Investigation of MSE Wall Corrosion in Wisconsin

Masoud Mousavi, PhD, PE
Antonios Vytiniotis, PhD, PE
W. Allen Marr, NAE, PhD, PE
Jerry DiMaggio, PE, BC.GE

Prepared by:
Geocomp, Inc.
Acton, MA

Prepared for:

WisDOT ID no. 0092-24-02

June 2025

RESEARCH & LIBRARY UNIT

WISCONSIN HIGHWAY RESEARCH PROGRAM

WISCONSIN DOT
PUTTING RESEARCH TO WORK

TECHNICAL REPORT DOCUMENTATION PAGE

1. Report No. WHRP 0092-24-02	**2. Government Accession No.**	**3. Recipient's Catalog No.**
4. Title and Subtitle Investigation of MSE Wall Corrosion in Wisconsin		**5. Report Date** June 2025 **6. Performing Organization Code**
7. Author(s) Masoud Mousavi, PhD, PE; Antonios Vytiniotis, PhD, PE; W. Allen Marr, NAE, PhD, PE; Jerry DiMaggio, PE, BC, GE		**8. Performing Organization Report No.** 221417
9. Performing Organization Name and Address Geocomp, Inc 125 Nagog Park, Acton, MA 01720		**10. Work Unit No.** 11. Contract or Grant No. WHRP 0092-24-02
12. Sponsoring Agency Name and Address Wisconsin Department of Transportation Research & Library Unit 4822 Madison Yards Way Room 911 Madison, WI 53705		**13. Type of Report and Period Covered** **Final Report** October 2024 to June 2025 **14. Sponsoring Agency Code**
15. Supplementary Notes		

16. Abstract

Mechanically Stabilized Earth (MSE) walls play a crucial role in transportation infrastructure due to their cost-effectiveness, ability to tolerate deformations, and resistance to seismic loading, among other advantages. While MSE walls are designed for long-term performance, the durability of their reinforcements is a key factor influencing their service life. When embedded in soil, steel reinforcements are susceptible to corrosion due to electrochemical interactions with the surrounding environment. As part of a highway widening project, WisDOT planned the removal of a 32-year-old MSE wall along I-43 in Glendale, WI, in 2024. The MSE wall was reinforced with galvanized steel strips. WisDOT sought to assess the reinforcements' condition to determine whether corrosion could pose a concern for its MSE wall assets. WisDOT contracted Geocomp to perform a field investigation and analysis of this MSE wall, aiming to: 1) assess the condition of the steel reinforcement and evaluate backfill electrochemical and geotechnical properties; 2) determine the remaining service life of the wall; and 3) evaluate WisDOT's design and maintenance practices to enhance the long-term durability and safety of the state's MSE walls. The study's findings emphasize the critical impact of pavement distress and salt intrusion on the deterioration of MSE wall reinforcements. Field investigations revealed that moisture and salt intrusion through pavement cracks and joints likely altered the backfill electrochemical properties over time, creating a highly corrosive environment. Geocomp excavations uncovered elevated chloride levels in the reinforced backfill and significant corrosion loss, as indicated by pitting corrosion loss as high as 90% of the strip's cross-sectional area in some locations. The excessive corrosion loss of metal strips extended to a depth of up to 13 feet from the top of the MSE wall. Deterministic stability analyses indicated that, had the MSE wall remained in service, an internal failure was highly probable within 10 to 15 years. These alarming findings underscore an urgent and immediate need for WisDOT to develop and implement a robust asset management program to proactively address corrosion risks, preserve infrastructure integrity, and ensure public safety.

17. Key Words Mechanically Stabilized Earth Retaining wall, Corrosion, De-icing Salt, Galvanized Steel, Pavement Distress	**18. Distribution Statement** No restrictions. This document is available through the National Technical Information Service. 5285 Port Royal Road Springfield, VA 22161

19. Security Classify. (of this report) Unclassified	**20. Security Classif. (of this page)** Unclassified	**21. No. of Pages** 55	**22. Price**
From DOT F 1700.7 (8-72)	Reproduction of completed page authorized		

DISCLAIMER

This research was funded through the Wisconsin Highway Research Program by the Wisconsin Department of Transportation and the Federal Highway Administration under Project WHRP 0092-24-02. The contents of this report reflect the views of the authors who are responsible for the facts and accuracy of the data presented herein. The contents do not necessarily reflect the official views of the Wisconsin Department of Transportation or the Federal Highway Administration at the time of publication.

This document is disseminated under the sponsorship of the Department of Transportation in the interest of information exchange. The United States Government assumes no liability for its contents or use thereof. This report does not constitute a standard, specification or regulation.

The United States Government does not endorse products or manufacturers. Trade and manufacturers' names appear in this report only because they are considered essential to the object of the document.

EXECUTIVE SUMMARY

Mechanically Stabilized Earth (MSE) walls play a crucial role in transportation infrastructure due to their cost-effectiveness, ability to tolerate deformations, and higher resistance to seismic loading than rigid concrete wall structures, among other advantages. These walls typically consist of metallic or geosynthetic reinforcing layers that provide tensile strength to the backfill and facing elements. A common configuration includes precast concrete facing panels connected to embedded steel grids or strip reinforcements. While MSE walls are intended for long-term performance, the durability of their steel reinforcements is a key factor influencing their service life. When embedded in soil, steel reinforcements are susceptible to corrosion due to electrochemical interactions with the surrounding backfill.

As part of a highway widening project, WisDOT planned to remove an MSE wall (RW-40-158, hereafter referred to as "the MSE wall") along I-43 in Glendale, Milwaukee County, in 2024. To our knowledge, no significant signs of distress were reported prior to removal, aside from a localized issue with one facing panel. The MSE wall, built in 1992, was reinforced with galvanized steel strips. Geocomp performed a field investigation and analysis of this MSE wall. The objectives of this study were to: 1) assess the condition of the steel reinforcement; 2) evaluate electrochemical and geotechnical properties of the backfill material; 3) determine the remaining service life of the MSE wall; 4) evaluate WisDOT's design and maintenance practices relative to corrosion of buried steel, and 5) provide recommendations to inform WisDOT's design and maintenance practices, enhancing the long-term durability and safety of the state's MSE walls.

The study's findings identified the critical impact of pavement cracks and joints, as well as moisture and salt intrusion, on the corrosion of MSE wall reinforcements. Field investigations revealed that moisture and salt intrusion through pavement cracks and joints likely altered the backfill electrochemical properties over time and created a highly corrosive environment. Geocomp's excavations uncovered significant corrosion loss in the reinforcing strips and elevated chloride levels in the backfill.

Geocomp investigated five 10 feet by 15 feet excavation sections (1 through 5) along the MSE wall by carefully deconstructing its components. The wall height decreased, and distance from the bridge increased, from Section 1 to 4. Section 5 was a shallow trench between Sections 1 and 2. Highly nonuniform corrosion was observed in the reinforcing straps in Sections 1, 2, 3, and 5. Pitting corrosion resulted in the loss of more than 90% of the strip's original cross-sectional area. The pitting corrosion indicated a likelihood of corrosion loss through salt attack. Corrosion severity was highest in sections closer to the bridge. In general, the severity of corrosion followed a gravity-driven pattern, decreasing with depth from the pavement surface. Sections with higher moisture and chloride content and lower resistivity exhibited deeper reinforcement straps experiencing excessive corrosion. Elevated moisture and chloride content, along with low resistivity, correlated with the presence of pavement cracks and joints. This indicated potential intrusion of moisture and salt.

The average resistivity of backfill within each excavation section appeared to correlate with the overall severity of corrosion loss of the reinforcement strips. However, the soil resistivity measured at a specific depth did not correlate with the corrosion loss of strips located at those depths. This discrepancy is likely due to temporal and spatial variations in soil resistivity, presenting a challenge to the reliability of field investigations that rely solely on measuring electrochemical soil properties to evaluate the corrosion loss of the reinforcements.

Geocomp excavation Section 4 exhibited the least corrosion, characterized by an almost intact galvanized coating, minimal pavement cracking, and backfill resistivity exceeding the AASHTO recommended minimum limit. In contrast, Section 1 showed the most severe corrosion, with heavily corroded reinforcement strips extending to depths of approximately 13 feet. Several key design and construction differences in Section 1 likely contributed to this excessive corrosion:

1. Section 1 had the lowest Pavement Condition Index (PCI) for the paved traffic lane and shoulder near the MSE wall.

2. The bridge deck and bridge abutment pavement were sloped toward this section, directing additional surface water runoff toward the reinforced zone.

3. The approach slab in this section included two 2-inch transverse expansion joints and multiple concrete joints and cracks extending over the reinforced zone.

4. A highly permeable layer of open-graded crushed stone existed beneath the concrete approach slab, likely facilitating water infiltration through its joints and cracks.

5. It likely received more salts due to anti-icing treatments, in addition to de-icing, before freezing events.

Geocomp's data revealed higher moisture contents in Section 1 compared to the other sections. Additionally, the average chloride content and minimum backfill resistivity in this section failed to meet current electrochemical design criteria. These findings indicate that moisture and salt intrusion likely played a significant role in the severe corrosion of the reinforcement strips observed in Section 1.

A comparison of measured and design-calculated corrosion losses for the reinforcing strips revealed that the shallow strips in Sections 1, 2, 3, and 5 experienced significantly greater corrosion loss than expected over the 32-year service period. Geocomp performed both deterministic and probabilistic stability analyses for the MSE wall at Section 1.

- Both deterministic and probabilistic analyses indicated that internal failure was likely within the design service life.
- The deterministic analysis showed that while the original design had an adequate factor of safety against slope stability, corrosion would reduce it to below 1.3 within approximately 40 years after construction.
- The probabilistic analysis indicated a failure probability exceeding 1% at 55 years.

Geocomp's findings suggested that the probabilistic approach estimates a data-informed longer service life compared to the deterministic analysis.

Geocomp recommends the following design and construction practices to reduce corrosion:

1. Use non-aggressive fills in the reinforced zone, use galvanized coated reinforcements, and design the reinforcements with a sacrificial thickness.

2. If possible, design the pavement cross slopes to force and manage the surface water to flow away from the reinforced zones.

3. Ensure uniform compaction of the backfill both near and farther from the MSE wall to minimize differential settlement in fill.

4. Use impervious membranes and drainage systems according to the WisDOT Bridge Manual to mitigate the intrusion of de-icing salts and chemicals into the reinforced backfill.

5. Design a dedicated drainage system for the bridge and its approach slab to prevent water infiltration into the backfill or retained zone in these areas.

6. If salt intrusion into the reinforced backfill is expected, the AASHTO simplified corrosion rates may not be applicable. The design should account for higher corrosion rates and increased sacrificial thickness for reinforcements.

7. In the absence of other design modifications, the upper rows of reinforcement straps are more exposed to excessive corrosion. Increasing the sacrificial thickness of these upper reinforcement rows could extend the service life of the MSE wall.

8. Consider installing test coupons at multiple depths and locations along the MSE wall during construction and retrieving selected ones at certain times to evaluate corrosion loss throughout the structure's service life.

9. Where beneficial from a risk management perspective, develop instrumentation specifications to monitor rate of corrosion loss of select strips using methods such as Linear Polarization Resistance (LPR).

Geocomp recommends the following to reduce corrosion:

1. Regularly maintain pavement surfaces and drainage structures associated with MSE walls reinforced with metallic elements to prevent moisture and salt intrusion. It is also recommended to conduct annual inspections and make necessary repairs prior to the onset of winter.

2. Give special attention to pavement directly above the reinforced zone, ensuring cracks and concrete joints are routinely sealed to prevent moisture and salt intrusion.

3. WisDOT might consider using less corrosive de-icing salts, such as calcium magnesium acetate, on MSE wall-supported pavements. A list of qualified corrosion-inhibited agents with their effectiveness is provided by the Clear Road research program.

Geocomp recommends a framework for a risk-based protocol to manage existing MSE walls potentially experiencing excessive corrosion. The risk-based protocol includes desk studies of condition states of the MSE wall, field assessment of performance states, and performing vulnerability, consequences, and risk evaluations. The recommended protocol results in an index that describes the risk associated with the failure of a given MSE wall.

ACKNOWLEDGEMENTS

The authors extend their sincere gratitude to the Wisconsin Department of Transportation (WisDOT) for sponsoring this study on the corrosion performance of the RW-40-158 MSE wall. We deeply appreciate the invaluable collaboration, efforts, and guidance provided by the Project Oversight Committee (POC) throughout the course of this research.

We would like to acknowledge the WisDOT staff and engineers for their significant contributions, including providing critical information on pavement condition indices and state de-icing salt practices. We also extend our appreciation to our subcontractor, GeoTesting Express, for their essential role in testing soil and strip samples, as well as to Hoffman Construction, the MSE wall demolition contractor, for their exceptional cooperation during the field investigation.

Finally, we wish to express our special thanks to the Geocomp engineers and staff who contributed to various aspects of this research, including Dr. Hala El Fil, Ms. Gail Lollis, Dr. Pooya Dastpak, Mr. Martin Hawkes, and Miss Hebatalla Ghoneim. Their expertise and support were instrumental in the successful completion of this study.

TABLE OF CONTENTS

LIST OF TABLES

LIST OF FIGURES

GLOSSARY OF TERMS

AASHTO	American Association of State Highway and Transportation Officials.
AC	Asphalt concrete.
CDR	Capacity demand ratio. The ratio of reinforcement capacity to the demand load.
Chloride content	Concentration of chloride ions in the soil.
Coefficient of Uniformity	The ratio of the diameter corresponding to 60% finer soil particles by weight to the diameter corresponding to 10% finer soil particles by weight, $C_u = D_{60}/D_{10}$.
Concrete approach slab	A reinforced concrete slab placed at the ends of a bridge or culvert to provide a smooth transition between the bridge structure and the adjacent roadway pavement.
Corrosion loss	Loss of steel reinforcement expressed as the percentage loss relative to the original (uncorroded) cross-sectional area of the reinforcement strip.
Crowned pavement	A crowned pavement is a roadway surface with a higher elevation in the center that gradually slopes downward toward the edges.
Depth of excessive corrosion	The maximum depth from the pavement surface at which a reinforcement strip exhibits excessive corrosion (i.e., see below for definition of excessive corrosion).
Degree of saturation	Percentage of volume of voids filled with pore fluid. A degree of saturation of 100% indicates all voids within the volume of soil are filled with water.
Excessive corrosion	Corrosion loss exceeding the estimated sacrificial thickness using the FHWA simplified design equations for strips in non-aggressive fill.
Facing	Component of MSE walls that forms the façade of the structure. *Facing Connection*: A structural element that connects a facing unit to reinforcement component in an MSE wall.
FHWA	Federal Highway Administration.
Field resistivity	Soil resistivity at in-place moisture content in field.
NCHRP	National Cooperative Highway Research Program.
Minimum resistivity (ρ_{min})	Minimum resistivity of soil at its near-to-full saturation measured using AASHTO T288.
MSE wall	Mechanically stabilized earth retaining wall.
Non-uniform corrosion loss	Maximum localized corrosion loss along a sample of reinforcing strip. Nonuniform corrosion loss of 100% indicates complete localized loss of the strip.
OSHA	Occupational Safety and Health Administration.

Pitting corrosion	Localized corrosion confined to small points, forming definite indentations in the metal surface.
PCI	Pavement condition index.
Reinforced Backfill	A soil mass with reinforcement inclusions that add tensile strength.
Reinforced zone	The reinforced backfill zone of an MSE wall.
Retained soil	The soil mass behind the reinforced zone of an MSE wall, retained by the reinforced backfill.
Retained zone	The zone of soil mass behind the reinforced zone of an MSE wall.
Service life	The predicted or actual time period a structure has before it ceases to perform its intended function
Service Limit State	Limit state relating to stress, deformation, and cracking applied to normal operating loads.
Strength Limit State	Limit state relating to strength and stability under statistically significant load combinations which are routinely experienced (i.e., not ship collisions, earthquakes, etc.).
Sulfate Content	Concentration of sulfate ions in the soil.
Surface Drainage	A system that collects and drains surface water.
Traffic Barrier	A structure on roadways that prevents vehicles from colliding with obstacles or leaving the roadway.
Uniform corrosion loss	Average corrosion loss along a reinforcing strip. Uniform corrosion loss of 100% indicates complete loss of the entire strip.

1 INTRODUCTION

Mechanically Stabilized Earth (MSE) walls play a crucial role in transportation infrastructure due to their cost-effectiveness, flexibility, ability to tolerate deformations, and higher resistance to seismic loading, among other advantages. These MSE walls typically consist of facing elements and reinforcing layers that provide tensile strength to the backfill. A common configuration includes precast concrete facing panels connected to embedded steel grid or strip reinforcements. While MSE walls are intended for long-term performance, the durability of their steel reinforcements is a key factor influencing their service life. When embedded in soil, steel reinforcements are susceptible to corrosion due to electrochemical interactions with the surrounding backfill.

To mitigate corrosion risks, modern design standards for MSE walls using metallic reinforcement specify the use of nonaggressive backfill materials that meet strict electrochemical criteria, along with the incorporation of sacrificial steel thickness and coating, to account for anticipated metal loss over time. Several case studies across the United States, including notable instances in Nevada, Utah, California, and New York, have documented significant corrosion-related deterioration of MSE wall reinforcements. Findings from these studies indicate that while existing corrosion models, such as those developed by FHWA and specified by AASHTO, tend to be conservative for nonaggressive fills, corrosion behavior in aggressive fills is highly variable.

The Wisconsin Department of Transportation (WisDOT) has used MSE walls extensively in highway projects, relying on galvanized steel reinforcements and low-corrosion-potential backfills to obtain long-term durability. However, a number of these MSE walls were constructed before 1990s, when standard specifications for assessment of corrosivity of fills and designing against corrosion loss were not well established. External factors such as moisture and salt intrusion into the reinforced backfill have been identified as potential causes of excessive corrosion (Elias, et al., 2009). These factors can increase the aggressiveness of the fill material over the structure's service life, even if the fill was originally designed and constructed to be nonaggressive.

WisDOT planned to remove an MSE wall (RW-40-158) along I-43 in Glendale, Milwaukee County in 2024. This was part of a highway widening project that presented a unique opportunity to evaluate the condition of an approximately 32-year-old structure which was constructed in 1992. To our knowledge, no significant signs of distress were reported prior to the MSE wall removal, aside from a localized displacement of one facing panel. The retaining wall consisted of a 616-foot-long MSE wall with a maximum height of 17 feet. The reinforcement consisted of galvanized steel straps.

1.1 PROJECT OBJECTIVES

The research objectives included the following:

- Document the condition of the subject MSE wall components at different locations throughout the reinforced backfill zone. The visual and physical condition of the steel straps and panel connections can indicate corrosion activity.
- Characterize the index and electrochemical properties of the reinforced soil to determine if the backfill satisfies current standards and if de-icing salts/chemicals have infiltrated the reinforced

zone creating corrosive conditions. Additionally, document spatial variations in the condition of reinforcement, connections, and reinforced zone material.

- Assess the remaining service life of the subject MSE wall based on measured corrosion rates and the condition of the MSE wall components.

1.2 ORGANIZATION OF THE REPORT

This report is organized into seven chapters, as follows:

- Chapter 1 provides an introduction to the study and the scope of the research.
- Chapter 2 examines the mechanisms of corrosion in buried metals, historical, current, and WisDOT practices for design against corrosion, previous MSE wall corrosion studies, and the testing methods used to characterize the corrosive potential of reinforced MSE backfills, testing methods for steel composition, thickness, and corrosion loss measurements.
- Chapter 3 provides background information about the design features of the study MSE wall.
- Chapter 4 summarizes the forensic field investigations performed by Geocomp prior to and during the MSE wall demolition.
- Chapter 5 discusses field and laboratory tests performed to characterize the collected samples from the study MSE wall reinforced backfill and reinforcing steels.
- Chapter 6 presents an assessment of the remaining service life of the MSE wall, and
- Chapter 7 summarizes the research findings and presents conclusions and recommendations based on the study findings.

2 BACKGROUND

This chapter provides general background on the corrosion of metals. It reviews the historical evolution of standards and guidelines related to the corrosion of metallic elements in MSE walls, as well as design guidelines developed by WisDOT. Additionally, it discusses previous studies on MSE wall corrosion, as well as testing practices used to characterize MSE wall backfill and reinforcement metals for corrosion assessment.

2.1 CORROSION PRIMER

Corrosion of metal reinforcements in soil is an electrochemical process in which metal deteriorates over time due to environmental exposure. Metals such as iron and zinc are inherently unstable in nature and tend to revert to more stable chemical forms through corrosion. The rate and severity of corrosion depend on factors such as soil moisture, soluble salt content, and pH, all of which influence electrons and ions transfer, the key drivers of corrosion. By controlling these environmental variables and through protective measures such as additional steel allowances or sacrificial galvanization, engineers can manage corrosion risks.

The spatial and temporal variability of soil conditions make corrosion prediction and prevention more challenging than in above ground or marine environments (NAE, 2023). Understanding the mechanisms of corrosion in soil is essential for understanding the key contributing factors, minimizing failures, and ensuring long-term performance. The following sections explore corrosion fundamentals, factors affecting corrosivity of soil, and corrosion prediction approaches for buried metal reinforcements.

2.1.1 Scientific background

Corrosion of steel buried in soil primarily occurs through an electrochemical oxidation-reduction process involving three essential components: an anodic site on the steel (where oxidation takes place and electrons are lost), a cathodic site on the steel (where reduction occurs and electrons are gained), and an electrolyte (e.g., soil moisture) that completes the circuit by conducting ionic current between the anodic and cathodic sites (NAE, 2023)[1].

Figure 1 provides a simple illustration of some of the electrochemical reactions involved in corrosion of steel. In the oxidation reaction, iron at the anodic site (labeled “A” in the figure) loses electrons to form iron ions (Fe^{2+}). In a reduction reaction, if dissolved oxygen is present in the soil, it can react with the released electrons at the cathodic site (labeled “C” in the figure) to form hydroxyl ions (OH^-). The interactions between iron ions and hydroxyl ions within the electrolyte can ultimately lead to the formation of red rust, iron oxide (Fe_2O_3).

Corrosion can involve different reactions depending on the acidity and oxygen availability of the electrolyte. While corrosion can also occur in anaerobic conditions, the rates are generally lower compared to aerobic conditions. The primary factors driving corrosion of steel are the unstable nature of iron, which causes the flow of electrons through the steel, and the presence of a conductive electrolyte, such as moist soil, which facilitates the flow of ions between the anodic and cathodic sites.

[1] National Academies of Sciences, Engineering, and Medicine.

2.1.2 Corrosivity of soils

The corrosivity of soil determines the rate at which corrosion progresses over time. Several factors such as moisture content, oxygen content, pH, electrical resistivity, soluble salt content, soil composition, compaction, grain size, and the presence of organic matter are conducive to or indicative of the corrosivity of fills. The effects of each factor, along with subsurface variability have a direct bearing on the ability to understand and predict the corrosion of steel reinforcements. It is crucial to understand that the corrosivity of soil is a dynamic property that can change over time due to variations in the composition of the pore space. The following sections describe the effect of key factors contributing to the corrosivity of soils.

Soil characteristics

The geochemistry of the soil, its density, gradation, and organic content affect its corrosivity. Grain size has important and complex impacts on parameters such as electrical conductivity, because the dominant soil mineralogy changes as grain sizes decrease. Coarse grained soils such as gravel and sand have lower electrical conductivity while fine-grained soils have higher. Coarse grained soils can provide better drainage of water and retain less water than fine-grained soils. On the other hand, if coarse-grained soils are subjected to cycles of infiltration, they can more easily feed the corrosion sites with fresh water high in oxygen content. Fine grained soils have lower permeability and allow water to infiltrate at a lower rate. A well-compacted soil and a soil with high fines content can retain higher moisture content compared to a loose or granular soil. Organic matter in soils can lower pH, participate in redox reactions, and promote microbial activity, all of which can accelerate corrosion.

Moisture content

Moisture content influences corrosion in opposing ways: higher saturation increases electrical conductivity, promoting corrosion, while lower saturation reduces oxygen levels and can limit it. Maximum corrosion rates typically occur at 60–85% saturation (Elias, 1990). In addition to moisture content, moisture infiltration can also alter pore fluid chemistry by transporting dissolved salts, oxygen, and contaminants. The significance of this is that these changes in pore fluid chemistry can increase the corrosivity of a soil that may have initially been noncorrosive.

Oxygen content

Corrosion rates are significantly lower in soils with low oxygen content. The amount of oxygen, free or dissolved, is affected by depth from the surface. In general, oxygen availability decreases as depth increases. This is because the rate of oxygen supply generally decreases with depth. Moisture infiltration and altering drying and wetting cycles of the soil have a significant effect on oxygen availability and corrosion of buried structures (Elias, 1990).

Soil electrical resistivity

Resistivity is the inverse of conductivity and is influenced by soil chemical composition, pore fluid characteristics, temperature, and degree of saturation. Generally, when all other factors remain constant, lower resistivity indicates higher conductivity, greater ion mobility, and increased corrosivity. Soil resistivity is inversely proportional to the concentration of soluble salts, such as chlorides and sulfates, as well as the degree of saturation. As soil saturation decreases, resistivity increases significantly. While the lowest soil resistivity occurs near full saturation, this does not necessarily correspond to the highest corrosivity, as oxygen availability becomes limited at saturations above approximately 85%, reducing the

rate of certain corrosion mechanisms. In fact, extracted steel piles have been found with very little corrosion below the minimum water line decades after installation. It is crucial to understand that current test methods, such as AASHTO T 288, are designed to measure minimum soil resistivity (ρ_{min}) under near-saturated conditions. While ρ_{min} is used as a criterion to assess the potential corrosivity of the soil, it does not necessarily reflect the actual resistivity or corrosivity during the structure's service life. Soil resistivity is particularly higher than its ρ_{min} value if the soil maintains low moisture content throughout the service life of the structure.

Soluble salts

Soluble salts, particularly chlorides and sulfates, play a significant role in the corrosion of metals. These salts reduce soil resistivity by increasing ion mobility, thereby enhancing electrochemical reactions that drive corrosion. Chlorides, in particular, are highly aggressive as they break down passive oxide layers on steel surfaces. This leads to localized pitting corrosion. Sulfates can also contribute to corrosion by supporting sulfate-reducing bacteria.

In addition to increasing conductivity, soluble salts can retain moisture at the soil-metal interface, even in relatively dry conditions, by forming a hygroscopic film. This retained moisture, combined with a high salt concentration, creates a highly conductive electrolyte, sustaining corrosion over time. In environments with fluctuating moisture levels, salt can dissolve and recrystallize, further damaging protective coatings and increasing exposure to corrosive conditions.

pH

For bare steel, corrosion rates are largely independent of pH between 4 and 10, relying instead on oxygen diffusion to the metal surface. However, extreme pH levels (below 4 or above 10) significantly accelerate corrosion. Zinc is particularly vulnerable in both strong acidic and alkaline soils (Elias, 2000). Note the local pH can vary widely with fluctuating wet and dry conditions.

2.1.3 Mechanisms of Corrosion

Steel corrosion can be broadly classified into general (uniform) corrosion and localized (non-uniform) corrosion. General corrosion results in relatively uniform material loss across the exposed surface, whereas localized corrosion involves concentrated attack in specific areas, potentially causing severe structural damage despite minimal overall mass loss. Localized corrosion may result from various electrochemical, environmental, or mechanical factors and, depending on the dominant mechanism, is further categorized into subtypes such as pitting corrosion and microcell corrosion.

In buried-steel applications, the most critical corrosion mechanisms to consider during design and performance assessment are general corrosion, pitting corrosion, and macrocell corrosion (NAE, 2023). Pitting corrosion occurs when protective surface films break down locally, resulting in deep, narrow pits that can severely compromise structural integrity, often with little visible indication. Macrocell corrosion involves the formation of distinct anodic and cathodic regions across the steel surface, typically driven by differences in moisture, oxygen, or electrolyte concentration in the surrounding soil. This leads to accelerated corrosion in the anodic zones. It is important to note that while corrosion engineers may distinguish between macrocell and pitting corrosion as separate mechanisms, the geotechnical community often categorizes both under the broader term “pitting corrosion”. According to FHWA, pitting corrosion is defined as localized corrosion confined to small points, forming definite indentations in the metal surface (Elias, et al., 2009). This study adopts the same terminology as FHWA for consistency. The

National Academies report on corrosion of buried steel at new and in-service infrastructure (NAE, 2023) provides a more comprehensive discussion of corrosion mechanisms in buried steel infrastructure.

2.1.4 Rate of corrosion

The most extensive data on underground corrosion comes from field tests conducted by the U.S. National Bureau of Standards (NBS). The data collection began as early as 1910 and involved buried metal pipes and sheet steel. These tests covered a broad range of burial conditions, not necessarily representative of the select backfill used in MSE structures. A key finding from these studies was that corrosion occurs most rapidly in the initial years after burial, before stabilizing at slower rates.

Based on these studies, Romanoff at NBS proposed an exponential equation to estimate general corrosion at a given time *t* after burial (Elias, 1990):

$$X = Kt^n \qquad \textbf{Equation 1}$$

Where *X* represents the metal's thickness loss or pit depth at time *t*, while *K* and *n* are soil- and site-dependent constants, with *n* being less than unity. The challenge in applying this model to galvanized steel lies in accurately determining *K* and *n* to account for environmental factors and the transition from galvanized protection to bare steel corrosion.

FHWA suggested the following equations for estimating galvanized steel loss considering a uniform corrosion model based on NBS data (Elias, 1990):

$$X = 25t^{0.65} \text{ (Average)} \qquad \textbf{Equation 2}$$

$$X = 50t^{0.65} \text{ (Maximum)} \qquad \textbf{Equation 3}$$

Equation 2 Equation and Equation 3 are representative of a wide range of soils, not necessarily those that meet the minimum or maximum requirements for electrochemical characteristics of backfill described in Section 2.2 of this report.

FHWA recommended a simplified model to determine the required sacrificial thickness of galvanized steel (Elias, 1990) which was later adopted by AASHTO as the required design consideration (AASHTO, 2002). It should be noted that this model is only applicable to soils meeting the electrochemical limits required by AASHTO described in Section 2.2 of this report. It also should be noted that the electrochemical properties of the soil are subject to change during the service life of the structure. Table 1 shows the simplified model recommended by FHWA and AASHTO.

2.2 HISTORICAL AND CURRENT PRACTICE

Early corrosion rate recommendations for steel reinforcement were based on field tests, studies like the NBS 45-year tests, French laboratory research, and buried pipe observations. By 1978, the French Ministry of Transport set electrochemical backfill standards: pH 5–10, minimum resistivity 1,000 ohm-cm, maximum chloride 200 ppm, and maximum sulfate 1,000 ppm (Blight & Dane, 1989).

It was not until the 1990s that the American Association of State Highway and Transportation Officials (AASHTO) included corrosion requirements for MSE walls in its Standard Specifications for Highway Bridges. In 1990, the FHWA published a comprehensive guide on design consideration for durability and corrosion of soil reinforced structures (Elias, 1990). One of the key objectives of this guideline was to

provide criteria for design engineers to assess potential corrosion losses in coated or uncoated steel reinforcements. In 1992, AASHTO introduced design requirements for reinforced structures, including electrochemical limits for fills and reinforcement corrosion rates (AASHTO, 1992), though no specific test procedures were outlined to verify the electrochemical limits. In 1996, AASHTO modified its specifications for standard corrosion rates and electrochemical properties (AASHTO, 1996), but it was not until the seventeenth edition that test procedures to measure corrosivity of soils were specified by AASHTO (2002). In 2000 and 2009, FHWA published follow-up reports that updated the Elias (1990) manual. The current practice incorporates the test methods discussed in the FHWA guideline (Elias, et al., 2009). This section describes the history of design and construction practices in regard to metallic reinforcement corrosion by FHWA and AASHTO.

2.2.1 FHWA-RD-89-186

In 1990, FHWA published the first comprehensive guideline on "durability/corrosion of soil reinforced structures" (Elias, 1990). The guideline provided criteria for assessing and designing against potential corrosion losses in soil reinforced structures. It provided an in-depth review of metallic reinforcement corrosion, corrosion indices, their effects, testing methods, and the design and evaluation of reinforced systems considering corrosion. The document also examined the prevailing FHWA corrosion design guidelines from 1986. The guideline indicated that the design practice in 1986 included the following key elements:

1. Reinforcement placement in select granular soil with electrochemical properties that meet specified limits, generally corresponding to mildly corrosive conditions,
2. a required service life of either 75 or 100 years, depending on the structure type, and
3. incorporation of a sacrificial thickness in the design to account for the expected mass loss due to corrosion over the service life.

The recommended electrochemical limits in 1986 for selecting backfills are provided in Table 2. FHWA-RD-89-186 (Elias, 1990) states that, at the time (i.e., 1986), the minimum required galvanization thickness in the U.S. was 86 μm per side, and the total sacrificial thickness for permanent structures was 0.65 mm.

FHWA-RD-89-186 (Elias, 1990) introduced updated design practices for corrosion protection of reinforcements. This included revised electrochemical limits, as outlined in Table 2. For determining the required sacrificial metal thickness, the guideline recommended design life values shown in Table 3.

For structures with backfills meeting the specified electrochemical limits, FHWA-RD-89-186 (Elias, 1990) recommended a uniform loss model to estimate the required sacrificial thickness, with the following corrosion rates:

(a)	Zinc corrosion rate first two years	15 μm/yr
(b)	Zinc corrosion to depletion	4 μm/yr
(c)	Carbon steel rate	12 μm/yr

The FHWA-RD-89-186 (Elias, 1990) guideline recommended a proportional reduction in tensile strength corresponding to the loss of steel thickness due to corrosion.

2.2.2 AASHTO (1992 and 1996)

Until 1992, the AASHTO Standard Specifications for Highway Bridges did not include provisions for the corrosion design of soil-reinforced structures. The 1992 edition was the first to introduce corrosion-related specifications for reinforced structures, including electrochemical limits for backfill materials, as shown in Table 4. In 1996, AASHTO revised these electrochemical limits (see Table 4). However, AASHTO (1996) did not specify the type of tests to characterize the soil material. In 2002, AASHTO specified the test methods to characterize the electrochemical properties of backfills. AASHTO (1996) adopted the same corrosion rates recommended in FHWA-RD-89-186 (Elias, 1990).

2.2.3 FHWA-NHI-00-044 and FHWA-NHI-09-087

In 2000, FHWA published a manual (i.e., FHWA-NHI-00-044) on "Corrosion/Degradation of Soil Reinforcements for Mechanically Stabilized Earth Walls and Reinforced Soil Slopes" (Elias, 2000). The manual updated the guidelines provided in (Elias, 1990). The key updates were the required electrochemical limits for acceptable backfill and the testing method to obtain them. The FHWA-NHI-00-044 (Elias, 2000) adopted the specified electrochemical requirements by AASHTO (1996). According to FHWA-NHI-00-044 (Elias, 2000), "*potential flow of salts from the retained fill must be considered in determining the long term regime within the reinforced backfill*."

In 2009, FHWA released the FHWA-NHI-09-087 manual, which updated the earlier FHWA-NHI-00-044 manual (Elias, et al., 2009). While the recommended criteria methods for reinforced backfill, as well as the predictive model for corrosion rates, remained unchanged, the updated manual provided more comprehensive content on corrosion. Table 2 presents the evolution of the electrochemical criteria and testing methods recommended by FHWA. With regard to electrochemical testing, the manual states that the required number of samples for testing is dependent on the number of stockpiles, history of laboratory testing on the source material, and the volume of material necessary for construction (Table 5). Another key addition was discussion on salt intrusion as a potential environmental agent that could accelerate corrosion during service of structures, particularly from sources such as de-icing salts. The manual also provides a review of state corrosion monitoring programs up to 2008.

2.2.4 FHWA-NHI-00-043 (Elias, et al., 2001)

This manual, entitled "Mechanically Stabilized Earth Walls and Reinforced Soil Slopes Design and Construction Guidelines", was issued in March 2001. The manual adopts the maximum and minimum requirements for electrochemical properties of the soils per FHWA (Elias, 2000) and AASHTO (2002).

The design recommendations to consider corrosion are consistent with AASHTO and FHWA specifications and guidelines discussed earlier as it requires:

1. Reinforcement placement in select granular soil with electrochemical properties that meet specified limits, generally corresponding to mildly corrosive conditions,
2. a required service life of either 75 or 100 years, depending on the structure type, and
3. the incorporation of a sacrificial thickness in the design to account for the expected mass loss due to corrosion over the service life.

The required electrochemical limits, testing methods, and predictive model for corrosion rates are the same as FHWA (Elias, 2000) manual. The manual recommends that consideration should be given to potential changes in backfill environment over the lifetime of the MSE wall. For example, de-icing salts may alter the reinforced backfill environment, particularly within the upper 2.5 m (i.e., 8 feet). In these

environments, FHWA recommends placing a minimum of 30 mil geomembrane below the road base. This membrane should be connected to a drainage system to reduce the penetration of de-icing salts into the backfill.

The manual provides recommendations for marine and chloride-rich environments outside of those that may be exposed to de-icing salts. For marine or salt intrusion structures and structures exposed to stray currents, the corrosion rate of 80 μm/year of carbon steel should be used for the first few years with a rate of 17 to 20 μm/year for the remaining life.

2.2.5 Contemporary AASHTO LRFD Bridge Design Specifications

AASHTO's contemporary LRFD Bridge Design Specifications generally follow the same approach as the FHWA (Elias, et al., 2009) guidelines for considering corrosion in the design of steel reinforcements, which is consistent with editions since 1992. This includes considering a sacrificial thickness based on a simplified corrosion rate in non-aggressive fills. Regarding electrochemical limits, AASHTO, in general, adopts the criteria outlined in the FHWA (Elias, et al., 2009) manual for characterization of non-aggressive fills (Table 4). The main difference between AASHTO and FHWA is the test method for chloride and sulfate contents. AASHTO also indicates that for soils with resistivities greater than 5,000 ohm/cm, the chlorides and sulfates requirements may be waved.

AASHTO C11.10.6.4.2a indicates that "*where deicing salts are used, adequate drainage provisions for salt laden runoff is required. In some cases, an impervious membrane may be required between the pavement structure and the select backfill.*" AASHTO adds "*These sacrificial thickness requirements are not applicable for soils which do not meet one or more of the nonaggressive soil criteria. Additionally, these sacrificial thickness requirements are not applicable in applications where:*

- *The MSE wall will be exposed to a marine or other chloride rich environment,*
- *the MSE wall has a metallic or wire mesh facing, or the metallic soil reinforcement is continuous, forming an electrically conductive circuit along the MSE wall length, and the MSE wall will be exposed to stray currents such as from nearby underground power lines or adjacent electric railways,*
- *the backfill material is aggressive, or*
- *the galvanizing thickness is less than specified in these guidelines".*

In terms of corrosion rates, AASHTO specifies the same rates as recommended by FHWA (Elias, 1990) guidelines (see Table 1) and provides the following provisions:

- *The metal loss rates shall be considered applicable to hot-dip galvanized steel and not applicable to black steel or steel coated by any other process. Other carbon steel loss rates shall be used for black steel and for steel coated by any other material or process.*
- *The sacrificial thicknesses account for potential pitting mechanisms and much of the uncertainty due to data scatter, and are considered to be maximum anticipated losses for soils which are defined as non-aggressive.*
- *Galvanized coatings shall be a minimum of 2 oz/ft² or 3.4 mils. in thickness, applied in conformance to AASHTO M 111M/M 111 (ASTM A123/A123M).*

2.3 WISDOT GUIDELINES FOR CORROSION DESIGN

2.3.1 1995 WisDOT Bridge Manual, Chapter 14 – Retaining Walls

WisDOT requirements for design against the corrosion of mechanically reinforced earth retaining walls (MSE walls) are provided in Section 14.3 of WisDOT Bridge Manual. The earliest available edition in 1995, revised in September 2000 indicates that the design methodology, in general, is in agreement with 1990 and 2000 FHWA guidelines. Section 14.3(F) dated September 2000 indicates that:

"*The galvanized steel reinforcement that is used for soil reinforcement is oversized in cross sectional areas to account for the corrosion that occurs during the life of the structure and the resulting loss of section. The net section remaining after corrosion at the end of the design service life is used to check allowable stress. MSE walls are designed for a minimum service life of 75 years. Corrosion of the wall anchors that connect the soil reinforcement to the wall must also be accounted for in the design.*" (WisDOT, 1996)

With respect to the acceptable backfill for the reinforced soil zone, Section 14.3(G) of WisDOT bridge manual, dated March 1996, states that:

"*The backfill material shall be free from organic and other deleterious materials and free of shale or other soft poor durability particles. It shall not contain foundry sand, bottom ash, blast furnace slag or other potentially corrosive material*" (WisDOT, 1996). The March 1996 manual indicates that the backfill shall be free from organics and shall meet the electrochemical criteria outlined in Table 4. The criteria established by WisDOT in 1996 appear to align with AASHTO's 1996 recommended limits, except for pH, which has a slightly wider acceptable range.

Section 14.3(G) of March 1996 WisDOT bridge manual recommends that "*the net area of steel reinforcement shall consider deductions for bolt holes and corrosion as stated in AASHTO 5.8.6.1 during the design life*" (WisDOT, 1996). AASHTO 5.8.6.1 specifies simplified corrosion rates recommended by FHWA guideline (Elias, 1990) as provided in Table 1.

2.3.2 2025-01 WisDOT Bridge Manual, Chapter 14 – Retaining Walls

Section 14.3.1.3, Site Characteristics describes that a part of site characterization includes determining the corrosion potential of the water at the site. *Section 14.4.7.8, Corrosion,* indicates that all metallic components of WisDOT retaining walls that may be subjected to corrosion should be designed in accordance with the Section 11.10.6 of AASHTO LRFD Bridge Design Specifications, 4th Edition, 2007.

Section 14.6.1.1, Usage Restrictions for MSE Walls, restricts the construction of MSE walls with either block or panel facing when soil is contaminated with corrosive material. WisDOT defines corrosive material as acid mine drainage, other industrial pollutants, or any other conditions which will increase the corrosion rate (e.g., stray electrical currents). *Section 14.6.2.1, Reinforced Earthfill Zone,* reiterates that potentially corrosive material shall not be used as backfill for MSE Walls. Table 14.6-1 in this section describes the requirements of electrochemical properties of reinforced fill in MSE walls and is provided in Table 4. WisDOT Bridge Manual does not specify the test method for electrochemical testing of backfill.

Section 14.6.2.2, Reinforcement, describes requirements for reinforcement of MSE Walls. The section indicates that metallic (inextensible) reinforcement can be either metallic strips, bar grids, or welded wire fabric. The metallic reinforcement is described as mild steel, typically galvanized or epoxy coated. The galvanized steel reinforcement cross sectional area is oversized due to anticipated corrosion that occurs throughout the structure's life and to account for section loss. The remaining section at the end of the design life, after corrosion, should be used in checking design requirements.

Section 14.6.3.8.7, Calculate T_{al} for Inextensible Reinforcement, provides the equation for tensile resistance (T_{al}) or reinforcement design strength of inextensible reinforcements as follows:

$$T_{al} = (A_C \times F_y)/b \qquad \textbf{Equation 4}$$

Where F_y = minimum yield strength of steel, b = unit width of sheet grid, bar or mat, and A_c = design cross sectional area corrected for corrosion loss. The corrosion loss is considered to be proportional to the loss of tensile strength.

Section 14.6.3.8.9, Design Life of Reinforcements, states that guidance presented in AASHTO LRFD Section 11.10.6.4.2a shall be the provision used for corrosion loss. AASHTO LRFD Section 11.10.6.4.2a was discussed in Section 2.2.5 of this report. *Section 14.6.3.8.10, Reinforcement/Facing Connection Design Strength,* indicates that connections between the steel reinforcement and wall facing units should also be designed to accommodate loss due to corrosion, and in accordance with AASHTO LRFD Section 6.13. Section 14.6.3.8.12, *Corrosion,* requires corrosion protection for all walls in aggressive environments as described in AASHTO LRFD Section 11.10.2.3.3. Typical aggressive environments in Wisconsin are described as areas typically associated with salt spray and areas near stormwater pipes in urban settings. This section indicates that MSE walls with steel reinforcement should have a properly designed impervious membrane layer below the pavement and above the first level of backfill reinforcement for protection (WisDOT, 2025).

2.4 CORROSION DESIGN IN COLD CLIMATE STATES

Cold Climate state DOTs have developed specific design and construction guidelines to mitigate salt-induced corrosion of MSE wall reinforcements. Common strategies include using impervious membranes to prevent salt and water intrusion, providing effective drainage layers to carry runoff away, enforcing strict backfill material specifications (such as AASHTO specified backfill electrochemical limits), applying zinc coatings to steel components, and in some cases restricting the use of metallic reinforcement under certain conditions. Below is a brief review of current practices in some states:

2.4.1 Michigan DOT (MDOT, Michigan Department of Transportation, 2019)

MDOT adopts AASHTO electrochemical limits for backfill and requires protective coating for reinforcements. According to MDOT bridge design manual (MDOT, Michigan Department of Transportation, 2019), section 7.03.012, a 30 mil thick PVC Liner (impervious membrane) is required between the roadbed and the soil reinforcement. The liner should be located a minimum of 8 inches above the soil reinforcement and extended 6 feet beyond the ends of the soil reinforcement. An underdrain should be placed one foot from the end of the PVC liner running transverse to the road and one foot from each

end of liner running longitudinally along the roadway. The underdrains are connected and dispense drained 3 feet minimum from any soil reinforcement.

2.4.2 New York (NYSDOT, State of New York Department of Transportation: Geotechnical Engineering Bureau, 2020)

NYSDOT requires the use of non-aggressive backfill and galvanized coating on metallic reinforcements. NYS standard specifications state that if the Contractor elects to provide an MSE wall which utilizes inextensible (metallic) reinforcing elements, the design submittal shall include a geomembrane barrier above the top layer of metallic reinforcements to protect the reinforcements from accelerated corrosion rates due to the infiltration of runoff containing deicing salts. If the design requires the geomembrane barrier to be installed at a lower elevation than the top layer of metallic reinforcements, the reinforcements situated above the geomembrane shall be designed for an exaggerated service life and supplied with identification markers for the Inspection Staff.

2.4.3 Pennsylvania (PennDOT, Pennsylvania Department of Transportation, 2019)

PennDOT's generic specifications require free-draining backfill meeting AASHTO gradation and corrosion criteria, to ensure low salt and moisture retention. PennDOT also requires specific designs to prevent salt intrusion. As documented in PennDOT's Design Manual (PennDOT, Pennsylvania Department of Transportation, 2019) guidance, "*For walls supporting roadways which are de-iced with chemical additives, an impervious membrane shall be placed above the reinforced zone and sloped to a collector drain to preclude infiltration of corrosion-causing elements*". PennDOT (2019) also emphasizes proper drainage for ground water, and states that "*walls in cut sections are advised to include chimney or blanket drains to intercept seepage before it reaches the reinforced soil*".

2.4.4 Minnesota (MnDOT)

MnDOT requires an impervious geomembrane barrier over the reinforced backfill zone for any MSE wall supporting a roadway that is salted in winter. This membrane should be installed between the roadway subbase and the top layer of reinforcement and sloped to drain salt-laden water to a collection system at the wall ends.

2.5 PREVIOUS MSE WALL CORROSION STUDIES

FHWA corrosion manual indicates that MSE wall corrosion assessment programs performed in nine states, including California, Florida, Georgia, Kentucky, North Carolina, New York, Nevada, Ohio and Oregon (Elias, et al., 2009). Figure 2 shows a summary of each program and references as provided in the FHWA manual (Elias, et al., 2009). The FHWA manual presents some of the key findings and results from the studies performed by Caltrans, FDOT, NYSDOT, and NCDOT.

In 2011, the National Cooperative Highway Research Program (NCHRP) project 24-28 included a performance database of MSE wall corrosion studies in various states (Fishman & Withiam, 2011). The report includes data from 170 sites located throughout the United States and Europe. The NCHRP report concluded that "*In general, metal loss models available from the existing literature, including the AASHTO model, were found to be conservative*." The NCHRP report made the following conclusions:

- Electrochemical properties of the reinforced fill have a significant impact on performance,
- the effect of time on the corrosion rate of galvanized steel is evident in the data, showing a decrease in corrosion rate over time,

- the spatial distribution of corrosion rates appears to be random, although spatial trends are apparent,
- no significant trends are observed between different climates for galvanized elements,
- marine environments had a detrimental effect on corrosion rates for plain steel (i.e., not galvanized) reinforcements, and
- seasonal variations affect measured corrosion rates, and considering the climate in the northeastern United States, measurements may vary by a factor of approximately 1.5 throughout a given year.

While the NCHRP report (Fishman & Withiam, 2011) noted no significant trends in corrosion severity across different climates, it is important to recognize that the underlying mechanisms and contributing factors likely vary by climate. Moreover, the report does not appear to isolate climatic effects while holding other variables constant. For example, if all other factors are equal, moisture and salt intrusion may be the dominant contributors in marine environments, whereas in cold climate regions, the use of de-icing salts may be the primary driver of corrosion.

The NCHRP report (Fishman & Withiam, 2011) indicates that although there is obvious trend between fill resistivity and corrosion rate, the data are highly scattered (See Figure 3). The report suggests that "*Some of the scatter may be due to spatial and temporal differences between measurement of corrosion rate and sampling and testing of reinforced fill materials.*" Electrical resistivity is only one factor influencing the corrosivity of fill. Laboratory tests typically measure the minimum electrical resistivity of soil under near-saturated conditions. However, actual soil resistivity can be significantly higher than this minimum value, indicating lower corrosivity, depending on the soil's moisture content throughout its service life.

Another critical factor is oxygen availability. For instance, if the fill experiences cycles of water intrusion through pavement cracks or an imperfect drainage system, it may undergo repeated fluctuations in moisture and oxygen content, promoting corrosivity and accelerating the corrosion rate. Conversely, even highly aggressive fill could result in a much lower corrosion rate than suggested by AASHTO if oxygen and/or moisture levels remain low. Therefore, while AASHTO's recommended electrochemical limits provide an indicator of fill aggressiveness, they are not a definitive condition, as other factors may play a more significant role.

2.6 TESTING PRACTICES TO CHARACTERIZE SOIL USED IN REINFORCED AND RETAINED SOIL

FHWA-NHI-09-087 manual (Elias, et al., 2009) provides the most recent recommended testing methods for characterization of MSE wall backfill. The recommended test procedures in the manual are provided in Table 2. AASHTO recommends the same testing methods for electrochemical limits, except for chlorides and sulfates. For chlorides and sulfates, AASHTO recommends the test methods AASHTO T 291 and AASHTO T 290, respectively (AASHTO, 2002).

FHWA further recommends that due to the variation in backfill sources, multiple tests should be performed to determine the mean conditions of the backfill. The manual indicates that the required number of samples for testing is dependent on the number of stockpiles, history of laboratory testing on the source material, and the volume of material necessary for construction. Table 5 shows the FHWA recommended sampling protocol for electrochemical testing of MSE wall backfill (Elias, et al., 2009).

2.7 STEEL REINFORCEMENT COMPOSITION TESTING AND CORROSION LOSS MEASUREMENT

2.7.1 Steel chemical composition

Several methods are used to test the chemical composition of MSE steel reinforcements. Combustion and inert gas fusion techniques, as outlined in ASTM E1019, are used to determine carbon, sulfur, nitrogen, and oxygen content in steel by measuring gases released during controlled heating. Similarly, ASTM E1479 specifies methods for determining the presence of trace elements such as boron using inductively coupled plasma atomic emission spectroscopy (ICP-AES). Optical emission spectroscopy (OES) and X-ray fluorescence (XRF) can be used for performing elemental analysis.

2.7.2 Steel reinforcement thickness

The nominal dimensions may be used with confidence for the steel reinforcement thickness (Elias, 2000). The thickness of bare steel in galvanized steel can be measured in the laboratory by first removing the zinc coating and then using a caliper to measure the remaining steel thickness. ASTM A90 outlines the procedure for sample preparation and zinc coating removal, which involves cutting a representative specimen from the coated steel product and immersing it in a hydrochloric acid solution with an inhibitor to dissolve the zinc layer without significantly affecting the steel substrate. The bare steel thickness is then measured at multiple locations along the sample to obtain an average thickness.

2.7.3 Galvanized coating

ASTM A90/A90M and ASTM B487 are standards used for measuring the thickness of zinc coatings on steel. ASTM A90 specifies a gravimetric method in which the zinc coating is chemically removed using an inhibited hydrochloric acid solution, and the coating weight is determined by the difference in mass before and after removal. This method is commonly used for hot-dip galvanized steel. ASTM B487 describes a microscopic method for measuring the thickness of metallic coatings, including zinc, by preparing a cross-section of the coated specimen and examining it under an optical microscope. This method provides a direct measurement of coating thickness. While ASTM A90/A90M provides an average value for thickness of the coating along the sample, ASTM B487 can provide minimum thickness of the coating and display coating thickness variation along the sample.

2.7.4 Corrosion loss

The reported corrosion losses in previous studies are mostly based on weight loss measurement of reinforcement samples and comparing it with the non-corroded weight of the same sample (Elias, 1990). The weight loss measurement provides an estimate of uniform corrosion of the reinforcement, i.e., assuming the corrosion is uniform along the metal strip. Corrosion loss also can be calculated by measuring section thickness at each retrieval interval (Elias, 2000). One challenge with such measurements is that the original weight or dimensions of the elements are uncertain if the corrosion monitoring is not initiated at the time of installation. According to FHWA (Elias, 2000), "*In these cases, the original dimensions or weights of the elements must be estimated to compute metal loss from observations of remaining thickness or weight. Nominal dimensions may be used with confidence for the steel thickness, however the original thickness of the galvanized layer is more uncertain. A minimum thickness of zinc coating is specified, however the hot dipped galvanization process specified by ASTM A123 (ASTM, 2007) results in galvanized layer thickness that may exceed the minimum by a wide margin*".

2.8 SUMMARY OF LITERATURE REVIEW

Understanding corrosion and assessing the risks of corrosion loss to structures requires knowledge of its mechanisms and the factors influencing its rate. The corrosivity of reinforced backfills plays a key role in determining the rate of corrosion over time. Several factors contribute to or indicate backfill corrosivity, including moisture content, oxygen availability, pH, electrical resistivity, soluble salt content, soil composition, compaction, grain size, and the presence of organic matter. Current practice focuses on designing for nonaggressive backfill material that meets specified electrochemical limits and incorporating sacrificial steel thickness based on recommended corrosion loss rates over the structure's service life. These guidelines assume that the fill remains nonaggressive throughout its design service life. Fill electrochemical properties can change over time due to environmental factors such as chemical intrusion and exposure to salt, such as de-icing salts. Specifically, in the case of MSE walls supporting roads with de-icing applications, previous studies showed temporal reduction in soil resistivity during de-icing season.

Studies conducted by state and federal agencies and private sectors have measured corrosion loss and evaluated the impact of electrochemical limits. Data suggest that AASHTO's predictive corrosion loss equations are generally conservative when the fill meets the recommended electrochemical limits by AASHTO and FHWA. In aggressive fill materials, electrical resistivity has been found to significantly affect corrosion loss, though the available data is highly scattered. This is likely due to the temporal variability of electrochemical properties of soil and effect of other contributing factors such as oxygen and moisture content. A key limitation of previous studies is their primary focus on the recommended electrochemical limits including minimum resistivity, pH, chloride, sulfate, and organic content, with limited information on the spatial and temporal variability of the electrochemical properties of soil as well as moisture and oxygen content. Even if a fill is classified as highly aggressive based on AASHTO electrochemical limits, actual corrosion loss may be limited depending on moisture and oxygen availability. In other words, classification of soil as aggressive based on electrochemical limits does not necessarily result in high corrosion loss if oxygen or moisture availability is low.

3 STUDY MSE WALL FEATURES

3.1 LOCATION

The MSE wall was located along Northbound of I-43 in Glendale, Milwaukee County, Wisconsin. Constructed in 1992 and scheduled for removal in 2024, the 616-foot-long Wall had a maximum height of approximately 17 feet and totaled 5,732 square feet of the MSE wall surface. Figure 4 shows the aerial view of the MSE wall and its approximate location along I-43. The wall began at Station (Sta.) 175+34.09 feet at the southern end and extended northward, reaching the existing grade of N Port Washington Rd at Sta. 181+50 feet.

3.2 DESIGN FEATURES

Geocomp reviewed relevant design and as-built information related to the study MSE wall. The following sections summarize key features of the MSE wall as they relate to this study. Appendix C includes copies of relevant drawings and reports.

3.2.1 Geotechnical Information

A design boring at STA 175+35 near the tallest section of the wall shows a subsurface profile consisting of approximately 2 to 3 feet of topsoil and fill, underlain by 21 feet of loose to medium dense sand, and very stiff to hard silt and clay layers, as shown in Figure 5.

According to the design drawings shown in Figure 6, the MSE wall system replaced a sloped embankment. A 2011 post-construction geotechnical investigation near the southern end of the wall indicated that the embankment was composed of a very stiff silty clay fill material. The silty clay fill would form the retained zone in the new retaining wall system. Geocomp did not find any information about the corrosivity of the retained fill in design and construction documents.

3.2.2 Typical Sections and Pavement Design

The typical roadway sections are shown in Figure 7 and Figure 8. The design drawings indicate that the road section immediately after the bridge abutment (between stations 175+35 and 175+55 feet) consisted of a concrete approach slab underlaid by crushed aggregate base (Figure 7). The drawings also show a pipe underdrain wrapped with geotextile underneath the edge of the approach slab close to the facing of the MSE wall. The design drawings show the road section beyond the concrete approach slab consisting of both an asphaltic and Portland cement concrete pavement. According to the design drawings, the road was to be constructed with a crowned[2] pavement along the MSE wall, which was to direct surface water towards the edges of the road.

Figure 9 presents the paving detail for the I-43 road along the RW-40-158 MSE wall. As shown in this figure, a concrete approach slab was designed at the southern end of the MSE wall immediately next to

[2] A crowned pavement is a roadway surface with a higher elevation in the center that gradually slopes downward toward the edges.

the bridge slab. The key feature of this approach slab potentially related to corrosion is multiple 2-inch expansion joints.

The design drawings show crowned pavement on top of the bridge (structure B-40-577) which is sloped downward toward the north (i.e., MSE wall) (Figure 7, Figure 8, and Figure 10). Thus, the surface water on the bridge and bridge slab was expected to flow toward the north and the two edges of the road, including the MSE wall. Specifically, most of the snowmelt and rainwater accumulated on the northern abutment of the bridge was expected to flow toward the MSE wall transversely to the direction of travel.

3.2.3 The MSE wall design

The MSE wall was designed by The Reinforced Earth Company. According to the MSE wall design drawings dated April 1, 1992, the design included the following criteria:

- Select granular backfill with friction angle of 34 degrees and unit weight of 125 pcf.
- Random backfill with friction angle of 30 degrees and unit weight of 125 pcf.
- Foundation material with a friction angle of 30 degrees.
- ASTM A-572 grade 65 reinforcing strips being 50 mm wide and 4 mm thick.
- Galvanized reinforcing strips in accordance with ASTM A-123.

The granular backfill was required to extend to the nominal length of the strips. The nominal length of strips varied between 11 feet and 10 feet at the taller wall sections. The wall facing consisted of precast concrete panels as shown on Figure 11.

According to the design drawings, the wall facing included a cast in place (CIP) concrete coping on top of. Based on the MSE wall design drawings, the wall sat on a leveling pad and the final grade in front of the wall was to be at least 3.5 feet above the top of the leveling pad.

The design drawings do not specify acceptable electrochemical limits for backfill corrosivity. AASHTO corrosion design specifications were not established until 1992. The reinforced granular backfill was designed to retain the fill within the existing embankment. As discussed in the previous section of this report, the retained fill consisted of silty clay, which is relatively impermeable. Consequently, the reinforced granular material is expected to function as a drainage layer for the retained fill due to its higher permeability. This could influence the backfill's corrosivity by increasing moisture content and facilitating flow from the retained fill into the backfill, if the retained soil is corrosive.

3.2.4 Drainage structures

The design drawings show two storm sewer inlets on the shoulder of the I-43 along the MSE wall. The storm sewer inlets are labeled as 271 and 273 on Figure 9. The storm sewer inlets were designed to collect the surface water flowing towards the edge of the road and direct it towards a stormwater collection system.

3.3 SUMMARY

The study MSE wall was constructed in 1992 and located along Northbound of I-43 in Glendale, Milwaukee County, Wisconsin. The MSE wall extended 616 feet from a bridge abutment on its south end and sloped down to natural ground toward the north. The reinforced system consisted of galvanized steel

ribbed straps and granular backfill. Geocomp identified several key design features that are likely to facilitate corrosion:

- The MSE wall replaced a sloped embankment consisting of compacted clay fill.
- The MSE wall was designed to consist of a reinforced granular backfill which retained the existing clay fill embankment.
- The retained soil was relatively impermeable and would direct the infiltrated water towards the highly permeable backfill.
- The I-43 roadway pavement system along the study MSE wall had two different section designs:
    - A short section at the south end of the wall immediately next to the bridge consisted of an approximately 20 feet concrete bridge approach slab with multiple joints, including 2-inch-wide expansion joints. The expansion joints were perpendicular to the wall alignment and extended to the pavement shoulder above the reinforcements.
    - The rest of the pavement beyond the approach slab towards the north consisted of an asphalt concrete pavement at the shoulder and concrete paved traffic lanes.
- The I-43 road pavement on the bridge and along the MSE wall both sloped downward and were crowned, directing the surface water and snowmelt toward the reinforced backfill.
- The concrete joints in the bridge approach slab and surface water flow toward the reinforced zone facilitated moisture and salt intrusion if the joints leak. Surface moisture and salt intrusion is not expected in the rest of the wall alignment, unless pavement cracks existed within or near the reinforced zone.
- The MSE wall design drawings did not specify criteria for determining acceptable noncorrosive backfill.
- The MSE wall design drawings did not include a geomembrane on top of the wall to impede moisture and salt intrusion into the reinforced backfill.

4 FIELD INVESTIGATION AND ANALYSIS

4.1 INITIAL SITE VISIT

Geocomp conducted a field visit of the MSE wall site on November 13, 2023, prior to its demolition. As part of the site visit, Geocomp, along with WisDOT staff, made observations, collected photographs, and documented several existing features, including:

- The approximate location, direction, openings, and condition of cracks in the shoulder pavement on top of the wall.
- Apparent movement on top of the wall, including lateral and downward movement of the shoulder pavement.
- The condition of the wall's drainage system.
- Rotation of concrete wall-facing panels in certain locations.
- Signs of water seepage from the face of the wall.
- The approximate free-standing wall height.

Representative photographs and Geocomp's observations during the initial site visit are provided in Appendix D. Table 6 summarizes key observations related to the top of wall and wall facing conditions, which are further discussed in the following sections.

4.1.1 Top of the Wall Conditions

- Geocomp was able to access only the paved area between the fences above the face of the MSE wall and concrete barriers as shown in Figure 12. Approximate stations along the wall were marked, where the MSE wall Sta. 0+00 feet was located at the south end of the wall immediately next to the bridge abutment slab as shown in Figure 13. Multiple concrete joints and signs of pavement distress were observed on the bridge abutment slab and concrete approach slab (Figure 13). The pavement distress on the concrete approach slab included a large area of repaired pavement on the second traffic lane and a transverse crack on the first lane that continued to the shoulder on top of the MSE wall. Geocomp observed that, at the MSE wall Sta. 0+00 feet, the top of concrete barrier on top of the wall facing was approximately ¾ inches lower than the top of concrete barrier on top of the bridge abutment.
- Both longitudinal (south to north) and transverse (east to west) cracks in the paved area between the concrete barriers and fences were observed along the MSE wall. An approximately 270-foot-long continuous longitudinal crack was observed from wall Sta. 0+20 to Sta. 2+90 feet. The longitudinal crack was approximately parallel to the edge of the wall and two to three feet away from it. The longitudinal crack opening was variable along the wall and generally ranged from less than 0.25 up to 0.5 inches. In general, the crack opening decreased as the wall height decreased. Geocomp measured excessive cross slope, up to 10%, in the shoulder area between the continuous longitudinal crack and the western edge of the concrete copings. Note that the cross slope at that area was to be 4% per design. The longitudinal crack discontinued at about Sta. 2+90 feet. Multiple isolated longitudinal cracks existed between wall stations 2+90 and 4+30 feet.

- The maximum measured cross slope in the shoulder area was less than 4% between wall Sta. 2+90 and 4+30 feet. Geocomp observed two storm sewer inlets approximately at wall stations 1+51 feet and 5+02 feet. The storm sewer inlets were partially covered by debris at the time of the observation. The storm sewer inlets appeared to collect and transfer the stormwater toward the center of the highway, as shown in design drawings (see 271 and 273 in Figure 9). Geocomp observed multiple transverse pavement cracks and pavement joints on the shoulder and traffic lanes. Some key observations made by Geocomp are provided in Table 6.

4.1.2 Conditions of the Wall Facing

Geocomp observed considerable horizontal displacement, bulging, and rotation of concrete coping and Wall facing panels at the Wall Sta 0+00 where the MSE wall met the bridge abutment (see Figure 14 for example). The outward displacement was approximately 4 inches. Geocomp measurements indicated considerable rotation of the top concrete panels along the wall and some to minimal rotation of concrete panels toward the bottom of the wall. Geocomp observed signs of water seepage through the concrete copings and MSE wall facing panels at multiple locations. Table 7 provides some of Geocomp's key observations.

4.2 MSE WALL 3-D MODEL

During the initial site visit, WisDOT used their drone to obtain video and photographs of the wall. Geocomp used data collected by WisDOT to develop an approximate 3-D model of the wall prior to demolition. Geocomp used Alicevision to construct the 3-D models from the source drone video. Figure 15, Figure 16, and Figure 17 show three different views of the texturized 3-D photogrammetry model. Geocomp used this data to have a record of the pre-existing condition of the wall. No apparent bulging of the wall is seen on these data. Figure 15 and Figure 16 show the presence of a berm at the highest part of the wall. The north part of the berm had been removed at the time of this video recording, as apparent by the distinct brown color at the face of the wall where the berm had been removed.

4.3 SELECT SECTIONS FOR FIELD TESTING AND SAMPLING

Based on the observations of wall conditions during the initial site visit, Geocomp selected four sections for field testing and sampling. The proposed excavation in each section included a trench with a 10 feet width parallel to the wall facing and approximately 15 feet length perpendicular to the wall facing. Section 1 was located at the concrete approach slab immediately next to the bridge abutment at the south end of the wall. Based on visual observations of the MSE wall performance, Sections 1 to 3 had relatively poor conditions and Section 4 had relatively good conditions in terms of wall facing movements and top of the wall pavement conditions. The height of the wall decreased from Section 1 to 4. During the field testing and sampling, an additional section (Section 5) was excavated. Section 5 was located between Sections 1 and 2. Table 8 presents key features of each section and Figure 18 presents their relative location along the MSE wall.

4.4 TRENCH EXCAVATION AND TESTING DETAILS

Geocomp performed field testing and sampling on March 6, 7, and 9, 2024 during the demolition of the MSE wall.

4.4.1 Section Excavation and Testing Details

The demolition contractor excavated the proposed sections under Geocomp's representatives' observation. Care was applied to not operate any equipment within 100 feet of each section during field testing. The excavation at each section had the following features:

- Excavation was at least 10 feet in width (north-south direction).
- Excavation extended at least 15 feet, perpendicular to the wall facing (toward west), from the face of the Wall.
- The demolition contractor sloped the excavation trench in accordance with OSHA's safe excavation standards.
- Except for Section 5 which was a shorter trench, excavation in each section extended vertically from the top of the wall to the bottom of the wall.

The sequence of excavation was as follows:

- The contractor removed the pavement layer from each excavation section while allowing Geocomp to measure the thickness of the concrete slab or asphalt concrete (AC) pavement layer.
- The sections were excavated in lifts. Each lift was excavated to uncover a row of reinforcing steel straps.
- For example, the excavation sequence in Section 1 was as follows:
    1. The demolition contractor cut the concrete approach slab to the top of the base course layer.
    2. The excavation proceeded using an excavator up to a few inches from the first row of the reinforcing straps.
    3. The demolition contractor used hand tools to excavate the fill and locate the reinforcing steel straps.
    4. To avoid disturbing the fill and reinforcing straps, only hand tools were used to uncover the reinforcing straps.
    5. The condition of each row of the reinforcing straps was recorded and samples were cut for further lab testing and measurement.
    6. Field testing including density, moisture content and soil resistivity test were performed at select lifts.
    7. Samples of fill material were collected for further laboratory testing.
    8. Steps 2 to 7 were repeated to uncover the deeper rows of reinforcing straps.

4.4.2 Field Testing and Sampling Schedule

Table 9 shows the schedule of field testing and sampling. Nuclear gauge tests were performed at two to four corners of the excavated section at given lifts of excavation. In addition to nuclear gauge tests, three sand cone tests were performed to evaluate the density of the fill. Soil resistivity tests were conducted in the field within each excavation section at selected excavation lifts, following the Wenner four-electrode method (ASTM G57). The soil resistivity tests were performed at the front and back of the lifts. To minimize the influence of deeper reinforcing strips, the electrodes were spaced 2 feet apart perpendicular to the orientation of the strips. The four-electrode array was positioned either immediately next to the wall or at the opposite end of the reinforcements, parallel to the wall (see Figure 19 for example).

Bulk soil samples were collected from each lift of excavation within each section and placed in double zipped bags to maintain their moisture. The samples were collected from opposing corners of each lift, one near the wall facing and the other at the far end of the trench. The bagged samples were stored in coolers and shipped to the GeoTesting Express facility for laboratory testing. Select metal straps were cut from each lift within each excavation section for laboratory measurements. Metal strip samples within each lift were collected randomly; however, more samples were generally taken from lifts exhibiting higher or more variable corrosion loss. In contrast, only one sample was collected from lifts where the metal straps appeared visually uncorroded. Each metal strap was cut into 3-5 segments to facilitate their shipment to the laboratory.

4.4.3 Key observations during field testing and sampling

Geocomp's staff were on site to document the condition of the fill and reinforcing straps during the excavation of the selected sections. Appendix E includes Geocomp's photographs during the field work. The following general observations were made during the field work:

- At Section 1, the pavement consisted of an 11-inch-thick concrete approach slab underlain by a 3- to 4-inch-thick open-graded base course (see Figure 20). This base course overlaid a relatively uniform sandy gravel fill that extended throughout the reinforced zone at Section 1 and other sections.
- At Sections 2 through 5, the pavement thickness ranged from 6 to 7.5 inches. No distinct base material, separated from the sandy gravel fill in the reinforced zone, was observed within the excavation footprint at these sections.
- Each concrete facing panel was connected to two rows (top and bottom) of reinforcing straps, with 2 to 4 straps per row.
- The reinforced fill within the excavated zone appeared to be compacted and relatively permeable.
- A compacted, relatively impermeable gravelly clay fill was observed in the retained zone at the western end of the excavations, approximately 3 to 4 feet beyond the ends of the reinforcing straps. The gravelly clay fill appeared to be part of the embankment that existed prior to the construction of the MSE wall.
- The longitudinal crack on the shoulder along the wall was exposed during pavement cutting at Sections 2 and 3 (see Figure 21). The crack appeared to be a top-down crack, with the crack opening decreasing with depth. At Section 2, the crack extended entirely through the pavement, while at Section 3, the crack opening was minimal at the bottom. Evidence of moisture infiltration was observed at the crack location in Section 2.
- Reinforcing straps were 11-feet-long in Sections 1, 5, and 2 and were 10-feet-long in Sections 3 and 4.
- Reinforcing straps at shallow depths within Sections 1, 2, 3, and 5 exhibited significant corrosion.
- Minimal to no corrosion was observed in the reinforcing straps at Section 4, which was noted to be in relatively good condition during the initial site visit.
- In general, visible corrosion decreased with increasing depth.
- Corrosion loss appeared to be more severe in sections with greater wall height and proximity to the bridge abutment (i.e., S1 > S2 > S3 > S4). Figure 22 presents photographs of reinforcing straps in Section 1 and Section 3.
- In Section 1, severe corrosion was observed in up to four lifts of excavation (approximately 10.5 feet below the pavement surface), while deeper straps appeared to be minimally to non-corroded.

4.5 SUMMARY OF FINDINGS

Geocomp conducted an initial site visit of the MSE wall site prior to its planned demolition. The purpose of this visit was to identify existing features of the Wall as well as I-43 pavement that might contribute to or indicate corrosion of the reinforcements. Geocomp's key observations included:

- Variations in pavement sections between the bridge approach slab and the remainder of the wall alignment, consistent with the design.
- Multiple concrete joints present in both the traffic lanes and pavement shoulder above the reinforced zone within the bridge approach slab. These joints likely facilitated water and salt infiltration, promoting reinforcement corrosion.
- An almost continuous longitudinal crack parallel to the wall, located approximately two to three feet from the wall face. The crack exhibited characteristics of a top-down crack, with surface openings of up to ½ inch. Generally, the crack narrowed and became intermittent as the wall height decreased.
- The pavement shoulder cross slope exceeded the design slope in areas where the Wall was taller. Outward rotation of the facing panels was observed in these locations, with the top panel near the bridge abutment showing excessive outward displacement of approximately 4 inches.
- Based on these observations, Geocomp selected four excavation sections (Sections 1 through 4) to represent both relatively poor and good-performing areas of the wall. Section 1 was located immediately adjacent to the bridge abutment, while Sections 2, 3, and 4 were progressively farther north. Generally, both wall height and cracking decreased from Section 1 to Section 4. Section 4 represented an area of relatively good performance, with minimal pavement shoulder cracking and panel rotation.

Geocomp subsequently performed field observations, testing, and sample collection of both soil and reinforcements during excavation of the selected sections. Key findings included:

- The reinforced backfill material appeared to be consistent along the wall alignment, consisting of sandy gravel. The retained soil, located at least 14 feet behind the wall face, was characterized as gravelly clay or clayey gravel.
- The steel reinforcements were galvanized ribbed steel and 11 to 10 feet long.
- Excessive corrosion of reinforcements was observed in shallow reinforcements within Sections 1 to 3. Corrosion generally decreased with increasing reinforcement depth or greater distance from the bridge abutment.
- Section 1 exhibited the most severe corrosion, with heavily corroded metal straps observed at depths of up to 12 feet. In contrast, Section 4 showed little to no reinforcement corrosion.

5 TEST RESULTS AND ANALYSIS

5.1 FIELD TESTS

5.1.1 Reinforced fill density and moisture content

Geocomp measured the in-situ dry and moist densities of the reinforced fill using the nuclear gauge and sand cone methods, Appendix F (pages F-1 to F-10) summarizes the results of these tests. The data are organized by section, lift, and test location within the excavation. For example, the sample ID "S1L1SE" indicates that the test was performed in Excavation Section 1, Lift 1, at the southeast corner of the excavation. Lift 1 refers to the first layer of excavation from the top of the wall, exposing the first row of reinforcing straps. Tests on the east side of the excavation were conducted near the ends of the reinforcing straps where they connect to the wall-facing panels, while tests on the west side were performed near the opposite ends of the straps. "South" and "North" refer to the location of the test relative to the southern or northern edge of the excavation.

The dry density of the fill material at the test locations ranged from 115.7 to 137.4 pounds per cubic foot (pcf), with an average density of 128.2 pcf. Moisture content ranged from 3.1% to 9.1%, averaging 5.5%. Except for Lift 4 of Section 4, which was nearly saturated, the degree of saturation ranged from 26% to 64%, with an average of 48%. These results indicate that the fill remained relatively moist and exhibited a relatively high water retention capacity despite its granular composition. Table 10 presents the average dry density, moist density, and moisture content for the tested sections.

5.1.2 Field soil resistivity tests

Geocomp performed in-situ resistivity tests at the front and back of each lift. The tests were performed using the Wenner four-electrode method (ASTM G57). The method used four metal electrodes placed 2 feet apart installed no deeper than 2 inches. The outermost electrodes provided a current source and a Miller 400A analog resistivity meter recorded the potential drop between the inner electrodes.

The Miller 400A measured the resistance (R) directly in ohms (Ω). The resistivity, ρ in ohm-cm was then calculated from Equation 5 according to ASTM G57.

$$\rho, \Omega\, cm = 191.5 a\, R \qquad \textbf{Equation 5}$$

Where a is the electrode spacing in feet.

Appendix F, page F-11, provides the results of field resistivity tests. Table 11 summarizes results of the field soil resistivity tests. The results indicate that Section 1 had the lowest average field soil resistivity. It is noteworthy that the field measured soil resistivity reflects the resistivity of the fill at in-place moisture content while the laboratory soil resistivity (e.g., using AASHTO T288) provides the minimum soil resistivity which usually occurs at or near saturation. Therefore, the values presented in Table 11 show the resistivity at in-place moisture content, not necessarily the minimum resistivity that fill could exhibit during the service life of the structure.

5.2 LABORATORY TESTS

Geocomp performed laboratory tests on the reinforced fill, retained soil, and reinforcing strap samples. See Appendix G for the test results on the reinforced fill and retained soil, including the following:

- Gradation per AASHTO T311 (Appendix G, pages G-2 to G-7).
- Moisture content per ASTM D2216 (Appendix G, pages G-8 to G-9).
- Proctor compaction test per AASHTO T99 (Appendix G, pages G-10 to G-11).
- Atterberg limits per AASHTO T90 (Appendix G, pages G-12 to G-13).
- Organic content per AASHTO T-267 (Appendix G, page G-14).
- Direct shear tests per AASHTO T236 (Appendix G, pages G-15 to G-16).
- Soil pH per AASHTO T289 (Appendix G, pages G-17 to G-18).
- Soil resistivity per AASHTO T288 (Appendix G, pages G-19 to G-21).
- Chlorides and sulfates content per ASTM D4327 (Appendix G, pages G-22 to G-26).

The following tests and measurements were performed on samples of reinforcing straps:

- Chemical composition of steel per ASTM E1019 and ASTM E1479.
- Galvanized coating thickness per ASTM A90/A90M and ASTM B487.
- Reinforcement thickness and width at multiple locations along each sample using a caliper.
- Sample weight loss for corrosion loss calculations.

The laboratory test results on chemical composition of steel and galvanized coating thickness is provided in Appendix G, pages G-27 to G-46. The results of dimension and weight measurements of reinforcements are provided in Appendix G, pages G-47 to G-49.

5.2.1 Gradation testing

Geocomp performed grain size analyses on five samples from the reinforced zone and one sample from the retained zone in accordance with AASHTO T311 for each location. The samples from the reinforced zone were selected to represent the fill at different elevations and locations along the MSE wall. Except for one sample, test results indicated that the reinforced fill consisted of sandy gravel with less than 5% fines. The sample collected from the second lift of Section 3 had a slightly higher sand content and a fines content just over 5%. These results were consistent with visual observations, confirming that the reinforced fill material was consistently similar material with depth and along the wall. Table 12 summarizes these gradation tests, and Figure 23 shows the particle size distribution curves for tested samples.

5.2.2 Moisture content testing

Geocomp tested select samples from the reinforced fill and retained soil for moisture content in accordance with ASTM D2216. Table 13 summarizes the range of moisture content and average values. Similar to the moisture content data from field tests, the laboratory test results show that the average moisture content decreases as the distance from the bridge abutment increases or as the height of the wall decreases.

5.2.3 pH testing

Geocomp measured the pH of select samples following AASHTO T289. In general, the pH of the reinforced backfill ranged from 8.36 to 9.58, while the sample from the retained zone had a pH of 9.15. All tested samples fell within the acceptable range for pH based on the 2025 WisDOT Bridge Manual criteria for non-aggressive fill.

5.2.4 Atterberg limits testing

Geocomp conducted Atterberg limits tests on a sample from the reinforced zone in Section 3 and a sample from the retained soil, both of which had a fines content greater than 5%. The tested sample from Section 3 was found to be non-plastic, while the retained soil sample was classified as lean clay.

5.2.5 Proctor tests

Proctor tests were performed on two select reinforced fill samples according to AASHTO T99. The samples were chosen to represent reinforced fill with dry densities approximately one standard deviation above and below the mean dry density of the reinforced fill. The results of the Proctor tests showed in-place relative densities of 97.7% and 88.5% for the tested samples. Table 14 summarizes the results of the Proctor tests.

5.2.6 Direct shear test

Direct shear tests were conducted on samples from Lift 2 of Section 3 and Lift 1 of Section 2. The samples were reconstituted to match the field-measured density. Testing was performed using a large-scale direct shear device with a 7-inch diameter. Soil samples passing the 5/8-inch sieve were compacted to their in-place dry densities. Each sample was tested at three different vertical effective stresses, including the estimated in-situ effective stress. Table 15 summarizes the direct shear test results. The results indicate that the peak friction angle of the samples was directly proportional to their initial dry density.

5.2.7 Soil resistivity testing

Geocomp performed soil resistivity tests on select samples of reinforced fill and retained soil in accordance with AASHTO T288. It is important to note that AASHTO T288 is used to determine the minimum resistivity of soil (ρ_{min}) at its near saturation condition. Table 16 presents a summary of the test data from excavation sections 1 through 5 and the retained soil.

The data showed that the backfill material in Sections 1, 2, and 5 had an average ρ_{min} value lower than 3,000 ohm-cm. The average ρ_{min} of the reinforced backfill in Section 3 was just slightly above 3,000 ohm-cm and Section 4 had an average ρ_{min} of 4,175 ohm-cm. The results show that a majority (58%) of the tested reinforced fill samples had a ρ_{min} value below 3,000 ohm-cm (Figure 24). The average ρ_{min} of all tested backfill samples was 2,655 ohm-cm. The ρ_{min} of the retained soil sample was 1,293 ohm-cm. It should be noted that fill with a minimum resistivity below 3,000 ohm-cm does not meet the 2025 WisDOT Bridge Manual requirements for non-aggressive fill. The noncompliant resistivities may result from salt intrusion during the service life of the structure.

5.2.8 Chloride content

Chloride content tests were performed on select samples of reinforced fill and retained soil in accordance with ASTM D4327. Table 17 presents the minimum, maximum, and average Chloride content in each excavated section. The average chloride content in all sections exceeded the 100 ppm maximum specified in the 2025 WisDOT bridge manual for noncorrosive fill. Figure 25 shows that 48% (14 out of 29) of the

tested reinforced fill samples had a chloride content exceeding 100 ppm. The sample collected from the retained zone had a chloride content of 131 ppm.

5.2.9 Sulfate content

Geocomp performed sulfate content tests on select samples of reinforced fill and retained soil in accordance with ASTM D4327. Table 18 presents the minimum, maximum, and average sulfate content in each excavated section. Results show that the sulfate content of the tested samples was well below the maximum sulfate content (i.e., 200 PPM), specified in the 2025 WisDOT Bridge Manual for a nonaggressive fill.

5.2.10 Steel chemical composition

Laboratory tests were performed on a selected strip sample from Lift 5 of Section 1 to determine the chemical composition of steel straps per ASTM E1019 and ASTM E1479. The details of the tests and results are provided in Appendix G. The chemical composition indicated that the steel from specimen S1L5 conforms to the chemical requirements of UNS G15260.

5.2.11 Galvanized coating and steel thickness

The zinc coating thickness was measured in accordance with ASTM A90/A90M and ASTM B487, as detailed in Section 2.6. The measurements were performed on samples that visually appeared to be uncorroded. Microscopic measurements using ASTM B487 indicated a minimum coating thickness of 54.43 µm, with an average thickness ranging from 93 µm to 132 µm per side. Measurements performed per ASTM A90 showed a coating thickness ranging from 110 µm to 210 µm per side. Table 19 provides a summary of the measurements. According to AASHTO M 111 and ASTM A123, the minimum required galvanization thickness for 4-mm-thick steel is 85 µm. The test results show that the visually uncorroded samples, on average, considerably exceeded the minimum required coating thickness. This finding aligns with previous studies, which reported that actual zinc coating thicknesses are highly variable and typically exceed the minimum required thickness. (Elias, et al., 2009).

Steel thickness measurement was conducted according to ASTM B487. The measurements indicated that the steel was slightly thicker than the required design thickness.

5.2.12 Corrosion loss

Weight loss and dimensional measurements (thickness and width) were conducted on collected metal strap samples to assess corrosion. As previously discussed, the straps were cut into four to five segments, and all measurements were performed on these cut segments.

- **Uniform (average) corrosion loss** was determined based on weight loss measurements for each segment.
- **Non-uniform (maximum) corrosion loss** was assessed through width and thickness measurements taken at the most corroded locations along each segment.

The following sections briefly discuss the means and methods used for measuring and calculating uniform and non-uniform corrosion loss.

5.2.12.1 Corrosion loss measurements

Before taking any measurements, all samples were cleaned to remove rust or residual particles using a brush and damp cloth. The unit weight of each segment was determined by weighing the segment on a scale, measuring its length, and calculating the weight per unit length. The thickness and width measurements of each segment followed these steps:

1. Visual Inspection: Identify two to three locations along each segment exhibiting the most significant corrosion loss.

2. Width Measurement: Measure and record the width at the selected locations using a caliper.

3. Thickness Measurement: Measure the thickness and width of the metal strap at two points along each selected location using a caliper and report the average value.

5.2.12.2 Corrosion loss calculation

Calculating corrosion loss was challenging due to the absence of original, uncorroded dimensions and weight data for the straps. Even if such data were available, variations in the measured galvanized coating thickness indicated that the original thickness and weight might have been inconsistent.

For this study, samples that visually appeared uncorroded were used as the reference baseline for unit weight and dimensional comparisons. Two sets of measurements were performed on each reinforcement sample. The first set used weight per unit length of samples to calculate an estimate of average or uniform corrosion loss along the sample. The second set measured localized minimum thickness and width of samples to calculate the maximum or nonuniform corrosion loss along the sample. The uniform (average) corrosion loss and non-uniform (maximum localized) corrosion loss were calculated as follows:

- **Uniform (average) corrosion loss** for each segment was determined by calculating the ratio of the segment's lost weight per unit length to the original uncorroded weight per unit length. A uniform corrosion loss of 100% indicates that the entire length of the strip segment is completely corroded.

- **Non-uniform (maximum localized) corrosion loss** was assessed by first calculating the cross-sectional area from the measured width and thickness at the location with maximum localized corrosion loss, then determining the corrosion loss as the ratio of cross-sectional area loss to the original cross-sectional area of the sample. A non-uniform corrosion loss of 100% indicates that the strip segment is 100% depleted by corrosion at a localized segment throughout its length.

5.2.12.3 Results

Figure 26 presents the uniform corrosion loss of the collected samples relative to depth from the top of the wall pavement for Sections 1 through 4. Overall, the data show that corrosion loss decreases with increasing depth of the reinforcing straps. The results show significant corrosion in metal straps at shallow depths, while minimal to no corrosion was observed beyond a depth of 10 feet. Additionally, metal straps in sections closer to the bridge, where the wall is taller, show higher corrosion levels. In contrast, Section 4 exhibited minimal corrosion, aligning with its selection as a representative "good" section based on visual assessments of surficial features such as pavement cracks and wall-facing conditions.

Figure 27 illustrates the nonuniform corrosion loss of the collected samples relative to depth from the top of the wall pavement for Sections 1 through 4. The data show similar trends to those observed in Figure 26, showing a decrease in corrosion loss with increasing depth. However, the magnitude of nonuniform corrosion loss is significantly greater than that of uniform corrosion loss, suggesting that pitting corrosion has been the dominant corrosion mechanism in most samples. The data show that in highly corroded segments, where uniform corrosion loss exceeds 10%, the nonuniform corrosion loss is generally about two times the uniform corrosion loss.

Figure 28 shows contour maps of both uniform and nonuniform corrosion loss along the length of the reinforcing strips. In these maps, the vertical axis represents the approximate elevation and the horizontal axis indicates the distance from the wall facing along the strip length. The plots reinforce the observed trend of reduced corrosion at greater depths; however, they do not reveal any clear relationship between corrosion loss and the distance from the wall facing along the strips.

5.3 DISCUSSION

5.3.1 Backfill compaction

The visual observations of the reinforced backfill showed that the backfill in general was well compacted. The collected density data in the field confirmed that the relative compaction of backfill further away from the MSE wall facing was higher than 95%. However, the data for the backfill immediately next to the wall indicate less compaction of the backfill. Figure 29 shows box-and-whisker plots comparing the in-place dry density of fill material near the wall facing to that at the free ends of the reinforcing straps, which are farther from the wall facing. The results indicate that, on average, the backfill dry density is lower near the wall facing compared to the areas further away. This is likely due to the design and construction practices at the time of the Wall construction which specified that "*compaction and operation equipment shall be kept a minimum distance of 3'-0" from the back face of the reinforced earth panels. Compaction within 3'-0" of the reinforced earth panels shall be achieved with at least three (3) passes of a lightweight mechanical tamper, roller or vibratory system*"[3]. As discussed in Section 4.1.1 of this report, the cross slope of the shoulder pavement near the wall facing was steeper than the design cross slope in the taller sections of the wall. This indicated that the shoulder likely experienced some settlement. The lower compaction of backfill within three feet of the wall panels was likely a contributing factor to this settlement.

Backfill compaction can influence corrosion both directly and indirectly. Indirectly, uneven compaction can lead to differential settlement and pavement cracking, allowing moisture and salt intrusion, as previously discussed. Directly, compaction affects permeability and moisture retention. A densely compacted backfill has lower permeability but higher moisture retention compared to a loosely compacted one. In a well-drained backfill, moisture retention can still significantly influence its corrosivity. High moisture retention leads to prolonged exposure of the reinforcement to a moist environment, increasing the potential for corrosion over time. Moisture retention is influenced by the gradation and density of the backfill material; in general, finer gradation and higher density result in greater moisture retention.

5.3.2 Backfill moisture content

The degree of saturation of soil can significantly affect the rate of corrosion. According to literature data, the corrosion rate is minimal in dry soil, and it peaks at 60 to 85% saturation (Elias, et al., 2009). Research

[3] Wall design drawings.

has shown that corrosion increased appreciably when the degree of saturation exceeded 50% and decreased as the degree of saturation reached 100% (Elias, 1990).

As previously discussed, backfill moisture content is a dynamic parameter that can fluctuate over time and seasonally as the backfill undergoes cycles of wetting and drying throughout its lifespan. These fluctuations are more pronounced when the design, construction, and conditions of the pavement facilitate moisture intrusion into the backfill. Based on the review of the wall and pavement design features, as well as observations of their condition, it was hypothesized that the reinforced backfill in the taller sections of the wall and areas closer to the bridge is more susceptible to moisture intrusion. The key design features and observed conditions supporting this hypothesis are as follows:

- The pavement design for the first 20 feet along the wall, extending from the bridge abutment, differed from the rest of the wall. Specifically, it incorporated concrete slabs with multiple joints and expansion joints, which could contribute to moisture intrusion.

- The bridge slab and concrete approach slab direct surface water toward the pavement shoulder, located above the reinforced zone of the wall.

- The concrete approach slab is underlain by a highly permeable open-graded crushed stone layer, facilitating the transfer of intruded water to the reinforced backfill. The design did not include an impermeable barrier, such as a geomembrane, to prevent this water intrusion.

- Relatively lower compaction within 3 feet of the wall-facing panels and thicker backfill zones likely resulted in settlement and longitudinal cracks along the wall. These cracks were observed to have wider openings in the taller sections of the wall, where the reinforced backfill is also thicker.

To evaluate this hypothesis, the average degree of saturation of samples from each section was calculated and plotted in Figure 30. The data presented in the figure illustrates the degree of saturation versus the approximate station of each excavation section. The average degree of saturation represents the mean degree of saturation in the top three lifts of excavation. The data were averaged only for the top three lifts to evaluate the effect of surficial water intrusion and eliminate the potential effect of groundwater capillary rise.

The data presented in Figure 30 shows that the in-situ degree of saturation decreases as the distance from the bridge increases or wall height decreases. This trend supports the initial hypothesis that water intrusion through pavement cracks and concrete joints likely contributes to moisture infiltration in the taller sections near the bridge. Section 1 and 5 had the highest average degree of saturation. The in-situ degree of saturation in these two sections ranged from 49 to 53%.

The backfill in most sections was classified as poorly graded gravel (GP) with less than 5% fines and relatively high permeability. Nevertheless, it maintained a relatively high degree of saturation, averaging 48%. This indicates that even granular materials can retain significant moisture depending on their gradation and exposure to infiltration. Therefore, relying solely on granular backfill for drainage may not be sufficient to limit moisture retention and reduce corrosion loss, as demonstrated by the findings of this study.

As discussed in chapter 2, moisture content can have opposing effects on the corrosion rate of metals. While high moisture content at full saturation is likely to result in oxygen depletion and reduced corrosion rate, the increase in saturation level decreases electrical conductivity, and increases the corrosivity of the

soil. For unsaturated soil (i.e., soil with degree of saturation less than approximately 85%), a significant decrease in soil resistivity occurs. Figure 31 presents the normalized resistivity versus moisture content for a number of tested samples, highlighting the effect of moisture content on electrical resistivity. Normalized resistivity was calculated as the ratio of measured resistivity at a given moisture content to the minimum resistivity of the sample. To examine this relationship, soil resistivity tests were performed on samples at their in-situ moisture content and at saturated condition. For reference, the in-place moisture content of samples was approximately 5% which corresponded to a degree of saturation of approximately 50%. Results showed that the resistivity of the samples at 50% saturation is 2 to 2.4 times higher than their minimum resistivity at near-saturated condition.

5.3.3 Electrochemical limits

The current practice in most states, including WisDOT, follows FHWA or AASHTO recommended electrochemical limits for backfill pH, minimum resistivity, chlorides, sulfates, and organic content to design for corrosion loss. This approach assumes that the backfill remains non-aggressive throughout the structure's service life, consistently meeting the recommended electrochemical limits.

Electrochemical tests conducted in this study showed that the MSE wall's reinforced backfill met the recommended limits for pH, sulfates, and organic content. However, the average chloride content exceeded the recommended threshold in all tested sections, and the average ρ_{min} fell below the acceptable limit in Sections 1, 2, and 5. It is important to note that these electrochemical properties were assessed after 32 years of service, and it remains unknown whether the backfill was nonconforming at the time of construction. In other words, it is likely that the chloride content and electrical conductivity of the backfill increased over time due to environmental conditions.

As discussed in the previous section, the data confirmed the hypothesis that considerable water intrusion likely occurred in the backfill near the bridge and/or in taller sections of the wall due to design features and surface conditions that facilitated moisture infiltration. One potential consequence of this intrusion is the reduction in soil resistivity caused by the presence of soluble chemicals, such as de-icing salts, transported by infiltrating moisture. However, water intrusion can also have the opposite effect by washing out soluble chemicals, such as salts deposited in the backfill pore space. As a result, the impact of water intrusion on backfill corrosivity can be both temporally and spatially variable. For example, previous research on de-icing salt infiltration in bridge approach embankments in Ohio found that elevated fill corrosivity was only observed for limited periods during the winter road-salting season (Timmerman, 1990).

Figure 32 presents the average ρ_{min} of the tested samples in each excavation section along the wall station. The data show a meaningful correlation between wall station and average ρ_{min}. Similar to moisture content, the fill exhibits higher corrosivity in sections near the bridge abutment and/or where the wall is taller. However, the correlation between wall station and resistivity is weaker than the correlation between wall station and moisture content ($R^2 = 0.74$ vs. $R^2 = 0.80$).

This study hypothesized that on Wisconsin roads de-icing salts are the main cause of elevated corrosivity. Previous studies have shown that electrical resistivity is a key indicator of soil corrosivity, as it reflects the total concentration of soluble salts, including sulfates and chlorides, in the pore fluid. Consequently, soils with high chloride contamination exhibit reduced resistivity.

Figure 33 plots the chloride content against the minimum resistivity of the tested samples, revealing a statistically significant correlation (p-value = 0.012). This finding suggests that chloride content plays a

dominant role in controlling backfill minimum resistivity and, by extension, its corrosivity in this Wall. A notable finding is that most backfill samples with chloride content exceeding the recommended 100 ppm limit also had minimum resistivity values below the 3,000 ohm-cm threshold for nonaggressive fill. This correlation suggests that elevated chloride levels are likely to be reflected in ρ_{min} measurements, making resistivity a reliable indirect indicator of chloride contamination, even in the absence of direct chloride testing.

Another notable finding is that the average minimum resistivity of the reinforced backfill in excavation Sections 3 and 4—where salt intrusion was expected to have less impact—was greater than 3,000 ohm-cm. This suggests that the reinforced backfill was likely nonaggressive at the time of construction and remained nonaggressive in areas less influenced by external environmental factors such as salt intrusion.

5.3.4 Corrosion loss

Previous studies have shown that resistivity can serve as an indicator of corrosivity. Data from the NCHRP study (Fishman & Withiam, 2011), which compiled 489 data points from 53 sites, demonstrated that fills with ρ_{min} values greater than 3000 ohm-cm generally exhibit corrosion rates approximately an order of magnitude lower than those with ρ_{min} values below 3000 ohm-cm (Fishman & Withiam, 2011) (Figure 3). However, significant data scatter was observed for fills with ρ_{min} values below 3000 ohm-cm, suggesting that reinforcement corrosion rates can vary by orders of magnitude even within fills of similar ρ_{min}. This indicates that while ρ_{min} values below 3000 ohm-cm may signal potential corrosivity, actual corrosion loss depends on additional factors such as oxygen availability and moisture content.

Figure 34 presents contour maps of uniform corrosion loss and minimum resistivity for Sections 1 through 4. A visual inspection of these maps does not reveal a meaningful correlation between corrosion loss and resistivity. For instance, corrosion loss data for Sections 1 to 3 clearly show reduced corrosion loss in deeper reinforcements. However, minimum resistivity does not appear to vary systematically with depth. Additionally, the contour maps indicate resistivity values of 3000 ohm-cm or lower in Section 4, yet the straps in this section exhibit minimal corrosion. This confirms that while minimum resistivity serves as an indicator of corrosivity, it does not necessarily predict elevated corrosion loss.

Geocomp performed a statistical analysis to identify the key drivers of observed corrosion loss. The statistical analysis compared the backfill properties with the corrosion loss of the strips at the sampled locations. The analysis included univariate and multivariate regression. The regression models accounted for both linear and transformed non-linear correlations between the variables and uniform corrosion loss. The variables assessed included:

- Minimum resistivity of backfill
- Backfill chlorides content
- Backfill pH
- Backfill in-place moisture content
- Backfill dry density
- Depth from pavement surface
- Wall station (i.e., distance from the bridge).

Results measured in terms of the coefficient of determination (R^2) and p-value, were used to assess the strength of the correlation and its statistical significance. The results of the single-variable analysis indicated that the best predictors of corrosion loss were wall station and moisture content (both with p-

values < 0.05). However, the R^2 values for these variables ranged from 0.43 to 0.44, suggesting a weak relationship. Wall station showed an inverse correlation with corrosion loss, while moisture content was directly proportional to corrosion loss.

The two-variable analyses, including combinations of depth and moisture content, moisture content and wall station, and dry density and wall station, exhibited stronger correlations with corrosion loss than any single variable alone. The analyses indicated that depth and wall station are inversely correlated with corrosion loss. In-place moisture content and dry density were directly proportional to corrosion loss. Results are shown in Table 20.

The inverse correlation between depth and corrosion loss as well as wall station and corrosion loss, aligns with field observations, which revealed that severity of corrosion loss decreased as the depth to the reinforcement or the distance from the bridge increased. Depth may indicate moisture and oxygen availability; deeper fills have lower oxygen availability and are less affected by moisture intrusion compared to shallower layers. Wall station represents the distance from the bridge and the height of the wall. As the distance from the bridge increased or the wall height decreased pavement joints, cracks, and openings which allowed moisture and salt intrusion also decreased.

Dry density likely affected the corrosion loss by influencing the moisture retention of the backfill. The more compacted the fill, the higher its ability to retain moisture. The higher the moisture content in unsaturated fill, the more corrosive it becomes until the degree of saturation reaches the level that reduces oxygen availability. It should be noted that more data are needed to support this observation as the data were limited in this study and the relationship between density and corrosion loss was not strong.

The analysis indicated there was no significant correlation between soil resistivity and corrosion loss when the backfill sample properties were compared to the corrosion loss of the strips at each depth. However, the results indicated that the mean resistivity of each excavation section is correlated with the severity of corrosion loss of the strips within that excavation section. There are several possible reasons for this observation. One factor is the temporal nature of resistivity. As shown in this study, chloride from deicing salts had a significant impact on resistivity. Since chloride is a soluble chemical, it can be washed out as water infiltrates the backfill. Therefore, measuring resistivity at just one point in time during the lifespan of the structure may not accurately reflect its long-term condition. Additionally, as discussed earlier, the average backfill resistivity was less than 3000 ohm-cm, indicating that the backfill is potentially aggressive in terms of corrosion potential. Thus, it can be concluded that while the fill remains aggressive in terms of minimum resistivity, other factors such as moisture and oxygen availability may have a greater influence on corrosion loss than the absolute minimum resistivity value. For example, if a fill with a ρ_{min} of less than 3000 ohm-cm remains dry throughout its service life, its actual resistivity would be orders of magnitude higher than ρ_{min}. Despite its potential corrosivity based on minimum resistivity, the fill is unlikely to cause significant corrosion under such conditions.

5.3.5 Pavement condition and corrosion loss

Data collected from this study indicate that moisture and salt intrusion through pavement joints and cracks was likely to cause the excessive corrosion loss of reinforcing strips. Initial site observations indicated that distress in the pavement shoulder, where the reinforced zone of the wall is located, was more pronounced in taller sections of the wall. Also, the concrete approach slab at the south end of the wall had multiple joints, including two 2-inch expansion joints, which can allow water intrusion into the backfill. These observations and findings aligned well with the corrosion data that indicated higher steel loss in taller sections and sections closer to the bridge. Specifically, the depth to excessive corrosion loss was

higher in sections that visually appeared to have more pavement distress. This is likely because larger volumes of water and salt intrusion could penetrate through the pavement in these sections, and moisture intrusion could reach deeper fill during each storm event. Geocomp evaluated two approaches, Pavement Condition Index (PCI) and crack infiltration, to quantify a correlation between corrosion loss and moisture intrusion through the cracks.

5.3.5.1 Pavement Condition Index

The Pavement Condition Index (PCI) is a widely used metric for quantifying the extent and severity of pavement distress. PCI values range from 0 to 100, where 0 represents a failed pavement section and 100 indicates a pavement in excellent condition. PCI captures a broad spectrum of distress. Some of the distress types that contribute to the PCI estimation are types such as asphalt concrete (AC) raveling and depressions that may not directly contribute to water intrusion.

In the case of the pavement along the study MSE wall, the predominant distresses were transverse and longitudinal cracks, which are highly susceptible to water infiltration. To assess pavement conditions near the reinforced zone, WisDOT provided PCI values from a survey conducted in 2022. The survey covered traffic lanes and shoulder pavement adjacent to the wall. The survey did not include the shoulder pavement between the concrete barrier and the wall facing, potentially omitting some distress features that may have contributed to water intrusion. Aerial imagery suggests that the pavement on I-43 along the MSE wall was resurfaced in 2014, meaning the reported PCI values may not fully capture the worst pavement conditions experienced over the service life of the MSE wall. WisDOT performed PCI assessments for 50-foot-long segments along the wall, covering the locations of Geocomp's excavation sections.

Table 21 shows representative PCI values for each excavation section, along with the depth of excessive corrosion loss[4] observed within the reinforcement zone. This depth is defined as the minimum depth at which the average uniform corrosion loss exceeds the estimated design loss, providing insight into the relationship between pavement condition and reinforcement corrosion. A greater depth indicates that deeper reinforcements have experienced corrosion levels beyond design expectations, potentially compromising the long-term performance of the Wall. Section 6.1 of this report provides a comparison between anticipated design corrosion loss and measured uniform loss.

The results indicate that the section with the greatest corrosion loss, extending to a depth of 12.8 feet, corresponds to the pavement section with the lowest PCI value—reflecting the worst pavement condition in terms of distress. Similarly, Section 4, which exhibited minimal corrosion, had the highest PCI value, indicating better pavement conditions. On this limited dataset, Geocomp found that even small reductions in PCI can contribute to substantial effects in increasing buried steel corrosion.

This comparison indicates a potential correlation between higher pavement distress and the extent of excessive corrosion throughout the MSE wall. PCI may serve as a potential indicator for assessing the likelihood of excessive corrosion, particularly when moisture and salt intrusion through the pavement are expected to contribute to corrosion. It is important to note that the dataset for this study is limited, and these findings may not be directly applicable to other MSE walls, especially those with different design and construction conditions.

[4] Geocomp defined excessive corrosion loss as the corrosion loss exceeding the FHWA simplified design estimated loss in nonaggressive fill.

5.3.5.2 Crack infiltration rate

The infiltration rate through pavement joints and cracks is influenced by several factors, such as the crack opening, the type of infill material within the crack, and the permeability of the pavement base material. Ridgeway proposed a method to estimate the infiltration rate through cracks (Ridgeway, 1976). The crack infiltration rate may be estimated using Equation 6:

$$q_i = I_c \left[\frac{N_c}{W} + \frac{W_c}{WC_s}\right] + k_p \qquad \textbf{Equation 6}$$

Where q_i is pavement infiltration rate in $ft^3/day/ft^2$, I_c is the crack infiltration rate in $ft/day/ft^2$, N_c is number of longitudinal joints or cracks, W_c is the length of contributing transverse joints or cracks in ft, C_s is spacing of contributing transverse joints or cracks in feet, and k_p is pavement permeability in $ft^3/day/ft^2$. This method is incorporated into the FHWA Drainage Requirements in Pavements (DRIP) for estimating water infiltration through pavements. FHWA recommends a value of I_c = 2.4 $ft/day/ft^2$ in the absence of more site-specific data and based on studies of saturated joints and cracks underlaid by a permeable base. For asphalt concrete (AC) and concrete pavements the pavement permeability is negligible, i.e., $k_p = 0$.

Geocomp calculated q_i values for four 20 feet by 20 feet pavement sections covering the locations of forensic excavation sections 1 through 4. This analysis did not consider cracks and joints beyond 20 feet from the MSE wall facing as the reinforcements extend up to 11 feet, making infiltration from more distant cracks less likely to impact the reinforced zone. The calculation only considered the cracks with medium to high severity and openings equal or larger than approximately ½". This was based on field observation that the shoulder cracks were mainly top-down cracks, and narrower cracks did not extend fully to the bottom of the AC.

For example, Figure 35 shows the cracks and joints identified in Section 1, which included the two transverse 2-inch expansion joints, one transverse crack, and two longitudinal concrete joints. Table 22 presents the parameters used to calculate the pavement infiltration rate and q_i in $ft^3/day/ft^2$. The results indicate that the pavement infiltration rate is highest in Section 1, followed by Section 2, then Section 3, and lowest in Section 4. This trend aligns with observed corrosion loss in these sections. Figure 36 presents the relationship between pavement infiltration rate and the minimum depth of strips not exceeding the design corrosion loss. The data show a strong correlation, with an R^2 value of 0.99, indicating that higher estimated pavement infiltration corresponds to deeper strips affected by excessive corrosion. This suggests that crack infiltration rate may serve as a useful indicator for assessing the likelihood of excessive corrosion, particularly in environments where moisture and salt intrusion through the pavement contribute to corrosion. However, it is important to note that the dataset for this study is limited, and these findings may not be directly applicable to other MSE walls, particularly those with different design and construction conditions.

5.3.6 Wisconsin Anti-icing and De-icing practices

Results from this study indicated that elevated chloride content was likely the main reason for the observed excessive corrosion loss of the reinforcing strips. Geocomp reviewed WisDOT Highway Maintenance Manual (HMM) to understand the level and frequency of snow and ice removal efforts by the state and how such efforts compare with collected data. Chapter 06, Section 15, subject 05 of HMM (HMM 06-15-05) outlines the level of effort that should be undertaken on the five different categories of roadway during a winter storm event. HMM discusses 5 categories, where category 1 is a major urban freeway with high traffic volume and category 5 is all other two-lane highways. In general, the level of effort for snow and

ice removal decreases from category 1 to 5, where category 1 has the highest effort with 24-hr maintenance of all lanes and ramps equally with extraordinary efforts if needed to remove snow, and category 5 receive 18-hr maintenance of only driving lanes and plow and sensible use of salting is recommended.

According to HMM 06-20-01, "*De-icing agents are used under appropriate winter maintenance conditions to: 1) prevent the formation of ice (anti-icing); 2) prevent the formation of a bond between accumulated snow, ice or slush and the pavement and keep the accumulation "plowable"; 3) de-ice, which is the melting of bonded ice or snow; and 4) keep abrasive material free flowing in freezing conditions*." The manual adds "*Anti-icing is best accomplished using direct liquid de-icing agent applications onto a dry roadway surface*".

HMA 06-15-55 states that "*Anti-icing should be conducted prior to forecasted frost, freezing fog, or black ice events on **bridge decks** and pavement trouble spots as a minimum, assuming conditions in this guideline*". HMM 06-20-20 provides guidelines for anti-icing application (Figure 37).

WisDOT confirmed that anti-icing of bridge decks and approach slabs is a common practice in most of counties. The anti-icing is in addition to de-icing efforts. Thus, the bridge and approach slabs receive more salt than the rest of the mainline. According to WisDOT, the main anti-icing agent is sodium chloride (salt) bring, applied at 40 gallons per lane mile, and at 2.29 lbs salt per gallon of brine. Milwaukee county commonly uses prewetted salt for de-icing application rate varying from 100-300 lbs/lane mile + prewetting at 8-10 gallon of brine per ton of salt. Calcium chloride is also used when temperatures drop for pre-wetting the rock salt at the 8-10 gallons of a 90% (NaCl brine)/10% (CaCl). The number of applications varies per year based on the number of events that happen.

The use of anti-icing specifically for bridge decks and approach slabs may explain the significant correlation found between distance from the bridge deck and corrosion loss in this study. The corrosion loss was much more severe in Geocomp excavation Section 1, which was next to the bridge deck and at the concrete approach slab compared to other sections further away from the bridge. Also, sodium chloride used for anti-icing and de-icing is known as one of the most aggressive de-icing agents in terms of corrosivity.

5.4 SUMMARY OF FINDINGS

- The reinforced backfill material across the excavation sections was relatively consistent, predominantly composed of poorly graded gravel.
- Backfill compaction varied with distance from the MSE wall, with material farther from the MSE wall being more compacted than that closer to the MSE wall. This variation in compaction, along with settlement and MSE wall rotation, likely contributed to the formation of longitudinal cracks in the shoulder pavement adjacent to the MSE wall.
- On average, backfill moisture content was highest in excavation Section 1. The average moisture content decreased with increasing distance from the bridge and decreasing MSE wall height.
- The average resistivity of the backfill, averaged across samples from each excavation section, was below the current AASHTO required limit in Sections 1 and 2.
- The average resistivity of backfill was highest Section 4. This section had minimal pavement cracks and joints and likely was not affected by moisture and salt intrusion.
- Chloride content was identified as the primary factor contributing to the low resistivity of the backfill.

- In highly corroded strips, nonuniform corrosion loss was considerably higher than the calculated uniform corrosion loss.
- With the exception of Section 4, where corrosion was minimal, corrosion loss generally decreased with increasing depth to reinforcement.
- Section 1 exhibited the most severe corrosion loss, with excessive corrosion extending to a greater depth (12.8 feet) compared to other sections.
- Although the study dataset was limited, there was a correlation between excessive corrosion loss and PCI, and excessive corrosion loss and pavement infiltration rate. Lower PCI values corresponded to increased cracking and joint formation in the pavement, greater moisture and salt intrusion, and deeper reinforcement straps affected by excessive corrosion loss.
- According to WisDOT, NaCl, a highly corrosive salt, is the primary de-icing agent used on WisDOT highways. Bridge decks and approach slabs may receive additional salt exposure compared to the mainline roadway due to anti-icing treatments. This likely contributed to the severe corrosion loss of reinforcing strips observed at Geocomp excavation Section 1, located underneath the approach slab.

6 REMAINING SERVICE LIFE OF THE STUDY MSE WALL

This chapter evaluates the service life of the studied MSE wall, assuming it was not demolished and remained in service. Section 6.1 compares the measured corrosion loss of the reinforcing straps to the anticipated corrosion loss using FHWA and AASHTO's recommended design corrosion rates. Section 6.2 calibrates an existing nonlinear corrosion predictive model to estimate future corrosion loss based on measurements taken during the investigation of the MSE wall. Section 6.3 integrates the design information, collected data, and predicted corrosion loss to estimate the remaining service life of the structure.

6.1 MEASURED AND DESIGN ESTIMATED CORROSION LOSS

As discussed in Section 2.2, the current practice relies on a simplified prediction model recommended by FHWA in 1990 and adopted by AASHTO to estimate corrosion loss of metal reinforcements over an MSE wall's service life. The design of MSE walls uses the predicted corrosion loss to determine the required sacrificial thickness of the metal reinforcements. The FHWA recommended corrosion loss predictive model estimates the maximum uniform corrosion loss of reinforcement over time and is based on two key assumptions:

1. The reinforced fill is classified as nonaggressive, meaning it satisfies the recommended electrochemical limits, and

2. the fill remains nonaggressive throughout the structure's service life.

For the MSE wall under study, data confirming whether the reinforced backfill was nonaggressive during its service life was not available. Laboratory testing by Geocomp on reinforcement samples taken after 32 years of service indicated that, on average, the reinforced backfill, did not meet the recommended electrochemical limits.

Geocomp applied the FHWA-recommended simplified corrosion loss prediction model to:

1. Estimate the expected corrosion loss after 32 years, assuming the fill was nonaggressive, and

2. compare the predicted corrosion loss with the actual corrosion loss measured in the reinforcements after 32 years.

Table 1 provides the FHWA's recommended corrosion loss prediction model. The corrosion loss estimation for the reinforcing straps requires baseline measurements of the thickness of uncorroded straps. Since this information was unavailable, measurements from visually uncorroded reinforcing straps were used to approximate the baseline thickness. These values are presented in Table 19. It should be noted that this approach may result in an underestimation of the original galvanized coating thickness. The average measured galvanized coating thickness was 0.33 mm, and the average bare metal thickness was 4.2 mm. Based on the corrosion loss prediction model, the estimated corrosion loss per side of the reinforcing strap over 32 years is 0.15 mm. This suggests that, had the reinforced fill met the FHWA recommended electrochemical limits throughout its 32 years lifespan, the maximum corrosion loss would have been less

than the galvanized coating thickness at the time of Geocomp's investigation. Figure 38 presents the measured uniform corrosion loss of reinforcement samples after 32 years in service, along with the corrosion loss values predicted by the FHWA's simplified model. A comparison of the measured and predicted values indicates that most samples from shallower depths in Sections 1 to 3 experienced corrosion loss significantly higher than the predicted values. The average fill resistivity in Sections 1 and 2 was below 3,000 ohm-cm, while Section 3 had an average fill resistivity slightly above 3,000 ohm-cm. Section 4 exhibited an average fill resistivity of 4,175 ohm-cm, exceeding the minimum resistivity recommended by the FHWA for a nonaggressive fill. The results presented in Figure 38 show that all reinforcement samples collected from Section 4 exhibited corrosion loss considerably lower than the predicted values. This suggests that the FHWA uniform corrosion loss predictive model likely provides a conservative estimate, assuming the fill remains nonaggressive throughout its service life. Since Section 4 was the section less likely affected by external factors such as salt intrusion, these findings suggest that the MSE wall backfill was likely nonaggressive as constructed and became aggressive due to salt intrusion throughout its service life.

6.2 CALIBRATED CORROSION PREDICTION MODEL

Geocomp used the exponential prediction model proposed by Romanoff (Equation 1) to estimate the corrosion loss over time. As discussed in Section 2.1.3, K and n in the model are soil- and site-dependent constants, with n being less than unity. FHWA proposed $n = 0.65$ for galvanized steel (Elias, et al., 2009). Geocomp adopted the proposed value for n and calculated K to calibrate the model based on field measurements collected during its investigation. The calibration aimed to match model predictions of corrosion loss to the average corrosion loss of reinforcing strips observed after 32 years of service. This calibration was performed individually for each row of reinforcements at specific depths (i.e., for each group of reinforcements exposed at a certain excavation lift). The model predicted corrosion loss on each side of the reinforcing strip for each year following construction. Geocomp utilized both uniform and non-uniform corrosion loss data to complete the calibration process. This was performed for reinforcements located in excavation Section 1, which was identified as the most critical section along the MSE wall in terms of corrosion loss.

Table 23 presents the calculated K values for reinforcements in lifts 1 through 5 of excavation Section 1, considering both uniform and non-uniform corrosion. Reinforcements in lift 6 exhibited little to no corrosion loss, with the galvanized coating appearing intact after 32 years in service. As a result, it was assumed that the corrosion loss in this lift would remain below the design sacrificial thickness over a 75-year service life. The calculated K values ranged from 18 to 96 for uniform corrosion and from 24 to 220 for non-uniform corrosion. For comparison, FHWA recommends $K = 25$ to estimate average corrosion loss of galvanized steel (Elias, et al., 2009). Additionally, FHWA suggests that non-uniform corrosion can lead to approximately twice the loss in tensile capacity relative to the average thickness loss, recommending $K = 50$ for estimating maximum corrosion loss.

A comparison between FHWA's recommended values and the calibrated value from this study indicates that the maximum K values obtained for uniform and nonuniform corrosion loss in this study were nearly four times the values suggested by FHWA model for average and maximum corrosion loss, respectively. The average K value for non-uniform corrosion loss was approximately twice the average K value for uniform corrosion loss. This is consistent with FHWA's findings, that loss in tensile strength capacity due to pitting is twice the loss relative to average thickness loss.

Geocomp applied the calibrated corrosion prediction model to estimate both uniform and non-uniform corrosion loss over the service life of the study MSE wall, focusing on excavation Section 1. Figure 39 and Figure 40 show corrosion loss per side of the reinforcing strip in excavation lifts 1 through 5 within Section 1 of the study MSE wall based on the uniform and nonuniform corrosion loss calculation, respectively. The corrosion loss values represent the reduction in thickness per side of each reinforcing strip, where a 100% loss indicates full depletion of the reinforcement's cross section. It is noteworthy that the model was calibrated based on a key assumption that the environmental conditions and backfill electrochemical properties would not change dramatically over time. For example, if corrosion loss or cracking of the pavement due to traffic loading dramatically promote the corrosivity of the backfill, the calibrated model may underestimate the corrosion loss in future. Also, there is inherent uncertainty in the model since the model was calibrated based on one measurement over the 32 years life of the reinforcements and data were not available to verify the evolution of the corrosion rate during this period.

The model predicts that uniform corrosion loss in lifts 1 through 3 will exceed half the original cross-sectional thickness (Figure 38). The maximum estimated uniform corrosion loss after the 75-year design service life is 1.6 mm per side. This is twice the maximum design sacrificial thickness for a 4-mm-thick galvanized strip, based on AASHTO's specified corrosion rates. the Figure 40 shows that non-uniform corrosion results in complete localized loss of reinforcing strips in lifts 1 through 4 within 42 to 65 years of service.

6.3 STABILITY ASSESSMENT OF THE STUDY MSE WALL

Geocomp evaluated the stability of the study MSE wall at the location of the excavation Section 1 of the Geocomp forensic investigation. The analyses were performed to evaluate overall slope stability, external stability, and internal stability of the MSE wall considering both uniform and nonuniform corrosion loss. The overall slope stability investigated "*all potential internal, compound and overall shear failure surfaces that penetrate the wall, wall face, bench, back-cut, backfill, and/or foundation zone*" per WisDOT Bridge Manual (2020). The internal stability evaluated pullout resistance and tensile capacity of the reinforcing strips at each reinforcement level. The external stability analyses evaluated the MSE wall stability against overturning, sliding, and bearing capacity failures in both the service and strength limit states. A deterministic approach which used the representative resistance values was used the perform overall slope, internal, and external stability considering both uniform and nonuniform cohesion losses. Geocomp also performed a probabilistic analysis to incorporate the actual distribution of the non-uniform corrosion loss measurements and estimates on the probability of failure of the structure. The following sections discuss the model geometry, input parameters, methods, and results for stability analyses.

6.3.1 Geometry

Geocomp determined the approximate MSE wall geometry at excavation Section 1 based on design drawings and measurements made during the forensic investigation. Section 1 was selected for the analysis because it was the tallest and had the largest corrosion loss. Figure 41 shows the base model for excavation Section 1.

Excavation Section 1 included six rows of reinforcement from top to bottom of the MSE wall. The horizontal spacing between the reinforcements in excavation Section 1 was variable through the depth and ranged from 1.45 feet to 2.50 feet center to center. Figure 42 shows the strip layout for Section 1. Figure 42 also shows the assigned lift number to each row of reinforcements. The vertical spacing between the reinforcements ranged between 2.30 feet to 2.60 feet. Figure 41 shows the distances between lifts for Section 1.

Geocomp applied a non-traffic uniform surcharge of 100 psf from the MSE wall face to 20 feet behind the MSE wall face and a uniformly distributed 240 psf traffic surcharge to the traffic lanes.

6.3.2 Soil Input Parameters

For its analysis, Geocomp used the Mohr-Coulomb failure criterion which is a widely used model in Limit Equilibrium Method (LEM) for assessing stability of retaining structures. This model defines the failure envelope as a linear relationship between shear strength (τ) and normal stress (σ), expressed as ($\tau = \sigma \tan(\varphi) + c$), where c is cohesion and φ is the internal friction angle.

Geocomp's laboratory testing indicated friction angles of 48° and 38° for the backfill material corresponding to dry densities one standard deviation above and below the mean dry density, respectively. Geocomp considered that the lower friction angle of 38° governs the critical slip surface and used this value in the stability analysis. It is noteworthy that the WisDOT Bridge Manual (2025) specifies a maximum allowable friction angle of 36° for the design of MSE wall backfills, regardless of higher values obtained from geotechnical testing. However, Geocomp's forensic evaluation was not aimed at designing the MSE wall but rather at assessing the stability of the structure under its current in-place conditions.

Geocomp modeled the MSE wall facing with a high cohesion value to prevent the slip surface from passing through individual MSE wall facing panels. The slip surface was only allowed to pass between the panels. Geocomp used a friction angle of 30^{o} for the retained soil per available soil boring data.

Table 24 summarizes the material properties used in Geocomp's stability analyses based on shop drawings, Geocomp forensic site investigation, WisDOT Bridge Manual (2020), and AASHTO recommendations.

6.3.3 Strip Input Parameters

The input parameters for the reinforcing strips included tensile strength, strip coverage area, and pullout resistance factor (F*). The horizontal coverage represented the percentage of the lateral area covered by reinforcing strips and was a function of their lateral spacing. The coverage area for each row of reinforcements in excavation Section 1 is presented in Table 25. According to the study Wall design drawings, the reinforcing strips were steel grade 65. The yield strength of steel grade 65 (T_n = 65 ksi) is used to calculate the tensile strength of uncorroded strips.

The tensile strength of the strips in each layer varied over time due to corrosion. The tensile capacity of reinforcing strips for a given year, from the initial construction of the MSE wall is dependent on corrosion loss. The loss of tensile capacity from the uncorroded condition was estimated based on percentage of estimated corrosion loss at a given year.

Geocomp calculated the pullout resistance factor, F*, in accordance with the guidelines in AASHTO and WisDOT Bridge Manual (2020). The F* was obtained based on the depth of embedment and default values provided in Figure 11.10.6.3.2-2 of the AASHTO specifications for ribbed steel reinforcement (Figure 43). Based on gradation tests on backfill material, the average Coefficient of Uniformity (C_u) for backfill material was 27. This resulted in a maximum F* value of 2. Table 25 presents the calculated F* for each row of the reinforcement.

6.3.4 Deterministic Stability Analysis

Geocomp's deterministic stability analyses included overall slope stability, and internal and external stability analysis of the MSE wall at the Wall Sta. 00+00 feet. The stability analyses were performed for different times within the service life of the MSE wall including:

- Initial construction,
- 32 years post-construction (demolition time),
- 37 years post-construction,
- 42 years post-construction, and
- 75 years post-construction.

Geocomp used Slide2 (2020) by Rocscience Inc. for the overall slope stability analyses. For internal and external stability analyses of the MSE wall, Geocomp used the software RSWall (2025) by Rocscience Inc.

Slide2 is a commercial software widely used by geotechnical practitioners for slope stability analyses including MSE wall analyses. Geocomp used the GLE-MP, Generalized Limit Equilibrium Morgenstern Price, method for determining the factor of safety (FS) using the Cuckoo search routine to generate potential non-circular slip surfaces. The overall slope stability analysis searched for any potential internal, compound, and external slip surfaces, according to the WisDOT Bridge Manual.

RSWall is a specialized software developed for the design and analysis of reinforced soil walls. RSWall can be used to perform bearing capacity, base sliding, overturning, pullout, and tensile strength stability analysis in accordance with standard specification such as AASHTO (2020). The software can perform stability analysis using load and resistance factors for service, strength, and extreme limit states. Table 26 shows the load and resistance factors for both service and strength limit states as per AASHTO (2020).

6.3.4.1 Uniform Corrosion Loss

Geocomp calculated uniform corrosion loss along each reinforcing strip at a given lift of excavation in the excavation Section 1. The uniform corrosion loss was averaged for strips at each lift to obtain the mean uniform corrosion loss for strips in a given lift of excavation. The mean uniform corrosion loss per lift was used to estimate the uniform corrosion loss at a given year within the service life of the MSE wall and evaluate its stability at excavation Section 1.

6.3.4.1.1 Overall slope stability

Geocomp performed overall slope stability for the MSE wall Sta. 00+00 feet in Slide2. The simulations were run for different times after construction to evaluate the potential effect of the corrosion loss on the stability of the MSE wall. The first set of analysis considered uniform corrosion loss of the reinforcing strips. It is noteworthy that based on the field observations, the corrosion loss was non-uniform, and the results presented in this section may provide an upper bound estimate of the stability of the MSE wall. Note that this approach may not be conservative, particularly in this study, where corrosion loss was determined to be nonuniform. Uniform corrosion assumes average section loss along the metal strips, whereas the tensile capacity of the reinforcements is more likely governed by nonuniform (maximum) corrosion loss along the strip.

The average uniform corrosion loss for each row of the strips at a given time after construction was determined as discussed in Section 6.1 of this report. The remaining tensile capacity for each row of the strips was calculated using the estimated corrosion loss. Geocomp assumed that the depletion of zinc

coating does not reduce the tensile capacity. The remaining tensile capacity was calculated having the tensile strength of uncorroded metal strips and calculating the remaining cross-sectional area after corrosion loss. Table 27 summarizes the average tensile capacity estimated for Section 1.

Figure 44 shows the trial slip surfaces for the simulated MSE wall section immediately after construction. The slope stability analysis yields a minimum factor of safety of 1.59. The slope stability analyses indicate that neither the factor of safety nor the shape of the slip surface would change in 75 years post construction, if uniform corrosion loss assumptions are used for the estimation of strips' tensile capacity.

6.3.4.1.2 Bearing capacity, Sliding, and Overturning – External Stability

Geocomp used RSWall to evaluate external instability of the MSE wall including bearing capacity, sliding, and overturning in both service and strength limit states. Bearing capacity failure occurs when the soil beneath the MSE wall cannot support the applied load, leading to excessive settlement or shear failure. Sliding failure happens when the entire MSE wall slides laterally due to insufficient friction or passive resistance between the MSE wall base and the foundation soil. Overturning failure occurs when the resultant force of lateral pressures causes the MSE wall to tilt or rotate forward about its toe.

RSWall calculates the Capacity-to-Demand Ratio (CDR) for each failure mode. A CDR less than 1 indicates inadequate capacity with respect to demand and potential failure of the MSE wall. Table 28 presents CDR values for the three modes of failure. The CDR is greater than 1, indicating adequate stability of the simulated section in both service and limit strength states for all three failure modes. It should be noted that the analysis of external stability is based on the assumption that the reinforced zone is internally stable. Therefore, the effect of corrosion loss on external instability of the MSE wall was not evaluated.

6.3.4.1.3 Pullout – Internal Stability

One failure mode of an MSE wall is pullout failure. Pullout failure occurs when one or more embedded strips are pulled out due to inadequate anchorage length or insufficient side resistance. This failure happens when the resisting force due to soil-reinforcement interaction is less than the applied tensile force, leading to the reinforcement being pulled out from the soil mass. The pullout resistance is dependent on the width and spacing of the reinforcements, among other factors. Geocomp considered that the corrosion loss reduced the thickness of the reinforcements and had negligible effect on the width. This was based on the observation and measurements of the corroded straps. Based on this, Geocomp considered that corrosion loss does not affect the pullout resistance of the metal strips. Accordingly, the pullout resistance was only calculated for right after construction, when the strips were not corroded.

Geocomp evaluated the CDR against pullout for reinforcements in rows 1 through 6 of the simulated section of the MSE wall. Table 29 summarizes the CDR for both service and strength limit states. Results showed a CDR below 1 for the first row of the reinforcement, for both service and strength limit states. This indicates that a localized pullout failure of the top panel of the MSE wall is likely. This aligns with Geocomp's field observation in which the top concrete facing panel was tilted and displaced approximately 4 inches outward as shown in Figure 45.

In the absence of project-specific data, Geocomp used AASHTO specified default values for F* to compute the CDR against pullout. Research has shown that, depending on type of backfill and embedment depth, AASHTO default F* values may be conservative. Specifically, Reinforced Earth Company (RECo) recommends higher values of F* than AASHTO default values (RECo, 2019) depending on type and properties of backfill material. Per RECo, a maximum value of F*= 4.0 may apply to the reinforced backfill of the study MSE wall. Using this value, the calculated CDR for service and strength limit states

are 1.34 and 0.89, respectively. This shows that even if the higher F* values are used, the pullout resistance would not meet the strength limit state CDR.

Geocomp review of MSE wall inspection reports indicate that the 4-inch displacement of top panel was reported in 2015. Also, Geocomp did not observe any tensile failure of the metal strips during its field investigation. These findings suggest that the observed 4-inch displacement was most likely caused by inadequate pullout resistance rather than by corrosion-related tensile failure.

6.3.4.1.4 Tensile Strength – Internal Stability

Tensile strength failure occurs when tensile stress with the reinforcing strips exceeds their capacity, leading to rupture or breakage of the strips. Geocomp assessed the internal failure due to tensile strength for both service and strength limit states. Table 30 summarizes the CDR at initial construction of the wall and after 75 years for both service and strength limit states. When uniform corrosion is assumed for the strips, the CDR is greater than 1, meaning the MSE wall would be internally stable in regard to tensile strength if uniform corrosion loss is considered to calculate the remaining tensile capacity.

6.3.4.2 Non-Uniform Corrosion

Geocomp calculated non-uniform corrosion loss along each reinforcing strip at a given lift of excavation in the excavation Section 1. The maximum non-uniform corrosion loss along each reinforcing strip was calculated, and the values were averaged for all strips within each lift to determine the average non-uniform corrosion loss per lift. Averaging the maximum losses was considered appropriate, as a potential slip surface in the event of instability would likely intersect multiple reinforcement strips rather than a single one. The resulting average non-uniform corrosion loss per lift was then used to estimate the corrosion loss at a given point in the MSE wall's service life and to evaluate the stability of the reinforcement in Excavation Section 1.

6.3.4.2.1 Overall Stability

Geocomp used the average non-uniform corrosion loss per lift to estimate the remaining tensile capacity of reinforcing strips. Table 31 represents the estimated ultimate tensile strength at different times after the MSE wall construction considering nonuniform corrosion loss.

Figure 47 and Table 32 show the factors of safety against overall slope stability for non-uniform corrosion loss models. The slope stability analyses show that the critical slip surface, which initially extends under and beyond the reinforcement strips except for lift 6, shifts toward the MSE wall and intersects with reinforcing straps as the top four strips lose their tensile strength. At 42 years after construction, the critical slip surface transitions into an internal slip surface, intersecting four reinforcing strips and passing through the intersection of the MSE wall facing panels (Figure 46). The factor of safety at this time reduces from 1.59 to 1.09. The FS further decreases to 0.74 when the MSE wall is 47 years post construction. Results indicate the failure of the MSE wall at excavation Section 1 would be likely within 10 to 15 years after its demolition (i.e., 42 to 47 years post construction), if it was still in service (Figure 47).

6.3.4.2.2 Tensile Strength – Internal Stability

Geocomp assessed the tensile strength internal failure at different times in relation to initial construction for both service and strength limit states. Table 33 and Table 34 summarize the CDRs at initial construction of the MSE wall, and after 32, 37, and 42 years for both service and strength limit states. The strips within lifts 2, 3, and 4 are likely to fail due to internal instability (CDR<1) after 42 years in service. The strength limit state analysis indicates that the design against internal stability would be unsatisfactory after 37 years of construction.

6.3.5 Probabilistic Slope Stability Analysis

6.3.5.1 Distribution Estimation

Geocomp conducted a probabilistic analysis of the MSE wall's overall slope stability. In this approach, all measured nonuniform corrosion loss data for each lift were considered to calculate the mean tensile strength and its standard deviation. Unlike the deterministic analysis, which only accounted for the maximum non-uniform corrosion loss averaged in each row of reinforcements to determine tensile capacity, the probabilistic analysis incorporated the distribution of measured nonuniform corrosion for all strips in a given row. Nonuniform corrosion loss was used in the analysis, as it dictates the tensile capacity of the reinforcements. The probability distribution of tensile capacity of reinforcements for each excavation lift is plotted in Figure 48. The only random variable in this analysis is the tensile strength of reinforcing strips.

The best distribution is fitted to the measured data using Kolmogorov-Smirnov test (KS test) method among Normal, Lognormal, Exponential, Gamma, and Beta distributions. The KS test was performed using the *kstest* function from the *scipy.stats* module in Python (SciPy Community, 2023). The KS test is a non-parametric statistical test that compares a sample dataset with a theoretical distribution. It measures the maximum difference between their cumulative distribution functions (CDFs). Based on the results of the KS test and the measured data, all lifts follow a Gamma distribution. It should be noted that, for lifts 5 and 6, substantial corrosion was not observed, and as such, Geocomp collected a limited number of samples. Therefore, a coefficient of variation (COV) of 5% was assumed for these lifts, which is considered reasonable based on the Geocomp field observations. Figure 48 shows that the tensile strength ranges from a maximum of 128,669 lb/ft to a minimum of zero lb/ft, corresponding to 0% and 100% corrosion loss, respectively.

Geocomp used the predictive model discussed in Section 6.2 of this report to estimate the distribution of non-uniform corrosion loss after different times after construction. For this purpose, Geocomp estimated the mean value for nonuniform corrosion loss of reinforcing strips at each lift and considered that the standard deviation remains the same. This is based on Geocomp's previous experience on another similar project in Utah. Geocomp's years of data collection in terms of both corrosion rate and corrosion loss indicated that it is reasonable to assume that standard deviation remains constant when estimating corrosion loss in time. Table 35 presents the calibrated values of n and K for each lift and the calculated corresponding tensile strength at different years.

6.3.5.2 Service Life Prediction Using All Measured Data

The input tensile strength is not factored by 0.75 as it is for allowable tensile strength, since the goal is to estimate the Probability of Failure (PF) at service life without any consideration of a reduction factor, and all possible tensile strength can be captured within the sampling of the distribution. Geocomp used Latin Hypercube Samling (LHS) with 10,000 samples for simulation. The corresponding PF is presented in Table 36 for each year after the MSE wall construction. While AASHTO does not specify a maximum PF for designing MSE walls, it indicates that "*past geotechnical design practice has resulted in an effective reliability index, β, of 3.0, or an approximate probability of a failure of 1 in 1,000, for foundations in general, and for highly redundant systems, such as pile groups, an approximate reliability index, β, of 2.3, or an approximate probability of failure of 1 in 100*". Geocomp's deterministic analysis indicated that the critical slip surface in a failure due to corrosion will be internal and a global failure of the MSE wall is not expected. As such, a PF = 1% may be appropriate for the probabilistic evaluation of service life of

the MSE wall considering corrosion loss at excavation Section 1. The MSE wall at Section 1 would have a PF greater than 1% after approximately 55 years of service, if it was still in service. This indicates that the MSE wall would have reached the end of its service life approximately 23 years after the demolition.

6.4 SUMMARY OF FINDINGS

Geocomp concludes:

- In excavation sections 1, 2, 3, and 5, the measured uniform corrosion loss of shallow reinforcing strips exceeded the AASHTO-estimated sacrificial thickness for an MSE wall in service for 32 years and constructed using nonaggressive fill.
- All reinforcing strips in Section 4 exhibited uniform corrosion loss significantly lower than the current design-estimated sacrificial thickness.
- Excessive corrosion loss extended to greater depths in excavation Section 1 than Section 2 and 3.
- The initial design of the MSE wall has an overall slope stability FS of 1.59. This FS remains constant when uniform corrosion is considered along the strips until the service life of the MSE wall (75 years).
- When the non-uniform corrosion loss is considered along the strips, the overall slope stability FS drops to 1.3 after 37 years, and further decreases to 1.0 after 40 years. The overall slope stability FS finally reaches a calculated value of 0.74 at 47 years of service.
- The first row of the reinforcing strips was likely under-designed or under-constructed against pullout capacity. Geocomp infers that the 4-inch outward movement of the MSE wall's top facing panel immediately next to the bridge abutment was most likely due to pullout failure.
- When Geocomp considered the nonuniform corrosion loss distribution corrosion within the strips, it estimated that the MSE wall would reach a target PF of 1% in approximately 55 years.
- The probabilistic analysis using the actual distribution of the corrosion loss can provide a robust framework to evaluate the remaining service life of the structure for a specific risk tolerance. This can help avoid using the conservative scenario of maximum non-uniform corrosion, which may result in underestimating the remaining service life of the structure.

7 CONCLUSIONS AND RECOMMENDATIONS

7.1 CONCLUSIONS

Geocomp conducted an evaluation of the corrosion affecting the reinforcing strips of a 32-year-old MSE wall in Wisconsin by performing field and laboratory tests in five excavation sections and documenting the condition of the reinforcing strips. The study's findings emphasize the critical impact of pavement distress, as well as moisture and salt intrusion, on the deterioration of MSE wall reinforcements. Field investigations revealed that water and salt intrusion infiltration through pavement cracks and joints likely altered the backfill electrochemical properties over time, creating a highly corrosive environment. Geocomp's excavations uncovered significant corrosion loss in the reinforcing strips and elevated chloride levels in the backfill.

Geocomp evaluated the design features of the study MSE wall that were likely to facilitate corrosion loss. The studied MSE wall extended from a bridge at its southern end and its height decreased to the north. The pavement cross slope along the MSE wall and bridge was crowned, directing surface water toward the MSE wall reinforced zone. The southernmost section of the MSE wall featured a concrete approach slab with multiple joints, including two 2-inch expansion joints, which likely facilitated moisture penetration into the reinforced backfill. The design did not include an impervious layer, such as a geomembrane, to mitigate water intrusion. Furthermore, the MSE wall replaced an existing sloped embankment, with the embankment fill forming the retained zone. Geocomp's laboratory testing indicated that the retained soil had relatively low resistivity and high chloride content. Flow of salts from the retained to the reinforced zone could, in principle, increase the corrosivity of the reinforced fill. However, no clear evidence of this mechanism was observed in this study. For instance, if retained fill had a significant impact, higher corrosion losses would be expected near the ends of the reinforcement strips adjacent to the retained zone, but such a pattern was not observed. Notably, the granular reinforced backfill extended at least 3 to 4 feet beyond the free ends of the strips in the study MSE wall, which likely mitigated contamination from the surrounding clayey fill in the retained zone.

Geocomp investigated five forensic excavation sections (1-5). Sections 1-4 extended to the MSE wall's base, with Section 1 adjacent to the bridge abutment. MSE wall height decreased and distance from the bridge increased from Section 1 to 4. Section 5 was a shallow trench between Sections 1 and 2. Significant and highly variable corrosion loss, characterized by pitting corrosion, was observed on the reinforcing straps in Sections 1, 2, 3, and 5. The pitting corrosion indicated a likelihood of corrosion loss through salt attack.

Geocomp's investigation found that corrosion severity was highest in sections closer to the bridge, where the MSE wall was taller, and decreased with reinforcement depth and distance from the bridge. This trend corresponded with pavement distress severity, moisture content, and fill corrosivity measured by soil resistivity. In general, greater pavement distress, higher moisture content, and more corrosive fill correlated with deeper straps experiencing excessive corrosion. While average soil resistivity of each excavation section appeared to be correlated with severity of corrosion loss of strips within that excavation section, the resistivity of soils at a given depth showed no significant correlation with the corrosion loss of strips at that depth. This is likely due to temporal and spatial variation of soil resistivity. This would challenge field investigations to evaluate corrosion loss by only measuring the electrochemical properties of the soil.

Section 4 had the least corrosion, with an almost intact galvanized coating, minimal pavement cracks, and higher-than-minimum average backfill resistivity. In contrast, Section 1 exhibited the most severe corrosion, with heavily corroded strips extending to a depth of approximately 13 feet.

Several key design and construction differences in Section 1 likely contributed to its excessive corrosion:

1. It was the section with the lowest PCI (i.e., highest pavement cracks and joints) for the paved traffic lane and shoulder near the MSE wall.

2. The bridge and abutment pavement sloped toward this section, directing surface water runoff toward the reinforced zone.

3. The approach slab in this section included two 2-inch transverse expansion joints and multiple concrete joints that extended over the reinforced zone.

4. A highly permeable layer of open-graded crushed stone beneath the pavement likely facilitated water infiltration from joints and cracks into the reinforced fill.

5. According to WisDOT, bridge decks and approach slabs are likely to receive more salt due to anti-icing treatments applied before freezing events. This is in addition to de-icing salts used during freezing conditions. The anti-icing salts are usually in liquid form with high mobility, allowing it to infiltrate more easily into the backfill through the pavement cracks and joints.

Geocomp's data and analysis showed higher moisture content in this section than in others. The average chloride content and minimum backfill resistivity did not meet current design electrochemical thresholds, indicating that moisture and salt intrusion likely contributed significantly to the severe corrosion loss of the reinforcing strips in Section 1.

A comparison of measured corrosion loss with expected values for reinforcing strips in nonaggressive fill showed that shallow strips in Sections 1, 2, 3, and 5 had significantly higher corrosion loss than anticipated over the 32 years of service. Geocomp estimated that the top three rows of reinforcing strips in Section 1, extending to a depth of 7.8 feet, would completely corrode within 50 years of service.

Geocomp performed deterministic and probabilistic stability analyses for the MSE wall at Section 1. The deterministic analysis, incorporating average non-uniform corrosion loss per row of strips, showed that while the original design had an adequate factor of safety against slope stability, corrosion would reduce it below 1.3 within approximately 40 years, leading to internal failure if the MSE wall remained in service. The probabilistic analysis, which considered the distribution of corrosion along strips rather than a mean value, indicated a failure probability exceeding 1% after 55 years. Both analyses confirmed that internal failure was likely within the design service life. Geocomp's findings suggested that a probabilistic approach provides a risk-based tool for cost-effective management, whereas the deterministic method may be more conservative.

7.2 RECOMMENDATIONS FOR DESIGN AND CONSTRUCTION

Geocomp's findings indicated that the sections of the MSE wall least affected by the external environment, such as Section 4, exhibited minimal corrosion. This suggests that FHWA recommendations for reinforcing strip sacrificial thickness will be adequate if:

1. The backfill is designed to be non-aggressive in accordance with the electrochemical limits specified by FHWA/AASHTO.
2. The reinforcing elements are galvanized in accordance with WisDOT requirements, and the design sacrificial thickness is calculated using AASHTO's simplified method.
3. The backfill remains non-aggressive throughout the service life of the MSE wall.

Since the late 1980s, FHWA and AASHTO guidelines and specifications have incorporated and enforced points 1 and 2 in MSE wall design. However, earlier design specifications lacked provisions to ensure that reinforcements remain in non-aggressive conditions throughout their service life. Additionally, there are no established guidelines for designing reinforcements in aggressive fills to account for corrosion loss.

Geocomp had access to the 2001, 2020, and 2025 WisDOT Bridge manuals. The 2001 WisDOT Bridge Manual did not include provisions to maintain non-aggressive conditions in reinforced backfill or to design for aggressive fills. In 2001, FHWA guideline acknowledged the potential change in backfill corrosivity in certain environments, stating:

"*For permanent structures directly supporting roadways exposed to deicing salts, limited data indicate that the upper 2.5 m (8 feet) of the reinforced backfill (as measured from the roadway surface) are affected by higher corrosion rates not presently defined*" (Elias, et al., 2001).

The FHWA guideline (Elias, et al., 2001) recommends designing an impervious membrane between the pavement base and reinforced backfill to mitigate the intrusion of deicing salts into the reinforced backfill. This is reflected in the recent WisDOT Bridge Manuals, including both 2020 and 2025 editions. WisDOT Bridge Manual indicates that in aggressive environments "*MSE walls with steel reinforcement should be protected with a properly designed impervious membrane layer below the pavement and above the first level of the backfill reinforcement*". The manual states "*Aggressive environments in Wisconsin are typically associated with salt spray and areas near stormwater pipes in urban areas*".

Current practice does not offer methodologies for estimating the corrosion rates of reinforced elements in fills that do not meet electrochemical criteria throughout their service life. Many MSE walls were constructed before salt intrusion mitigation measures were required, and current design guidelines do not establish performance criteria to ensure the long-term effectiveness of salt intrusion mitigation systems.

Based on the findings of this study, Geocomp recommends:

1. Use non-aggressive fills in the reinforced zone according to FHWA electrochemical criteria and estimate sacrificial thickness using the FHWA simplified model for non-aggressive fills.
    a. Based on findings that the recommended sacrificial thickness is likely conservative if the backfill remains non-aggressive throughout its service life.
2. If possible, design the pavement cross slope and manage the surface water to ensure it flows away from the reinforced zone and not into the reinforced zone.
    a. Excessive corrosion loss was found to be inversely related to backfill moisture content.
    b. Design and construction practices should ensure uniform compaction of the backfill both near and farther from the MSE wall to minimize differential settlement in fill. Differential settlement in fill can cause pavement cracks on top of the MSE wall.

3. Implement impervious membranes and drainage systems according to WisDOT bridge manual to mitigate the intrusion of de-icing salts and chemicals into the reinforced backfill, or else suitable alternatives to impervious membranes and drainage systems.
    a. Moisture and salt intrusion was found as main factors causing excessive corrosion.
4. WisDOT may explore an alternative approach to the impervious membrane, such as placing a non-aggressive, low permeability engineered fill between the top of the first row of reinforcements and the pavement to serve as a moisture intrusion barrier. This requires detailed backfill and drainage design.
5. WisDOT may consider designing a dedicated drainage system for the bridge and its approach slab to prevent water infiltration into the backfill or retained zone. This system could include impervious barriers designed to keep the water away from reinforced backfill and channel it towards designated drainage paths.
    a. The study found several cracks and pavement joints in these areas.
    b. These areas likely receive more salt due to application of anti-icing.
    c. The most severe corrosion loss was found in the excavation section within these areas.
6. If moisture and salt intrusion into the reinforced backfill is expected, the FHWA simplified corrosion rates may not be applicable. The design should account for higher corrosion rates and increased sacrificial thickness for reinforcements at least 13 feet deep from the pavement surface.
    a. Corrosion loss of strips in excavation sections affected by moisture and salt intrusion exceeded the sacrificial thickness estimated by FHWA simplified model.
7. The non-uniform corrosion rates estimated in this study may be used for assessing corrosion loss in non-aggressive fills that become aggressive through de-icing salt intrusion. However, caution is needed as non-uniform corrosion rates can vary significantly and be hard to predict.
8. In the absence of other design modifications, the upper rows of reinforcement straps are more exposed to excessive corrosion. Increasing the sacrificial thickness of these upper reinforcement rows could extend the service life of the MSE wall.
    a. The corrosion loss was found to be, in general, more significant in shallower depths.
9. Consider installing test coupons at multiple depths and locations along the MSE wall during construction to evaluate corrosion loss throughout the structure's service life to develop project specific and localized design methods and/or predict remaining life.
10. Consider developing instrumentation specifications to monitor the rate of corrosion loss of select strips using methods such as Linear Polarization Resistance (LPR). The select strips are expected to have higher exposure to corrosion based on findings from this study. The measurements would assist in verifying whether or not the actual rate of corrosion loss exceeds the design rate and predicts remaining life so maintenance and replacement can be planned and programmed.

7.3 RECOMMENDATIONS FOR MAINTENANCE OF MSE WALL SUPPORTED PAVEMENTS

Findings from this study indicate a correlation between the severity of corrosion loss and pavement cracks and joints near the top of the MSE wall. Geocomp's 2023 site visit, along with a review of historical road images from 2002 provided by WisDOT, suggests that WisDOT routinely maintained the I-43 pavement by sealing cracks and concrete joints on the traffic lanes. However, many cracks and joints within the

pavement shoulder, located between the traffic barrier and the MSE wall, directly above the reinforced zone, were not sealed.

Additionally, there is no data confirming that the maintenance was both timely and effective in preventing salt intrusion into the reinforced zone. For example, expansion joints on the bridge approach slab may lose their sealing due to repeated expansion and contraction. Notably, pavement contraction (i.e., increased joint opening) coincides with the application of deicing salts in winter, potentially exacerbating salt intrusion into the backfill.

Based on the findings of this study, Geocomp recommends the following to reduce corrosion rates:

1. Regularly maintain pavement surfaces and drainage structures associated with MSE walls reinforced with metallic elements to prevent moisture and salt intrusion. It is recommended to schedule annual maintenance and repairs to be completed prior to the onset of winter.
    a. Cracks and joints were found to be major contributors to corrosion.
2. Give special attention to pavement directly above the reinforced zone, ensuring all cracks and concrete joints are routinely sealed to effectively prevent water and salt intrusion infiltration.
    a. This area showed less maintenance despite its direct effect on the reinforced backfill condition.
3. WisDOT may consider using less corrosive de-icing salts, such as calcium magnesium acetate, on MSE wall-supported pavements. A list of qualified corrosion-inhibited agents with their effectiveness is provided by the Clear Road research program.
    a. Sodium chloride, widely used by WisDOT, was found to be strongly linked to excessive corrosion.

7.4 RECOMMENDATIONS FOR ASSET MANAGEMENT OF EXISTING MSE WALL SYSTEMS

Geocomp recommends that WisDOT consider initiating a risk-based asset management program to identify MSE walls potentially subject to excessive corrosion. The objectives of this program are to:

1. Collect an inventory of the MSE walls with risk of failure due to corrosion,
2. validate the applicability of the findings from this study to other MSE walls, and
3. supplement the data from this study with additional relevant information and update the risk-based framework.

In 2018, Geocomp developed a risk-based protocol for the asset management of MSE walls (hereafter referred to as “Geocomp risk-based protocol”) (Govindasamy, et al., 2018). The qualitative risk-based protocol results in an index that describes the risk associated with the failure of a given MSE wall. This risk index, which combines the effect of vulnerability and consequence of MSE wall failure, can be used to prioritize MSE walls within an asset inventory and optimize the time and effort needed to manage this inventory by focusing attention on relatively high-risk structures. MSE walls with high and very high risk levels are shortlisted for risk mitigation strategies. These risk mitigation strategies include performing further investigative studies to determine MSE wall service life, implementation of site-specific risk monitoring programs, and implementation of rehabilitation measures.

The key variables used in the qualitative risk-based protocol are Condition States, Performance States, Vulnerability, Consequence, and Risk. The Condition states are characteristics that pertain to the quality of design and construction of structures and can be determined by a desk study. Performance states are characteristics that pertain to the in-service performance of structures. The performance states can be determined by a field reconnaissance study. Vulnerability is an indicator of the likelihood (probability) of the MSE wall failing. Consequence is an indicator of the impact of MSE wall failure, where failure represents the condition when Ultimate Limit State is reached. Risk is a measure that combines vulnerability and consequence, i.e. it combines how likely it is an MSE wall will fail and what level of undesirable impact will arise from that failure.

MSE walls potentially experiencing excessive corrosion loss can benefit from a field reconnaissance to collect data, a subsurface exploration to supplement data, and a study to develop an inspection and maintenance program for existing MSE walls. Data from this study indicated that corrosion loss severity correlated with proximity to the bridge, pavement distress, moisture content, and average resistivity of backfill in excavation section. This information will be used to guide the preliminary evaluation and field investigation efforts to locate reinforcements with excessive corrosion.

7.4.1 Condition states from desk studies

Condition states are characteristics that pertain to the quality of design and construction of structures. These characteristics may affect MSE wall performance but are not a direct result of MSE wall response to loading or its environment. As an example, an MSE wall that has not exhibited any signs of distress could still be assigned a poor condition state if it was constructed with poor backfill or reinforcement. Checklists provided in Figure 11 through Figure 14 of Geocomp's risk-based protocol can be used to assess the component condition state indicators that are specific to the following MSE wall components, respectively: (a) Reinforced backfill; (b) Structural metallic components (reinforcements, facings, and facing connections); (c) Drainage; and (d) Other MSE wall components (foundation, non-metallic facing, utilities, and surroundings). Each component condition state indicator is assigned one of the following three levels of severity: poor, marginal, and good (Govindasamy, et al., 2018).

Based on experience from this study, an MSE wall with the following characteristics should be categorized as poor with respect to drainage conditions:

- The reinforced backfill is not protected against deicing salt intrusion by an impervious layer,
- The MSE wall extends from a bridge and includes a concrete bridge approach slab, and
- The pavement section directly above or near the reinforced zone of the MSE wall consists of concrete slabs with joints.

7.4.2 Performance states from field investigations

Performance states are characteristics that pertain to the in-service performance of structures. These characteristics are a direct result of MSE wall response to loading and/or its environment. Examples of performance states of MSE walls include excessive deformations, bulging of the MSE wall face, and broken reinforcements. Checklists in Figure 17 through Figure 20 of the Geocomp risk-based protocol can be used to assess the component performance state indicators that are specific to the following individual MSE wall components, respectively: (a) Reinforced backfill; (b) Structural metallic components (reinforcements, facings, and facing connections); (c) Drainage; and (d) Other MSE wall components (foundation, non-metallic facing, utilities, and surroundings). Each component performance state indicator

is assigned one of the following three levels of severity: unfavorable, neutral, and favorable (Govindasamy, et al., 2018).

The field investigation may include a subsurface exploration. Based on the experience from this study, the following items should be considered as a guide for subsurface exploration:

- The subsurface exploration should be performed when there is considerable pavement cracks and joints that facilitate salt intrusion and there is no impervious layer to protect backfill against salt intrusion. In such cases, "other MSE wall components" conditions shall be considered as unfavorable.
- Pavement condition index (PCI) may be used to evaluate the significance of pavement cracks. It is recommended that:
    - PCI be calculated for the traffic lane and pavement shoulder near and on top of the MSE wall reinforced zone.
    - Lowest PCI during the service life of the structure be calculated.
    - PCI be calculated for no more than 50 feet intervals along the MSE wall.
    - PCI calculations exclude the distresses that are not contributing to or not indicative of corrosion loss, such as AC raveling.
    - This study indicated that sections with PCI values less than approximately 75 had reinforcements with excessive corrosion loss.
- The subsurface exploration should be conducted in locations susceptible to water intrusion. These include locations covered with concrete pavements with joints extending within the reinforced zone and locations with significant pavement cracks.
- The subsurface exploration may be performed by soil borings from the top of the MSE wall pavement, trench excavation, or coring through the MSE wall facing.
- In case the backfill consists of gravelly soil, soil sampling may not be possible through soil boring using a conventional split spoon sampler. Alternatives include an oversized split spoon sampler, recovery of auger cuttings, or a test pit.
- Backfill samples should be collected at multiple depths and distances from the MSE wall facing.
- In case of limited resources, a shallow test pit uncovering the first row of the reinforcement may be excavated to collect samples and observe the reinforcement conditions. The location of the trench excavation should be selected where excessive corrosion loss is anticipated per findings in this study.
- Corrosion loss of reinforcements should be measured, at the minimum, in locations where the average soil resistivity is less than 3000 ohm-cm. Data from this study showed less than expected corrosion loss in Section 4, where average minimum resistivity was slightly over 4000 ohm-cm.
- If the maximum corrosion loss exceeds the design sacrificial thickness for the service life of the structure, the corrosion should be considered severe.

7.4.3 Risk analysis

The risk analysis is performed by vulnerability and consequence analyses. Within the risk-based protocol, vulnerability is a measure that combines the overall condition state and overall performance state to obtain an index that represents the potential for the MSE wall to reach its ultimate limit state. Consequence is an indicator of the impact of MSE wall failure, where failure represents the condition when Ultimate Limit

State is reached. In the risk-based protocol, risk is a measure that combines vulnerability and consequence, i.e., it combines how likely it is an MSE wall will fail and what level of undesirable impact will arise from that failure. The outcome of the investigation will be a risk state for each MSE wall. Risk is characterized into five states: very low, low, medium, high, and very high. MSE walls with high and very high risk levels are those whose risk level is sufficient that they require immediate attention.

7.4.4 Asset management

MSE walls with high and very high risk levels require further investigative studies. This approach involves the collection of more information about the condition states and performance state to revise the risk assessment. This investigation program may include test pits, borings, soil sampling, reinforcement sampling, and field and laboratory testing. It might result in undertaking work to predict the remaining service life of an MSE wall using quantitative methods. It involves the determination of the corrosion rate of structural metallic components (reinforcements, facings, and facing connections) as well as the corrosivity potential of reinforced and retained backfill via a prioritized investigation program. Collected data should be used to improve the condition assessments and ratings in previous sections.

If the predicted remaining service life determined from the further investigative studies is inadequate, rehabilitation measures should be taken to ensure that the MSE wall has sufficient service life. Alternatively, a site-specific risk monitoring program can be implemented. This approach involves the development and execution of a site-specific risk monitoring program which could include MSE wall instrumentation and monitoring as well as more frequent MSE wall inspections. Risk monitoring might be used to defer expensive remediation work until the measurements indicate that such work is clearly needed. If the predicted service life is adequate, the MSE wall should be re-assessed using the qualitative risk-based protocol within a period of 5 years.

7.4.5 Update condition and performance assessment protocols

The collected data should be used to verify and supplement findings in the current study. Specifically, the new findings should be used to guide and improve the condition state and performance state assessment methods and ratings to characterize the risk. Analysis should be done to evaluate the rate of corrosion loss of MSE walls and calibrate predictive models to estimate corrosion loss. Data in this study indicated that soil resistivity, when averaged for samples taken from an excavation section, can be used as an indicator of excessive corrosion loss. Also, the pavement cracks and joints correlated with observations of excessive corrosion loss. However, these observations pertained to one MSE wall with set conditions and performance. A comprehensive dataset is required to develop a reliable risk and asset management effort to include a wide variety of indicators and direct the level of maintenance of existing MSE walls.

7.5 RECOMMENDATIONS FOR FUTURE RESEARCH

Geocomp identified limitations in the current body of work and available literature, primarily due to the limited and non-uniform data collection methods. To address these gaps, Geocomp recommends that WisDOT take advantage of opportunities to collect corrosion-related data from additional MSE walls using the procedures applied to this work to refine our findings and recommendations.

1. For existing MSE walls scheduled for demolition, WisDOT can establish a standard specification for wall deconstruction. This would require collection of data on deconstruction of existing MSE walls, such as uniform corrosion loss and backfill electrochemical properties. Developing a consistent and cost-effective database over time would significantly improve understanding of

corrosion trends. Additionally, WisDOT should conduct pre-demolition condition evaluations, including collecting design and construction records, performing PCI calculations, and inspecting the MSE wall facing and supported pavement. By implementing these measures, WisDOT could build a comprehensive corrosion dataset at minimal cost with time. To the extent such a specification can be shared and co-developed with other DOTs this will assist even more with expanding our understanding of corrosion and how to better control it.

2. For new MSE wall construction, WisDOT can develop a long-term data collection program to assess the MSE wall performance, including corrosion rates, backfill electrochemical properties, and pavement and MSE wall conditions. This could involve instrumentation for monitoring moisture and oxygen levels, as well as measuring corrosion rate changes using techniques such as Linear Polarization Resistance (LPR) or manually by extracting coupons and measuring corrosion. Long-term data collection would eliminate uncertainties caused by temporal variations in backfill properties and corrosion loss, ultimately supporting the development of more reliable and effective corrosion-resistant design strategies.

8 REFERENCES

AASHTO, 1992. Standard Specifications for Highway Bridges. Washington, DC.

AASHTO, 1996. Standard Specifications for Highway Bridges. Washington, DC.

AASHTO, 2002. Standard Specifications for Highway Bridges. Washington, DC.

Blight, G. E. & Dane, M. S. W., 1989. Deterioration of a wall complex constructed of reinforced earth. *Géotechnique.*

Elias, V., 1990. Durability/Corrosion of Soil Reinforced Structures.

Elias, V., 2000. Corrosion/Degradation of Soil Reinforcements for Mechanically Stabilized Earth Walls and Reinforced Soil Slopes.

Elias, V., Christopher, B. R. & Berg, R. R., 2001. Mechanically Stabilized Earth Walls and Reinforced Soil Slopes Design and Construction Guidelines.

Elias, V., Fishman, K. L., Christopher, B. R. & Berg, R. R., 2009. Corrosion/Degradation of Soil Reinforcements for Mechanically Stabilized Earth Walls and Reinforced Soil Slopes.

Govindasamy, A. V., Marr, A., DiMaggio, J. & Morsy, A., 2018. *Risk-Based Protocol for Asset Management of Metallically Reinforced Mechanically Stabilized Earth Walls.* Louisville, KY, The 49th Annual Southeastern Transportation Geotechnical Engineering Conference.

MDOT, Michigan Department of Transportation, 2019. *MDOT Bridge Design Manual,*.

NAE, 2023. Corrosion of Buried Steel at New and In-Service Infrastructure. *National Academies of Sciences, Engineering, and Medicine.*

NCHRP Project 24-28, 2011. LRFD metal loss and service-life strength reduction factors for metal-reinforced systems.

NYSDOT, State of New York Department of Transportation: Geotechnical Engineering Bureau, 2020. *Geotechnical Engineering Manual: Mechanically Stabilizied Earth System Inspection Manual (GEM-16).*

PennDOT, Pennsylvania Department of Transportation, 2019. *Design Manual Part 4 (DM-4) guidance*.

RECo, 2019. Pullout Resistance and Apparent Coefficient of Friction (f*) of High Adherence (HA) Reinforcing Strips In AASHTO MSE Backfill. *Tech Bulletin.*

Ridgeway, H., 1976. Infiltration of water through the pavement surface Transportation. *Research Record No. 616. Transportation Research Board. Washington, D.C.*

Timmerman, D., 1990. Evaluation of Mechanically Stabilized Embankments as Support. *Ohio Department of Transportation Interim Research Report.*

WisDOT, 1996. WisDOT Bridge Manual, Chapter 14 - Retaining Walls.

WisDOT, 2025. WisDOT Bridge Manual, Chapter 14 - Retaining Walls.

APPENDIX A: FIGURES

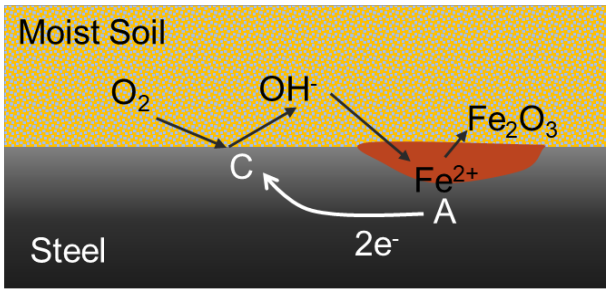

Figure 1. Electrochemical reactions involved in the corrosion of iron.

State	Description	References
California	Have been installing inspection elements with new construction since 1987, and performing tensile strength tests on extracted elements. Some electrochemical testing of in service reinforcements and coupons has also been performed. LPR and EIS tests were performed on inspection elements at selected sites as part of NCHRP Project 24-28 and results compared with direct physical observations on extracted elements.	Jackura et al. (1987), Elias (1990), Coats et al. (1990), Coats et al. (2003- Draft Report)
Florida	Program focused on evaluating the impact of salt-water intrusion, including laboratory testing and field studies. Coupons were installed and reinforcements were wired for electrochemical testing and corrosion monitoring at 10 MSE walls. Monitoring has continued since 1996.	Sagues et al. (1998, 1999, and 2000), Berke and Sagues (2009)
Georgia	Began evaluating MSE walls in 1979 in response to observations of poor performance at one site located in a very aggressive marine environment incorporating an early application of MSE technology. Exhumed reinforcement samples for visual examination and laboratory testing. Some in situ corrosion monitoring of in service reinforcements and coupons at twelve selected sites using electrochemical test techniques was also performed.	McGee (1985), Deaver (1992)
Kentucky	Developed an inventory and performance database for MSE walls. Performed corrosion monitoring including electrochemical testing of in service reinforcements and coupons at five selected sites.	Beckham et al. (2005)
Nevada	Condition assessment and corrosion monitoring of three walls at a site with aggressive reinforced fill and site conditions. Exhumed reinforcements for visual examination and laboratory testing; performed electrochemical testing on in service reinforcements and coupons. A total of 12 monitoring stations were dispersed throughout the site providing a very good sample distribution.	Fishman et al. (2006)
New York	Screened inventory and established priorities for condition assessment and corrosion monitoring based on suspect reinforced fills. Two walls with reinforced fill known to meet department specifications for MSE construction are also included in program as a basis for comparison. Corrosion monitoring uses electrochemical tests on coupons and in service reinforcements.	Wheeler (1999, 2000, 2001, 2002a and 2002b)
North Carolina	Initiated a corrosion evaluation program for MSE structures in 1992. Screened inventory and six walls were selected for electrochemical testing including measurement of half-cell potential and LPR. This initial study included in service reinforcements but coupons were not installed. Subsequent to the initial study, NCDOT has installed coupons and wired in-service reinforcements for measurement of half-cell potential on MSE walls and embankments constructed since 1992. LPR testing was also performed at approximately 30 sites in cooperation with NCHRP Project 24-28.	Medford (1999)
Ohio	Concerned about the impact of their highway and bridge deicing programs on the service life of metal reinforcements. Performed laboratory testing on samples of reinforced fill but did not sample reinforcements or make insitu corrosion rate measurements	Timmerman (1990)
Oregon	Preliminary study including 1) a review of methods for estimating and measuring deterioration of structural reinforcing elements, 2) a selected history of design specifications and utilization of metallic reinforcements and 3) listing of MSE walls that can be identified in the ODOT system.	Raeburn et al. (2008)

Figure 2. Summary of state DOT MSE wall corrosion assessment programs provided in 2009 FHWA guideline (Elias, et al., 2009).

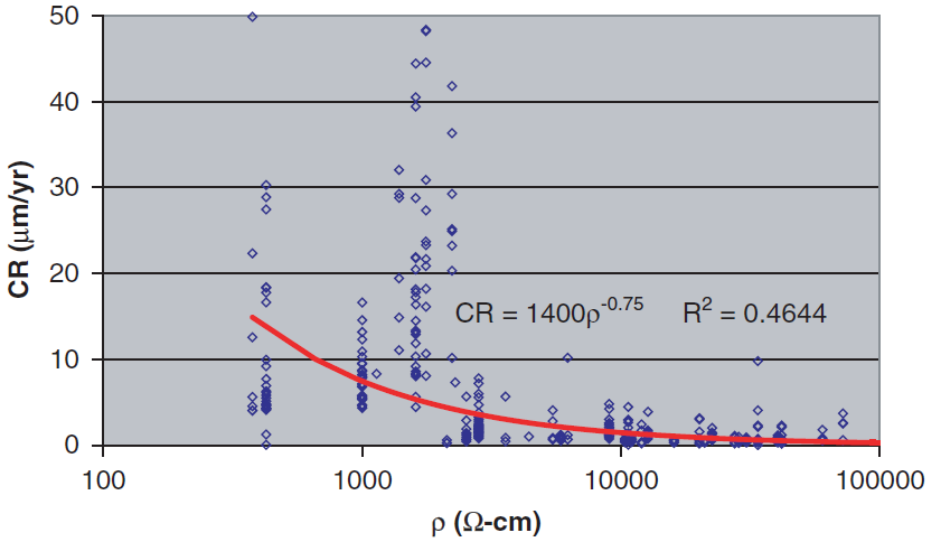

Figure 3. Excerpt of fill resistivity (r) versus corrosion rate (CR) reported by NCHRP (Fishman & Withiam, 2011).

Figure 4. General location of the RW-40-0158 MSE wall in Glendale, WI (Google Earth, 2023).

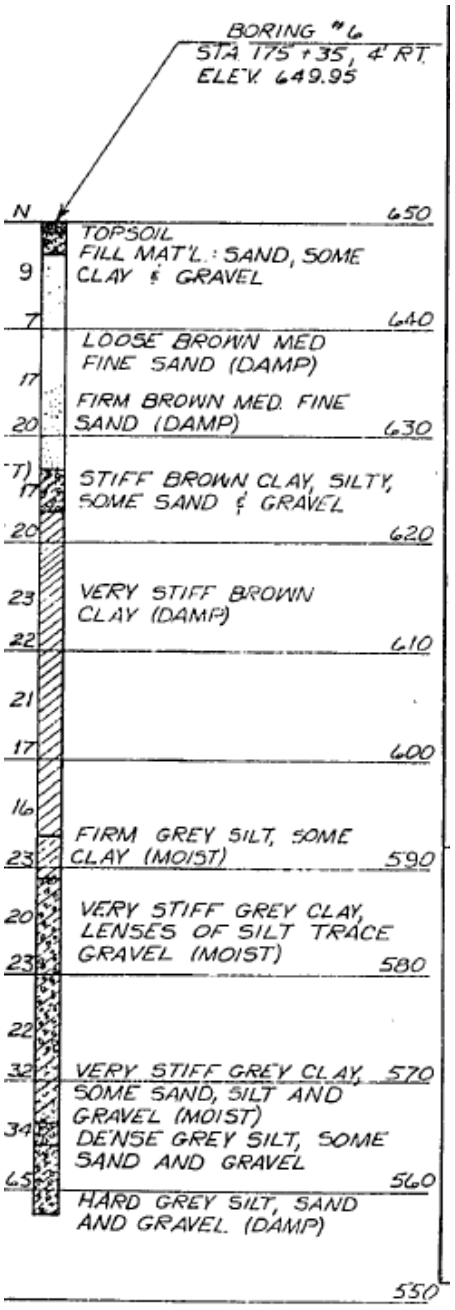

Figure 5. Design boring log located at station 175 + 35 near the south end of the MSE wall.

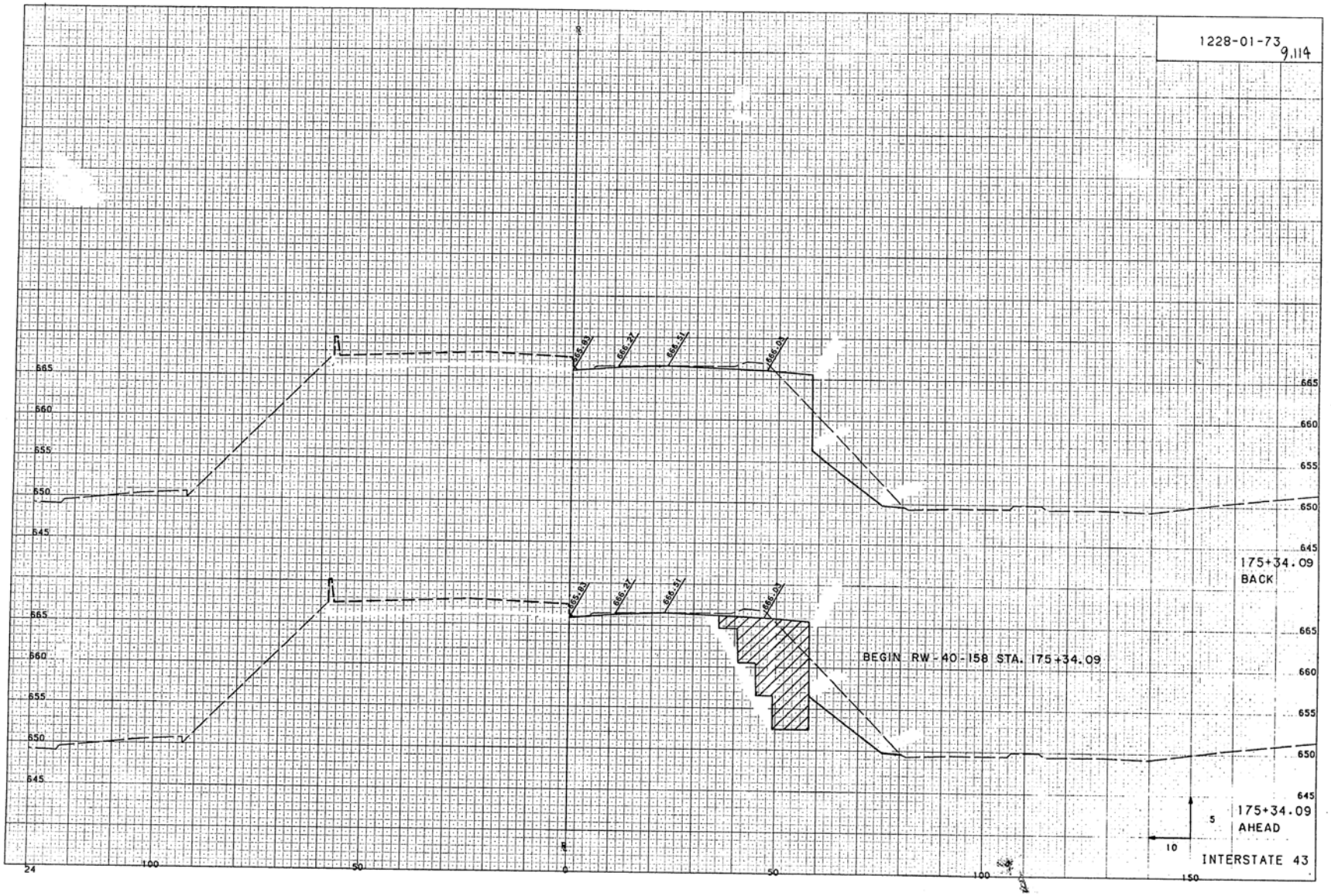

Figure 6. Example design cross sections showing existing and proposed surface ground elevations. The hatched area shows the location of reinforced fill material and dashed line shows the existing ground prior to the construction of the MSE wall.

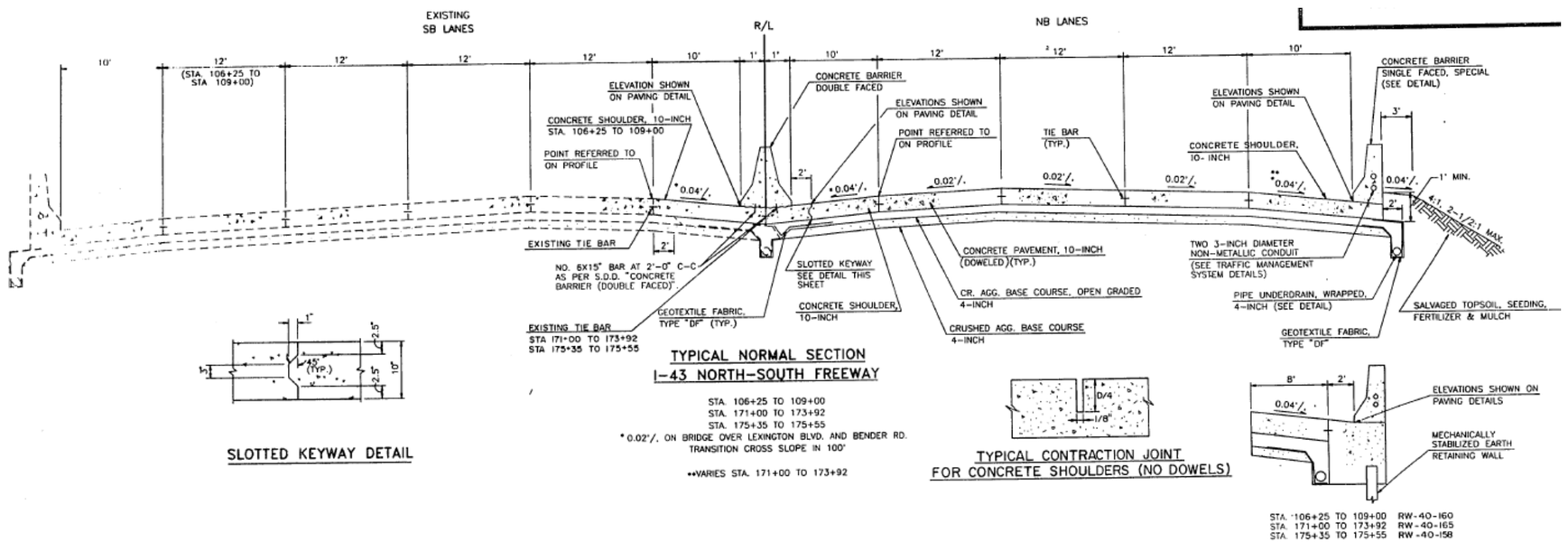

Figure 7. Typical section of the I-43 highway at the bridge approach slab between stations 175+35 and 175+55.

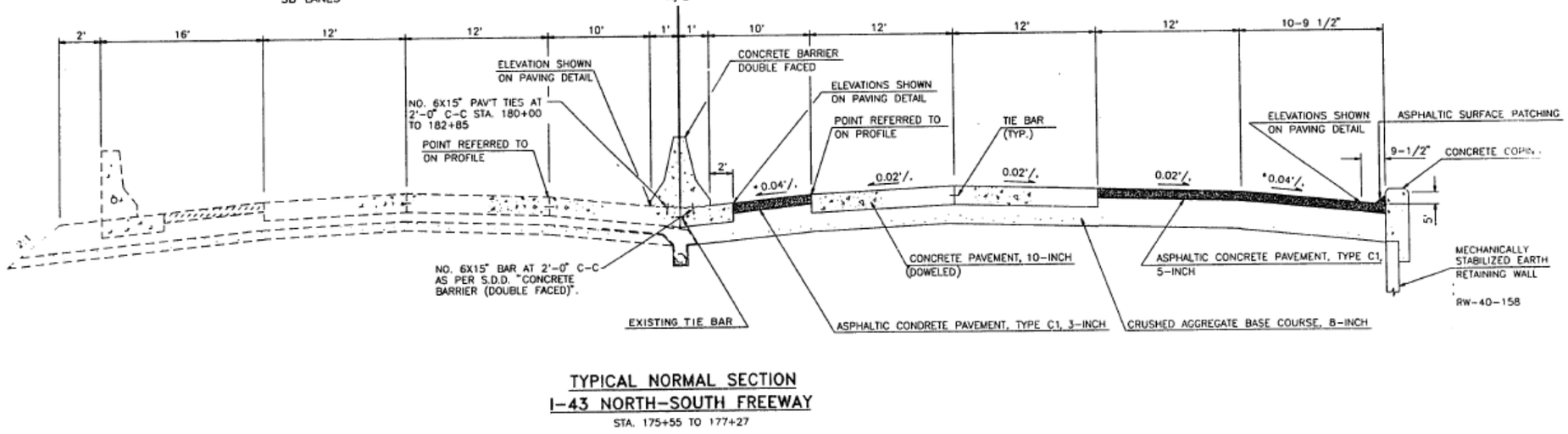

Figure 8. Typical section of the I-43 highway beyond the bridge approach slab between stations 175+55 and 177+27.

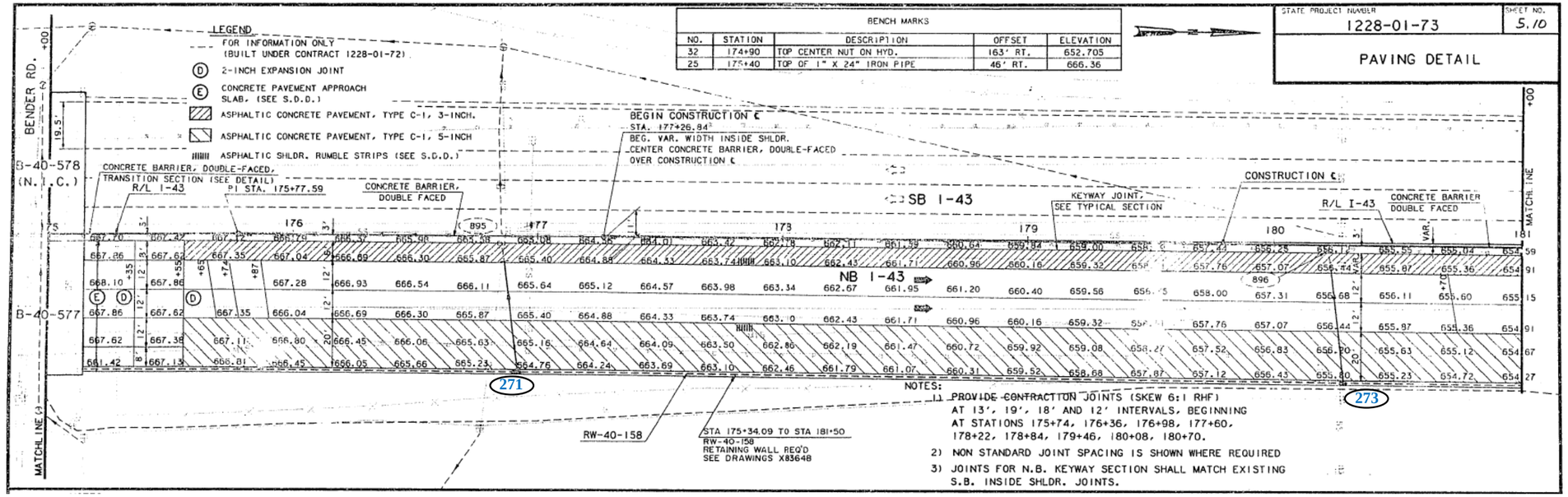

Figure 9. Paving design for the northbound of I-43 highway with the length of the MSE wall.

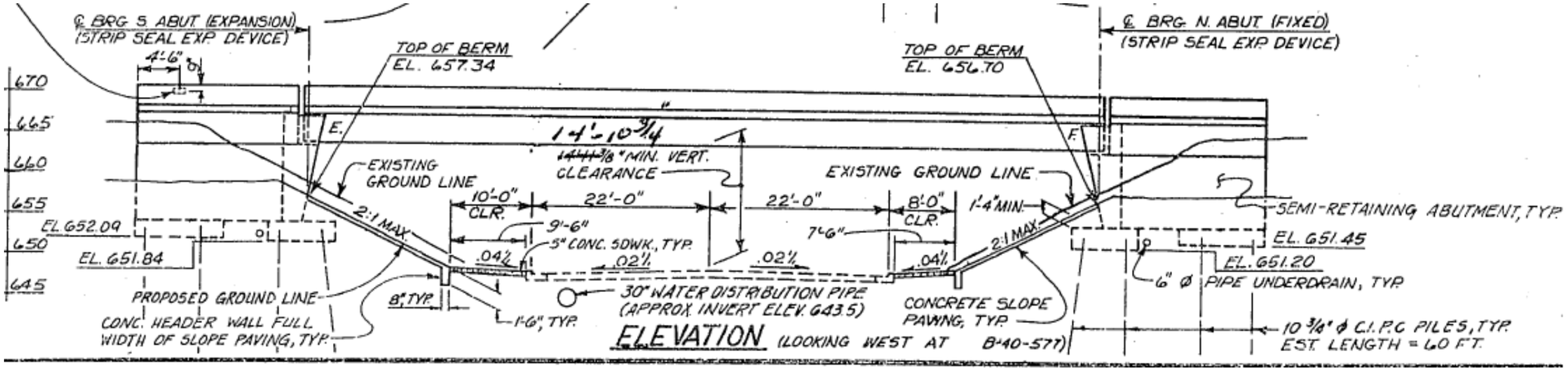

Figure 10. Design drawings for structure B-40-577 located at the south end of the MSE wall.

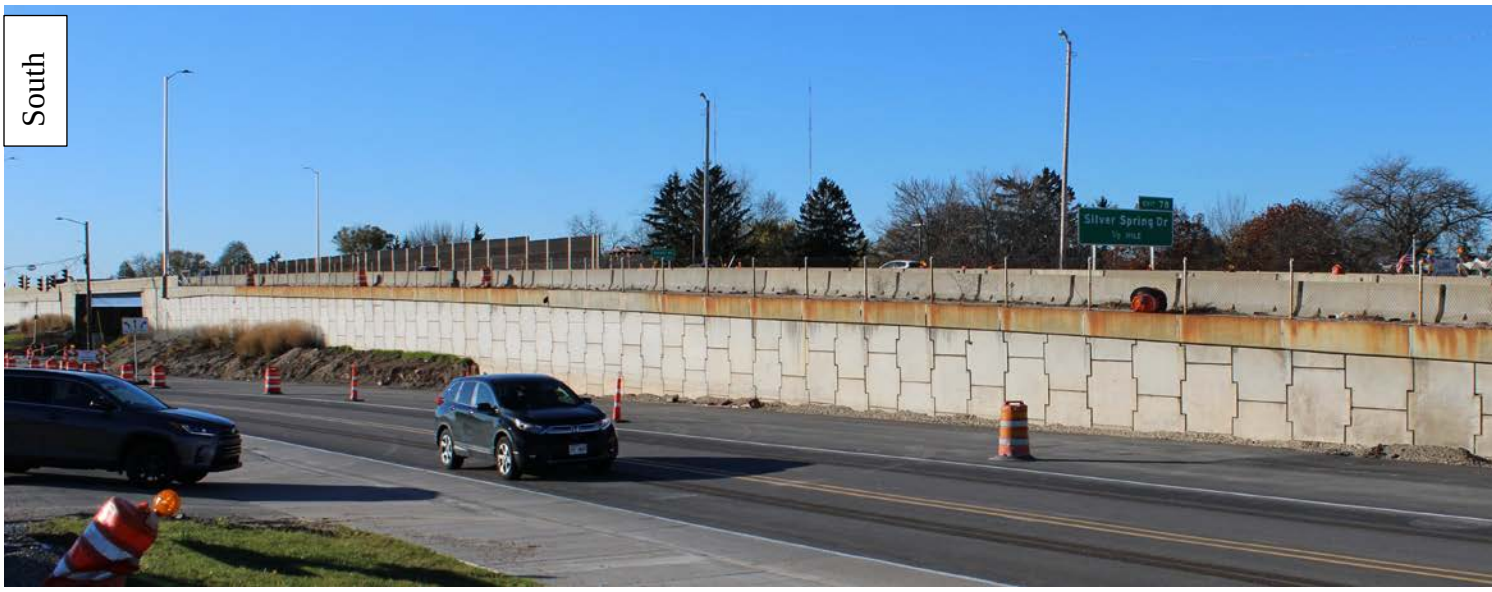

Figure 11. Photograph taken in November 2023 showing the MSE wall facing.

Figure 12. The accessible area on top of the MSE wall. The photograph is taken at the wall STA 00+20 feet looking to the north.

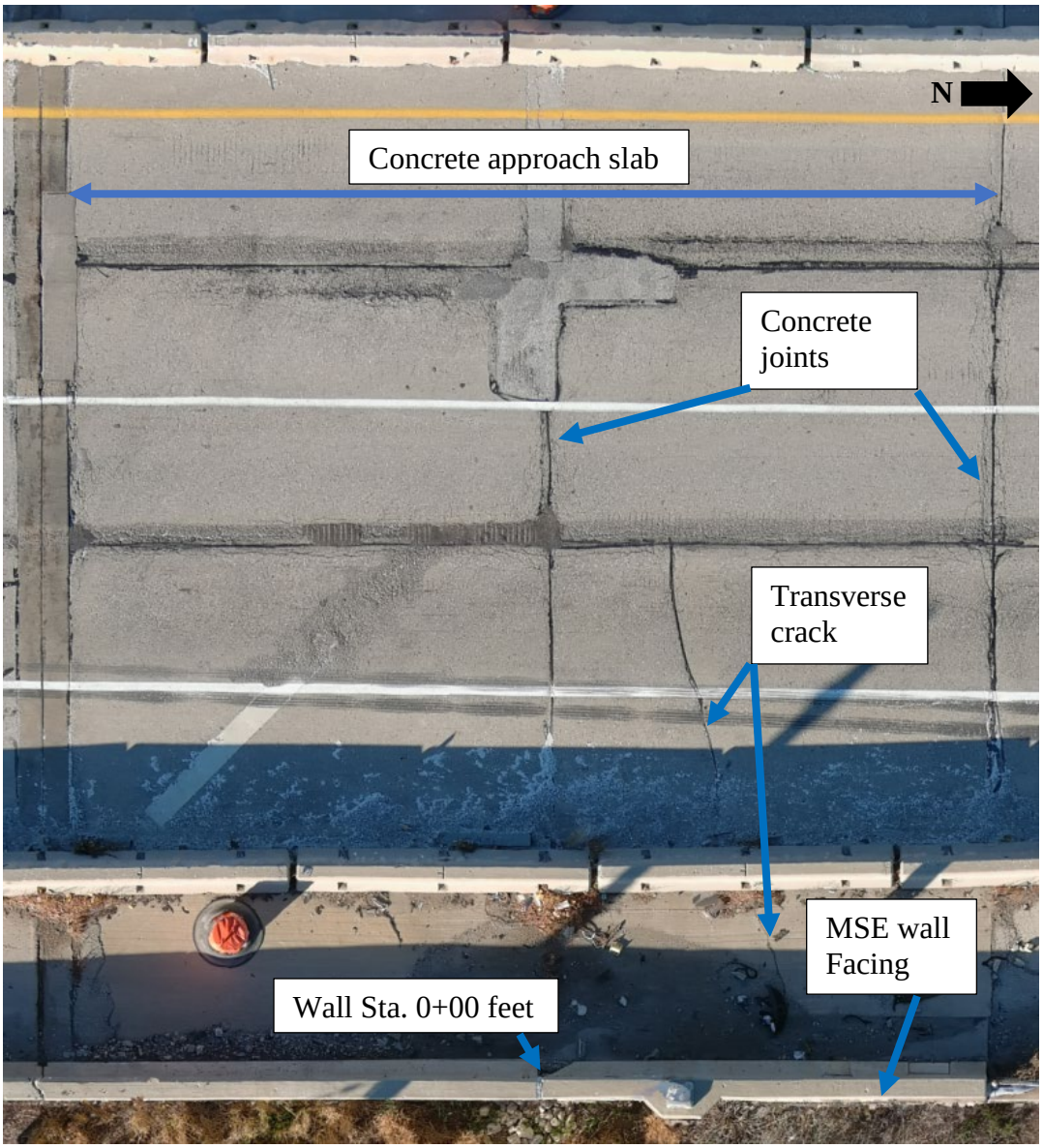

Figure 13. The aerial photograph taken by WisDOT in November 2023 showing the top of the bridge approach slab, MSE wall, and I-43 traffic lanes.

Figure 14. Relative movement of the concrete coping and concrete panel at the south end of the MSE wall to the bridge abutment wing.

Figure 15. Top view of the texturized 3-D photogrammetry model.

Figure 16. East part of the texturized 3-D photogrammetry model, looking west.

Figure 17. Zoomed in part of the texturized 3-D photogrammetry model next to the bridge, looking west.

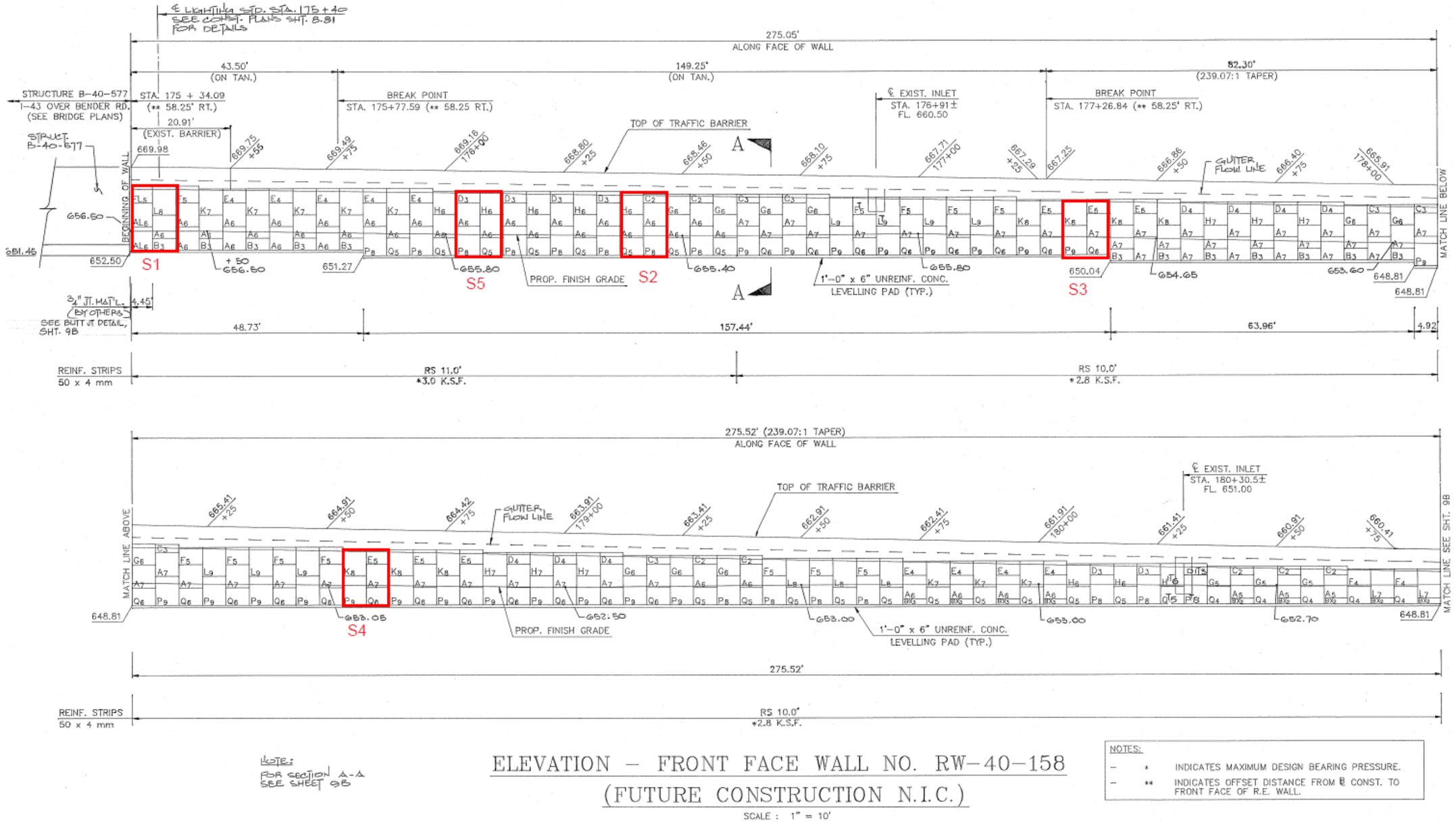

Figure 18. Approximate location of excavation trenches along the RW-40-158 MSE wall (the figure shows snips of MSE wall's design drawings with Geocomp's annotations in red).

Figure 19. Soil resistivity testing in the field.

Figure 20. Concrete slab and underlying layers at the Section 1's excavation trench.

Figure 21. The longitudinal crack on the shoulder pavement along the MSE wall at Section 3.

(a) (b)

Figure 22. Photographs of reinforcing straps in (a) Section 1 lift 1 and (b) Section 3 lift 4.

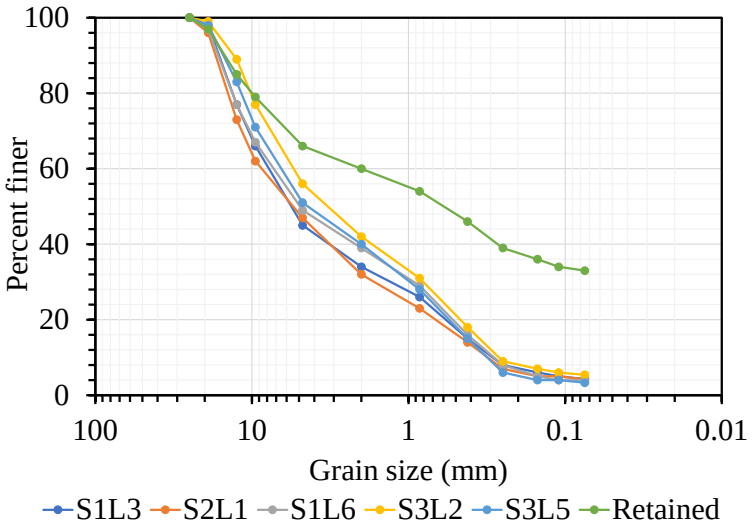

Figure 23. Particle size distribution of samples.

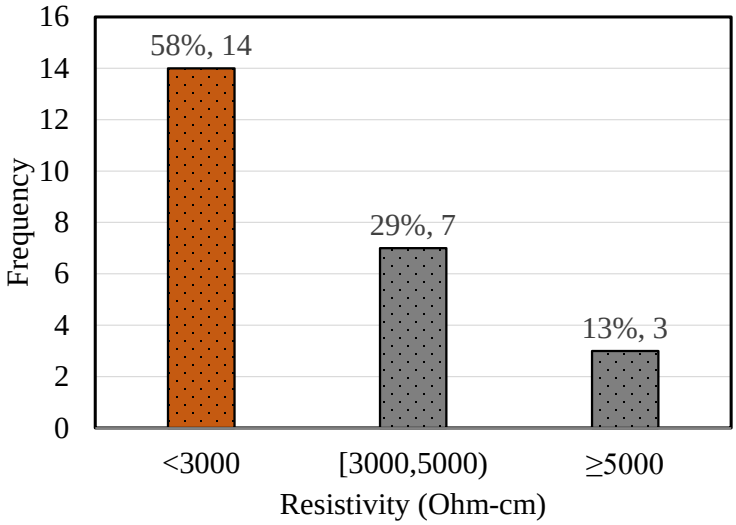

Figure 24. Soil Resistivity statistics.

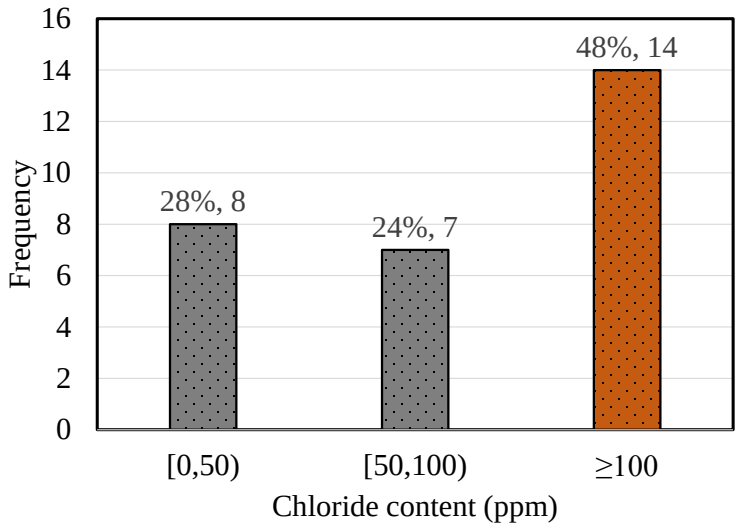

Figure 25. Chloride content statistics.

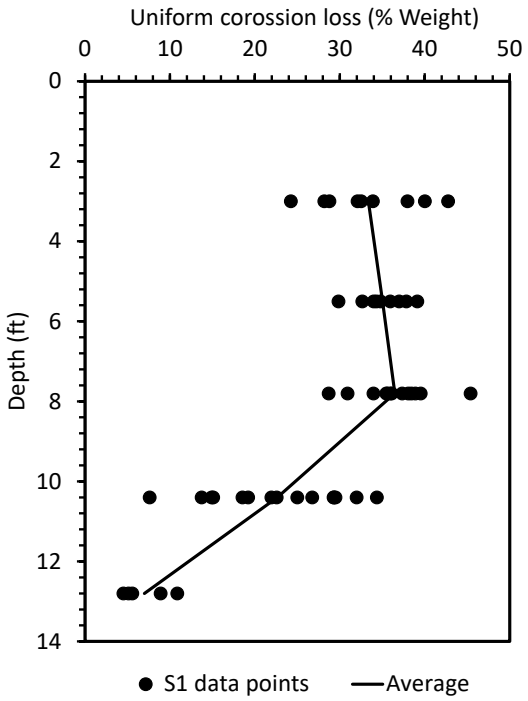

(a)

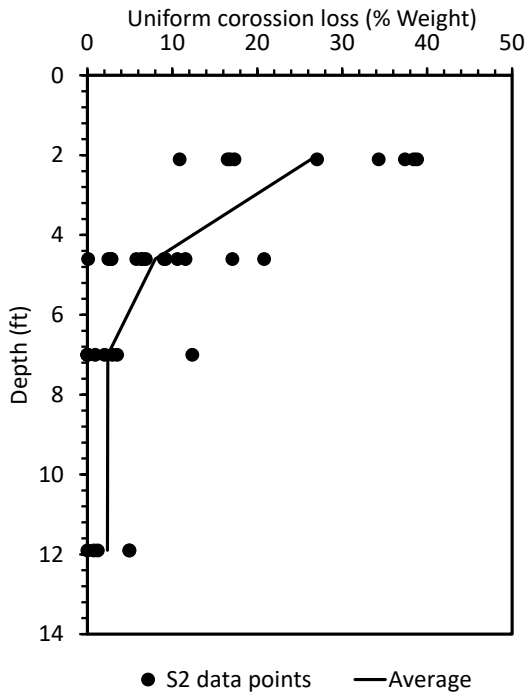

(b)

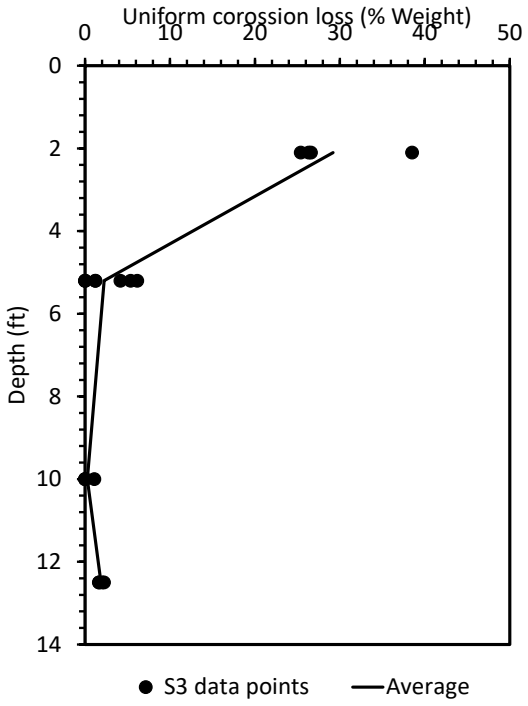

(c)

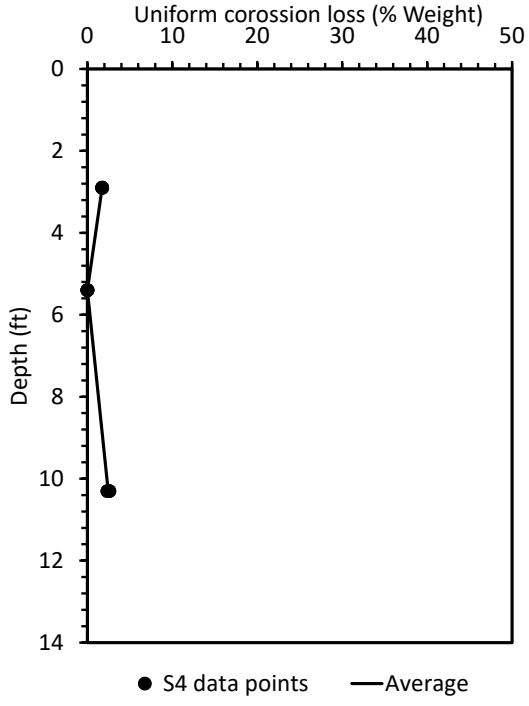

(d)

Figure 26. Uniform corrosion loss versus depth for (a) Section 1, (b) Section 2, (c) Section 3, and (d) Section 4.

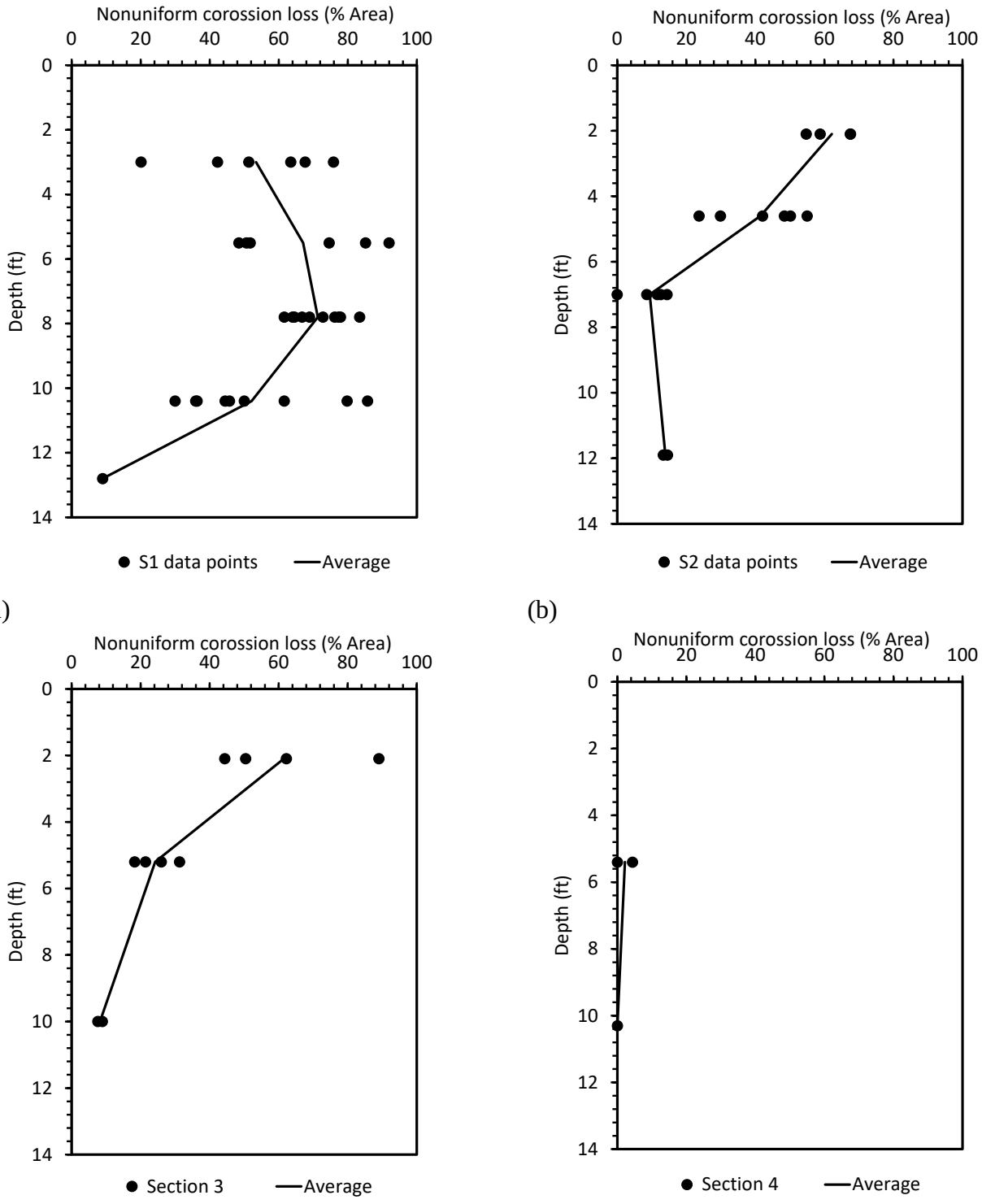

Figure 27. Nonuniform corrosion loss versus depth for (a) Section 1, (b) Section 2, (c) Section 3, and (d) Section 4.

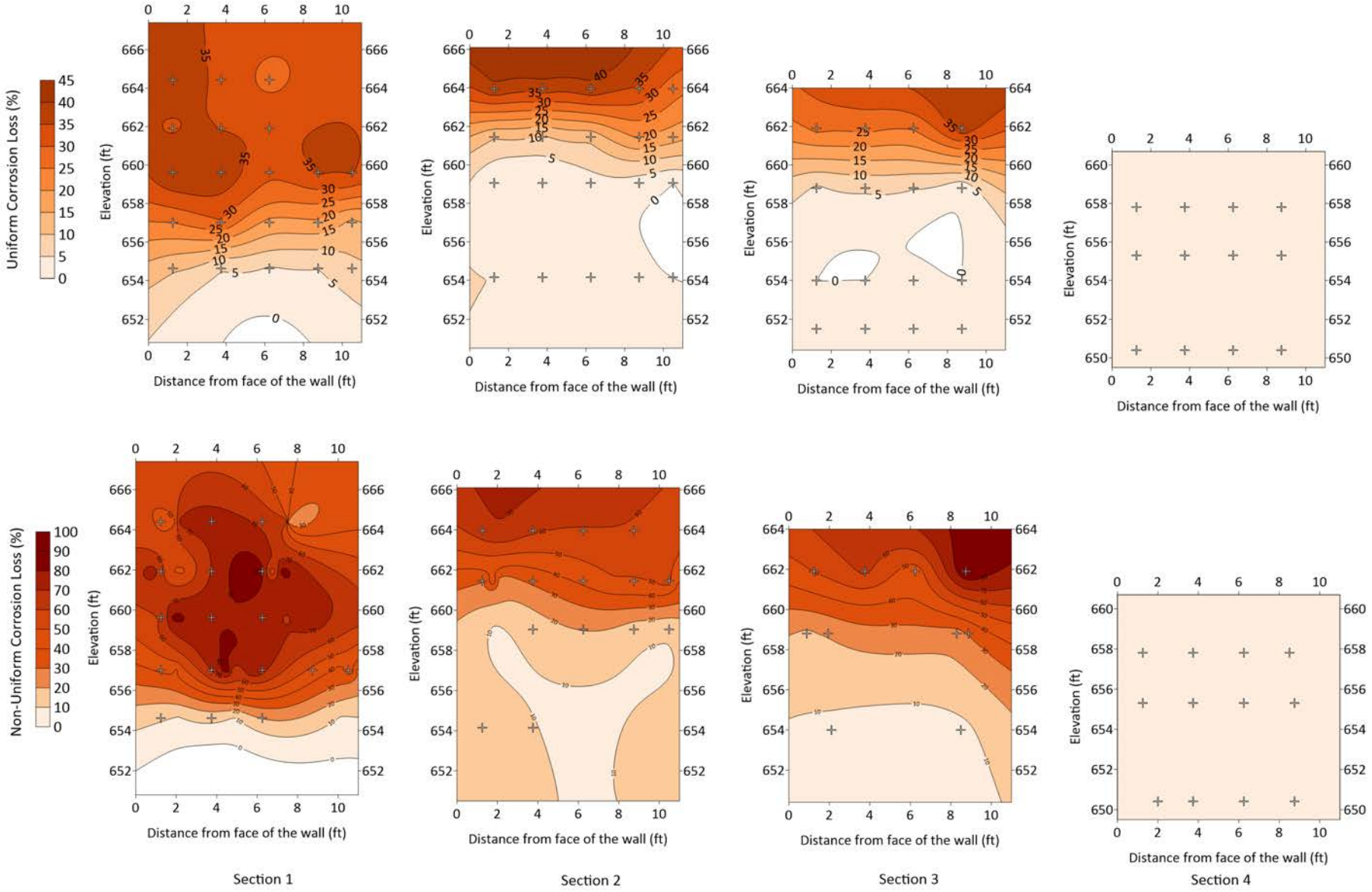

Figure 28. Uniform and nonuniform corrosion loss along the strips for excavation Sections 1 through 4. The "+" sign on the figure represents the sample locations.

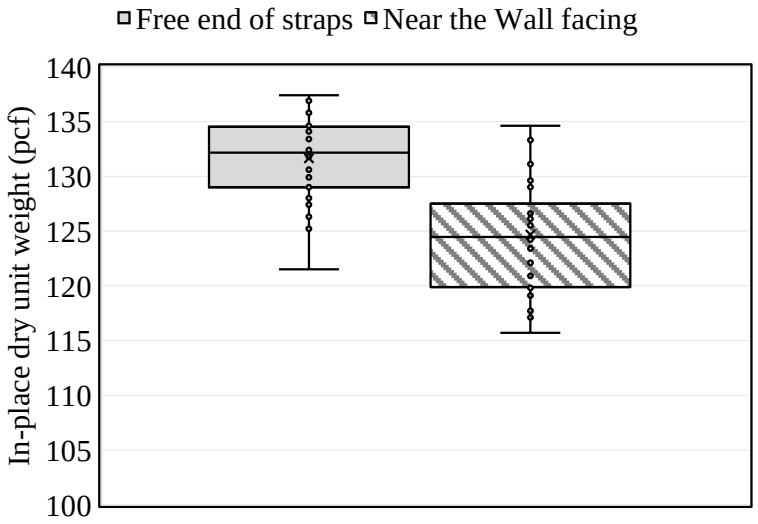

Figure 29. In place dry density of reinforced backfill next to the MSE wall facing and near the end of reinforcing straps.

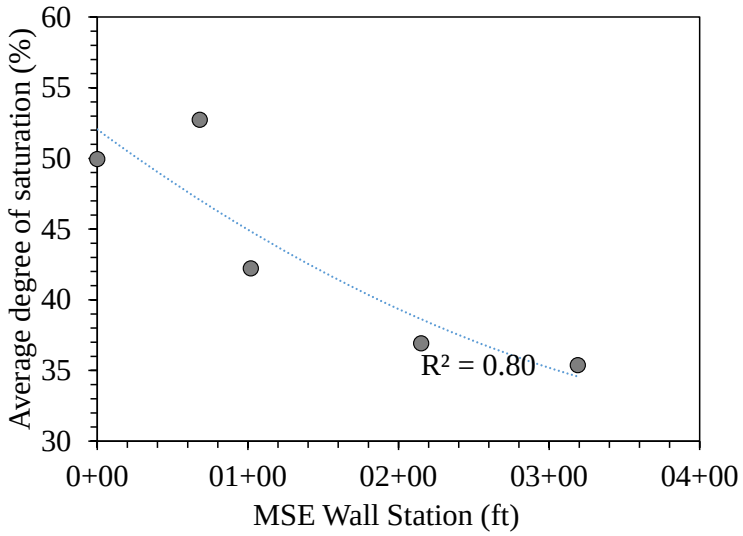

Figure 30. Degree of saturation versus MSE wall station. The data presents the average degree of saturation of the tested samples from each excavation section.

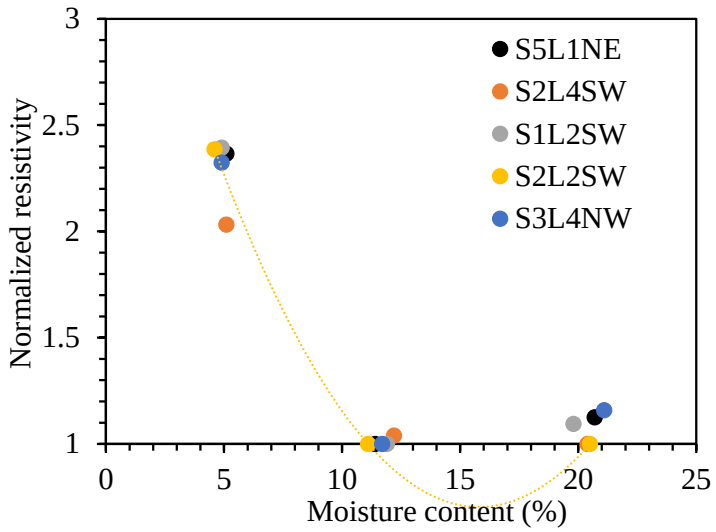

Figure 31. Normalized resistivity versus moisture content.

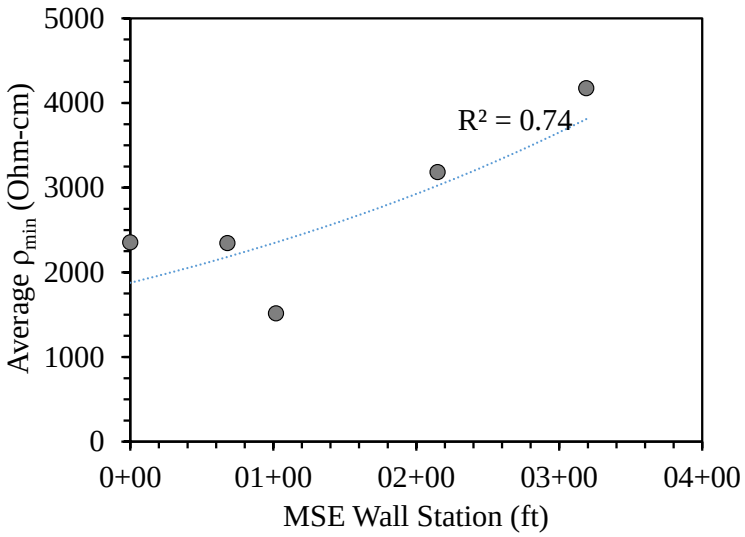

Figure 32. Average ρ_{min} of reinforced backfill versus MSE wall station.

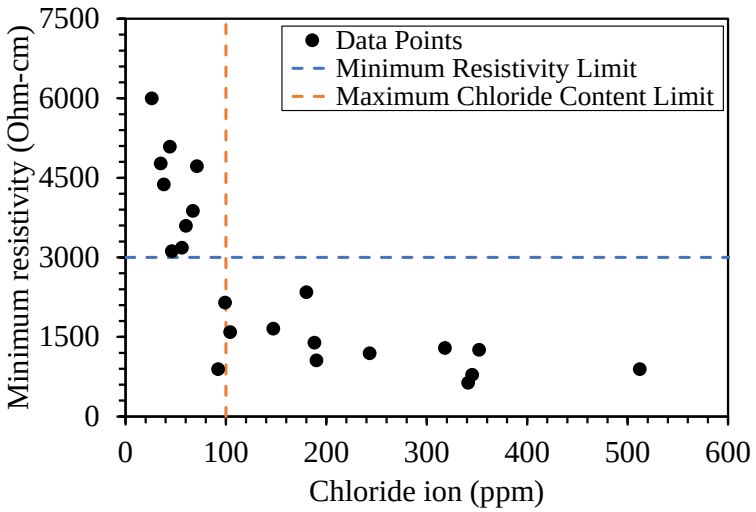

Figure 33. Electrical resistivity versus chloride content of the tested reinforced backfill samples.

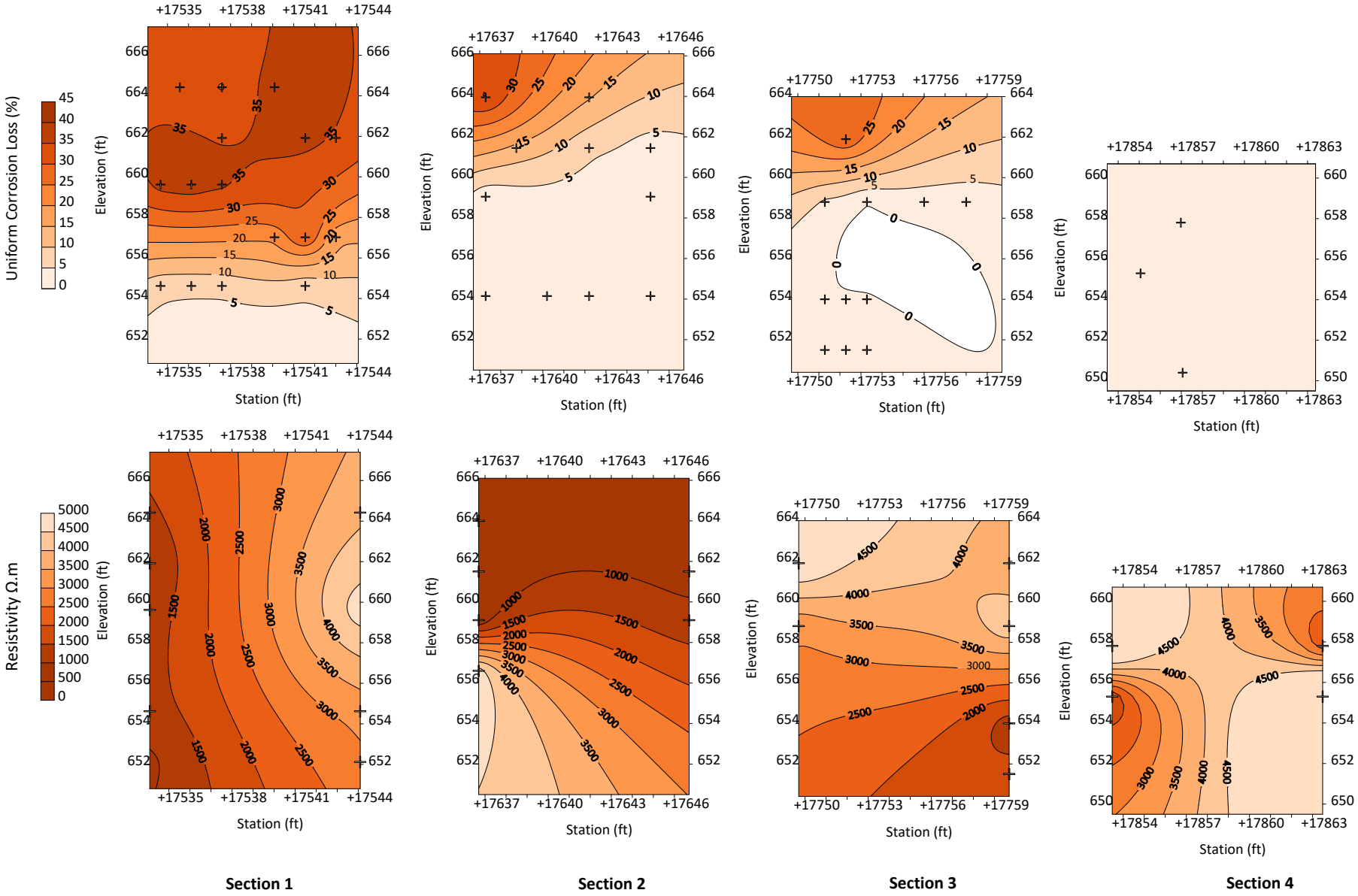

Figure 34. Uniform corrosion loss and minimum resistivity contour plots for excavation sections 1 through 4. The "+" sign on the figure represents the sample locations.

Figure 35. Cracks and concrete joints considered for calculation of crack infiltration rate in Section 1.

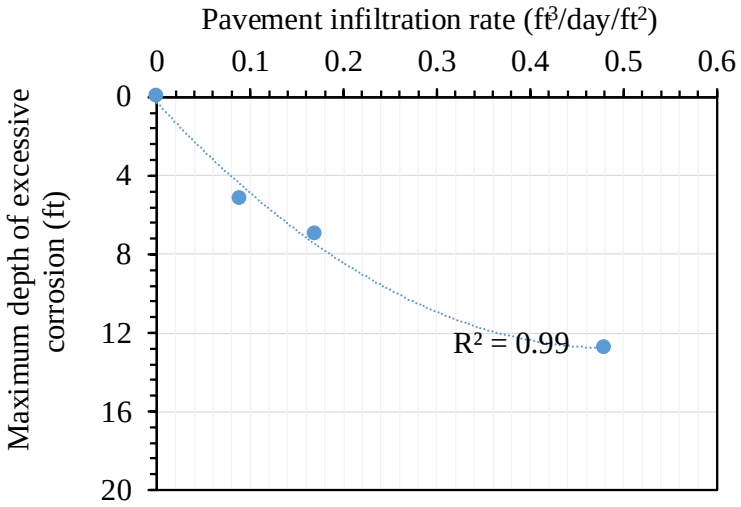

Figure 36. Crack infiltration rate versus the maximum depth of excessive corrosion loss.

Guidelines Anti-Icing				
PREDICTED PRECIPITATION EVENT	Recommended Locations	Application Rate Liquid (gal/lane-mi.)	Application Rate Pre-wetted Salt (lb/lane-mi)	*COMMENTS*
Frost or Black Ice	Bridge Decks and Trouble Spots	20-30 (frost) 30-40 (Black Ice)	50-150	1) Consider treating approaches as well as bridge decks. 2) Treat ice patches, if needed, with pre-wetted salt at 100 lb/lane-mi.
Sleet	Bridge Decks and Trouble Spots and Intersections	20 Recommended 30 Maximum	200-400(1) 100-300(2)	1) Consider treating approaches as well as bridge decks.2) Treat ice patches, if needed, with pre-wetted salt at 100 lb/lane-mi.
Freezing Rain	Any area of concern	Not Recommended	200-400(1) 100-300(2)	It is not recommended to apply liquid de-icing agents in an anti-icing mode prior to freezing rain events.
Light Snow (< 1/2" in./hr.)	Trouble Spots and Intersections	30 Recommended 40 Maximum	100-200	If anti-icing is performed prior to a snow event, re-application may be necessary to prevent re-freeze. It also may be necessary to switch to a de-icing mode.
Moderate or Heavy Snow (≥ 1/2 in./hr)	Trouble Spots and Intersections	40 Recommended 50 Maximum	100-300	1) Do not apply liquid anti-icing agents onto heavy snow accumulation or packed snow. 2) Applications will need to be more frequent at lower temperatures and higher snowfall rates. 3) If anti-icing is performed prior to a snow event, re-application may be necessary to prevent re-freeze. It also may be necessary to switch to a de-icing mode.

Notes:

- Anti-icing operations typically should be conducted during normal, non-overtime working hours and low traffic volume periods.
- It is not recommended to apply de-icing agents in an anti-icing mode when the pavement temperature is below 15ºF or drifting is a problem.
- Time initial anti-icing agent applications and subsequent de-icing agent applications to prevent deteriorating conditions or development of packed and bonded snow.

(1) 4-Lanes and Greater
(2) 2 Lanes

Figure 37. Anti-icing guidelines per HMM 06-20-20 dated January 2012.

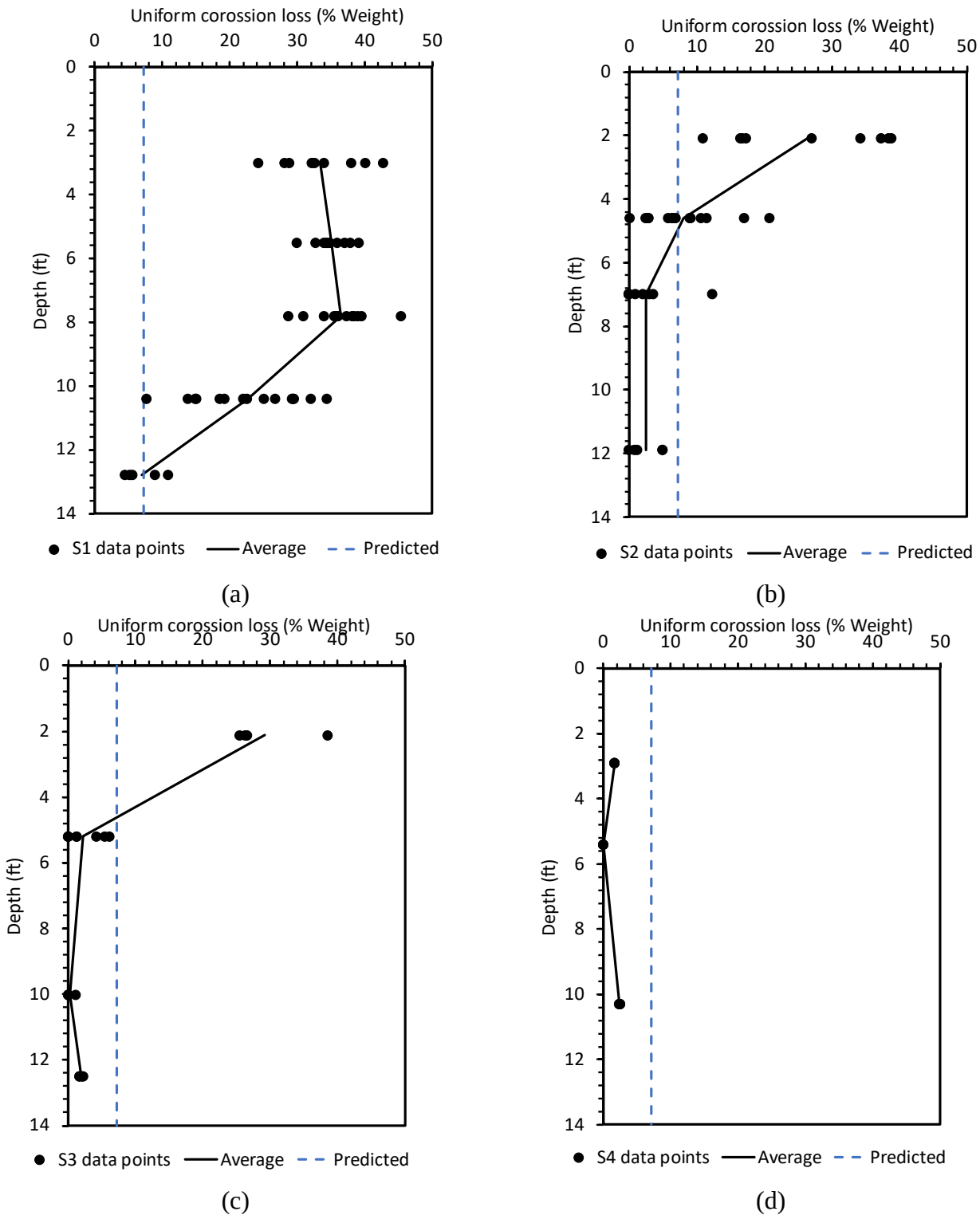

Figure 38. Predicted uniform corrosion loss of reinforcement in nonaggressive fill after 32 years of service and measured uniform corrosion loss for (a) Section 1, (b) Section 2, (c) Section 3, and (d) Section 4.

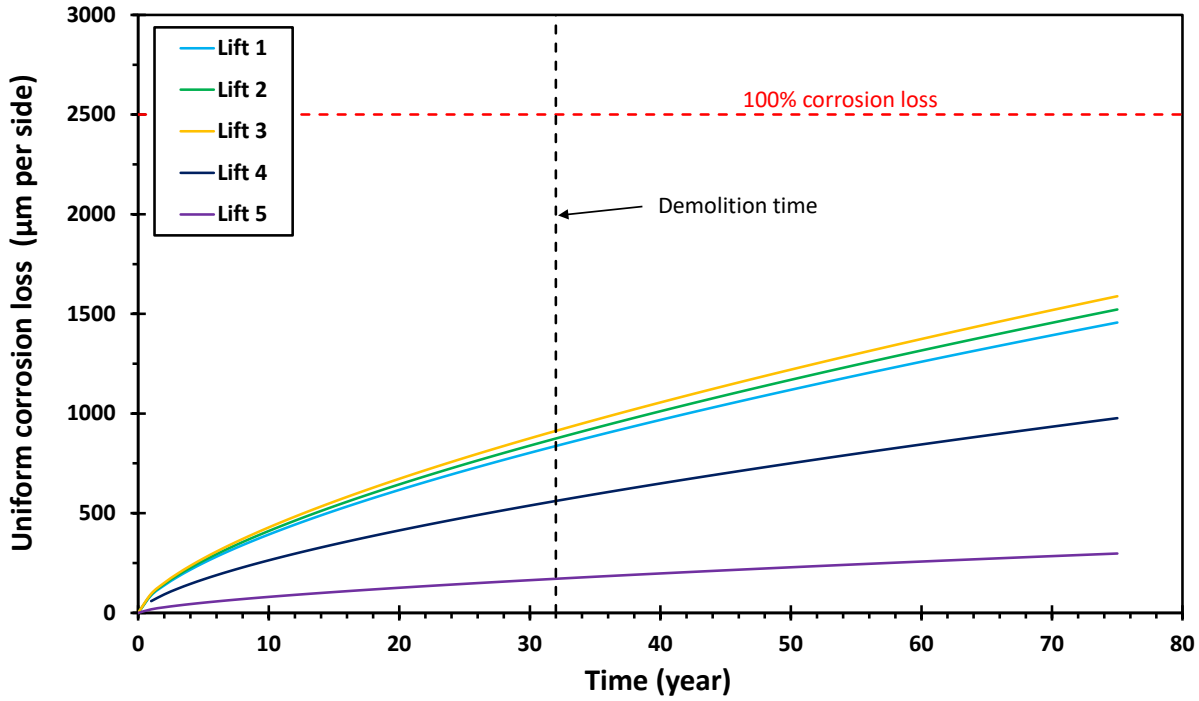

Figure 39. Uniform corrosion loss of reinforcing straps in lifts 1 through 5 of excavation Section 1 over service life of the study MSE wall.

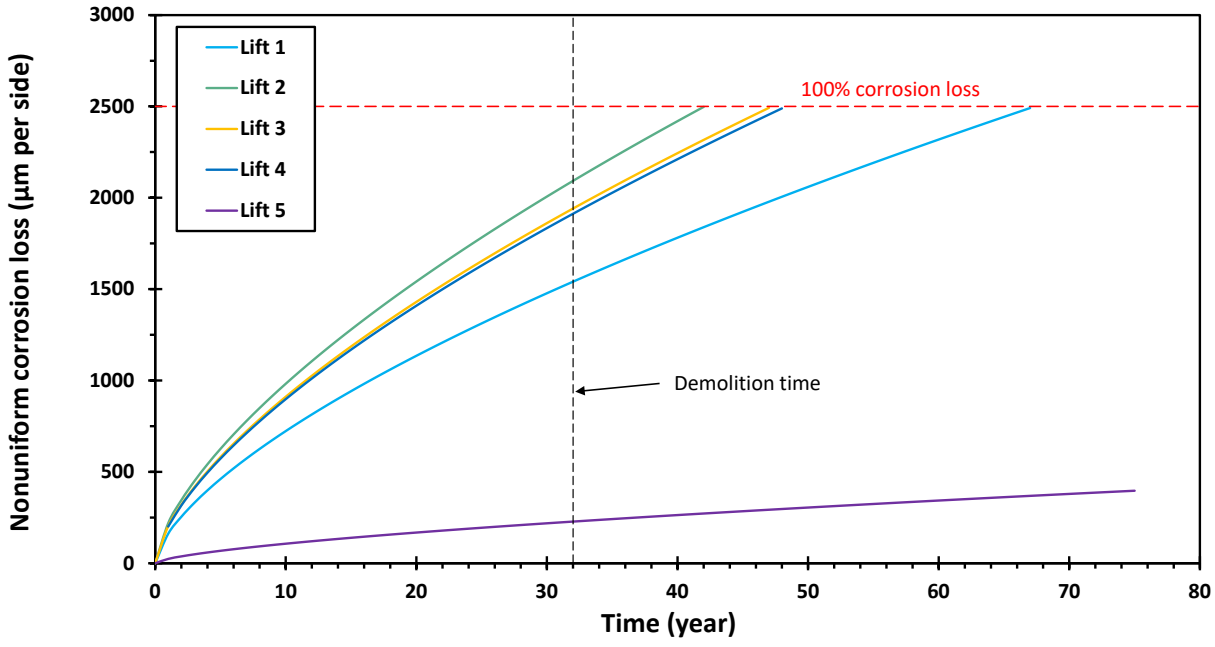

Figure 40. Nonuniform corrosion loss of reinforcing straps in lifts 1 through 5 of excavation Section 1 over service life of the study MSE wall.

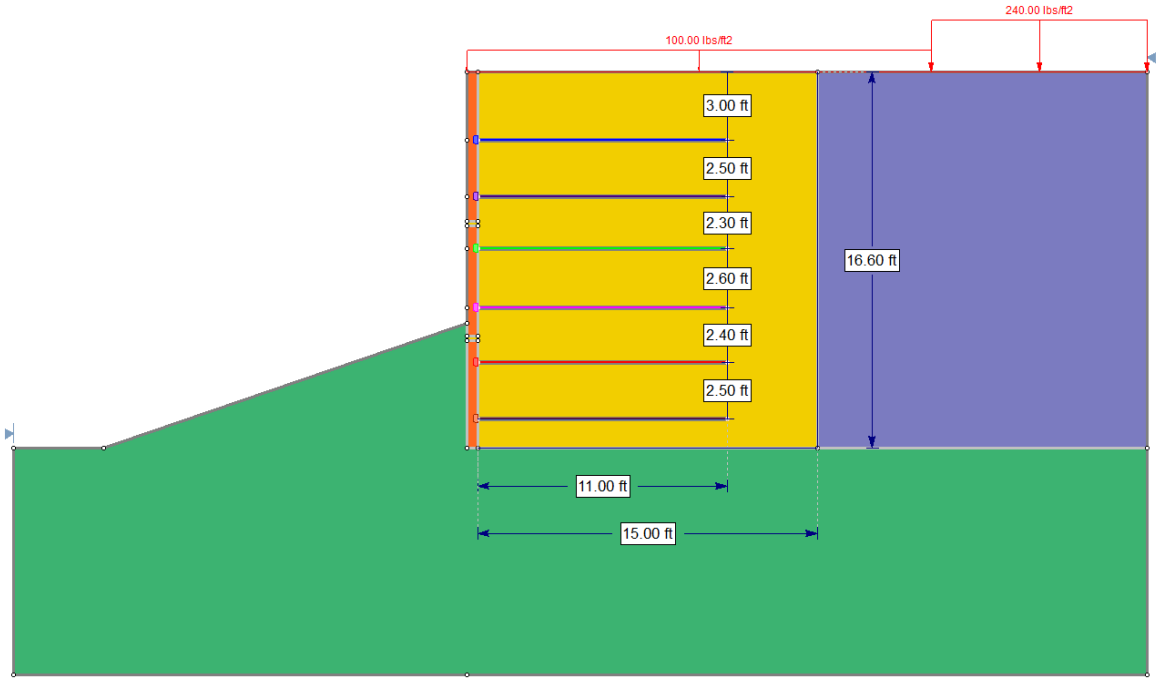

Figure 41. 2D cross section geometry of the MSE wall at the excavation Section 1 (units are in foot).

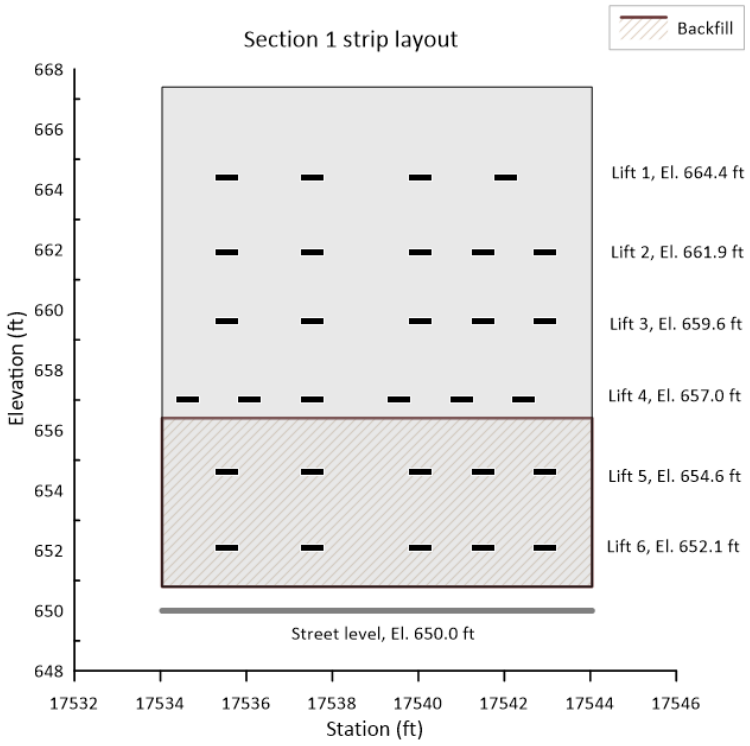

Figure 42. Elevation view showing the reinforcing strips' layout in Section 1 (strip dimensions are not to scale).

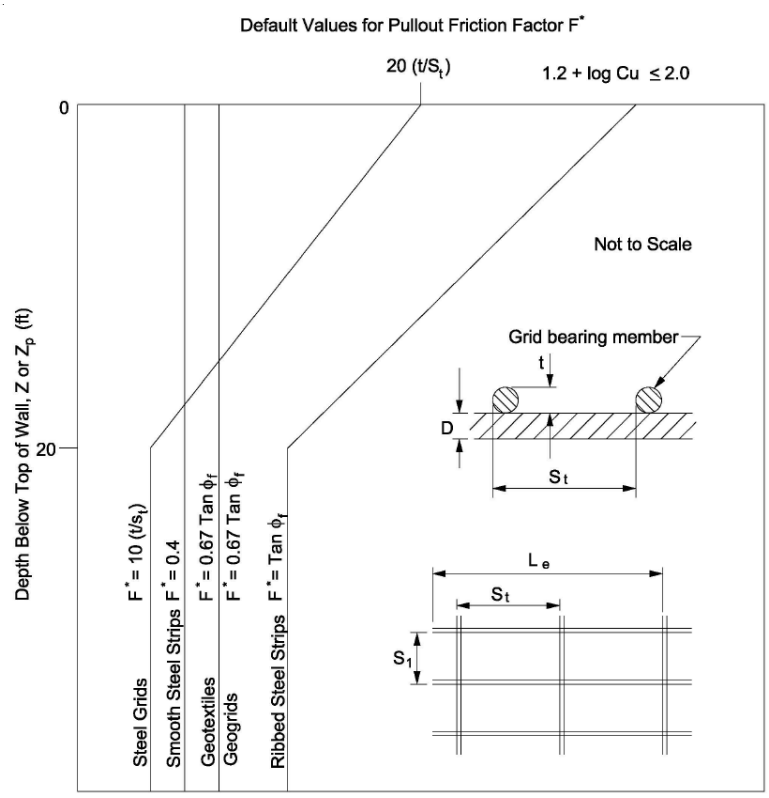

Figure 43. Default value of F* (pullout resistance factor) from AASHTO [Figure 11.10.6.3.2-2].

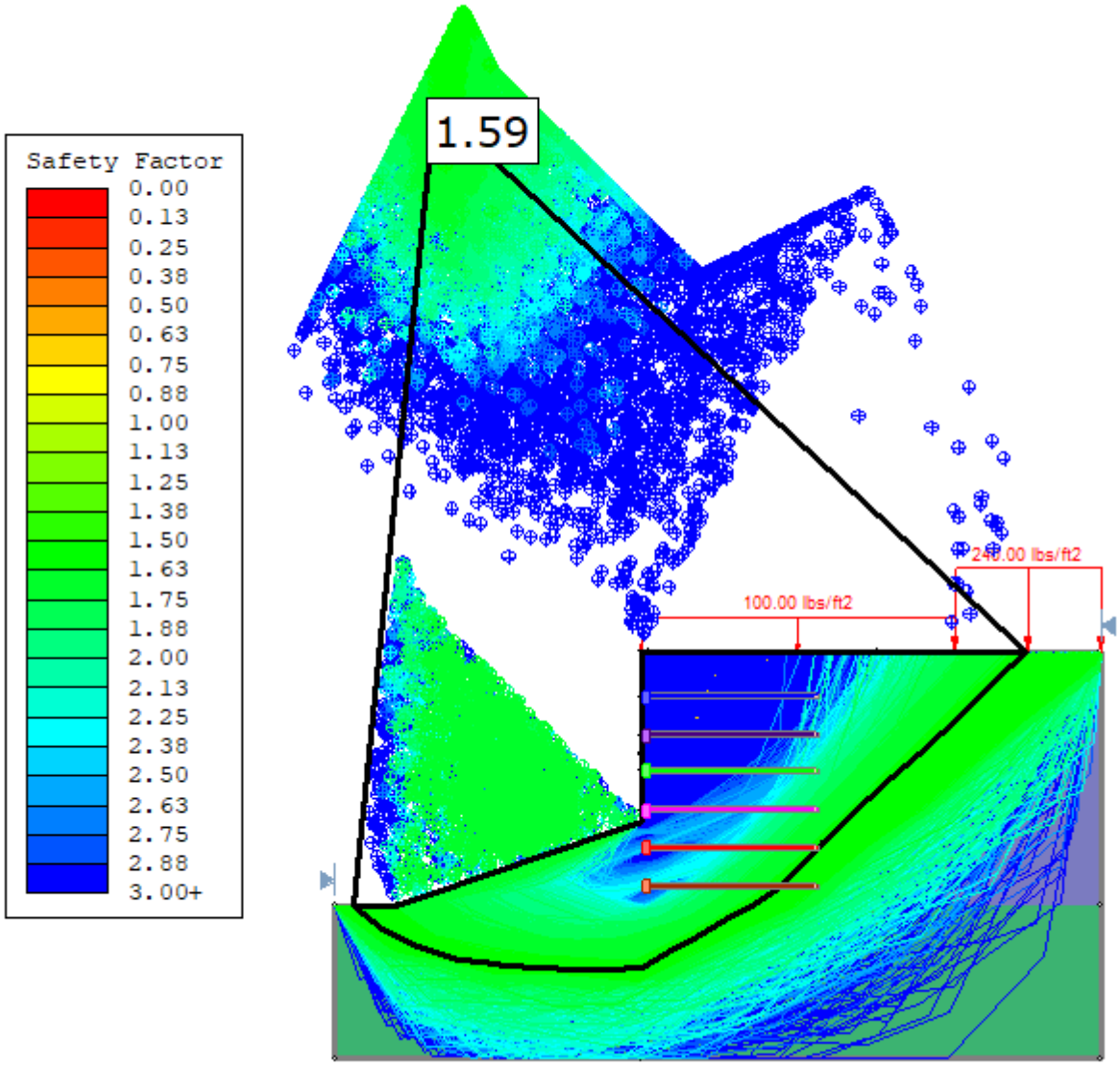

Figure 44. Critical slip surface for global stability of the MSE wall considering uniform corrosion loss. This slip surface remains the same for all times until 75 years post construction.

Figure 45. The 4-inch outward displacement of the top panel immediately next to the bridge abutment.

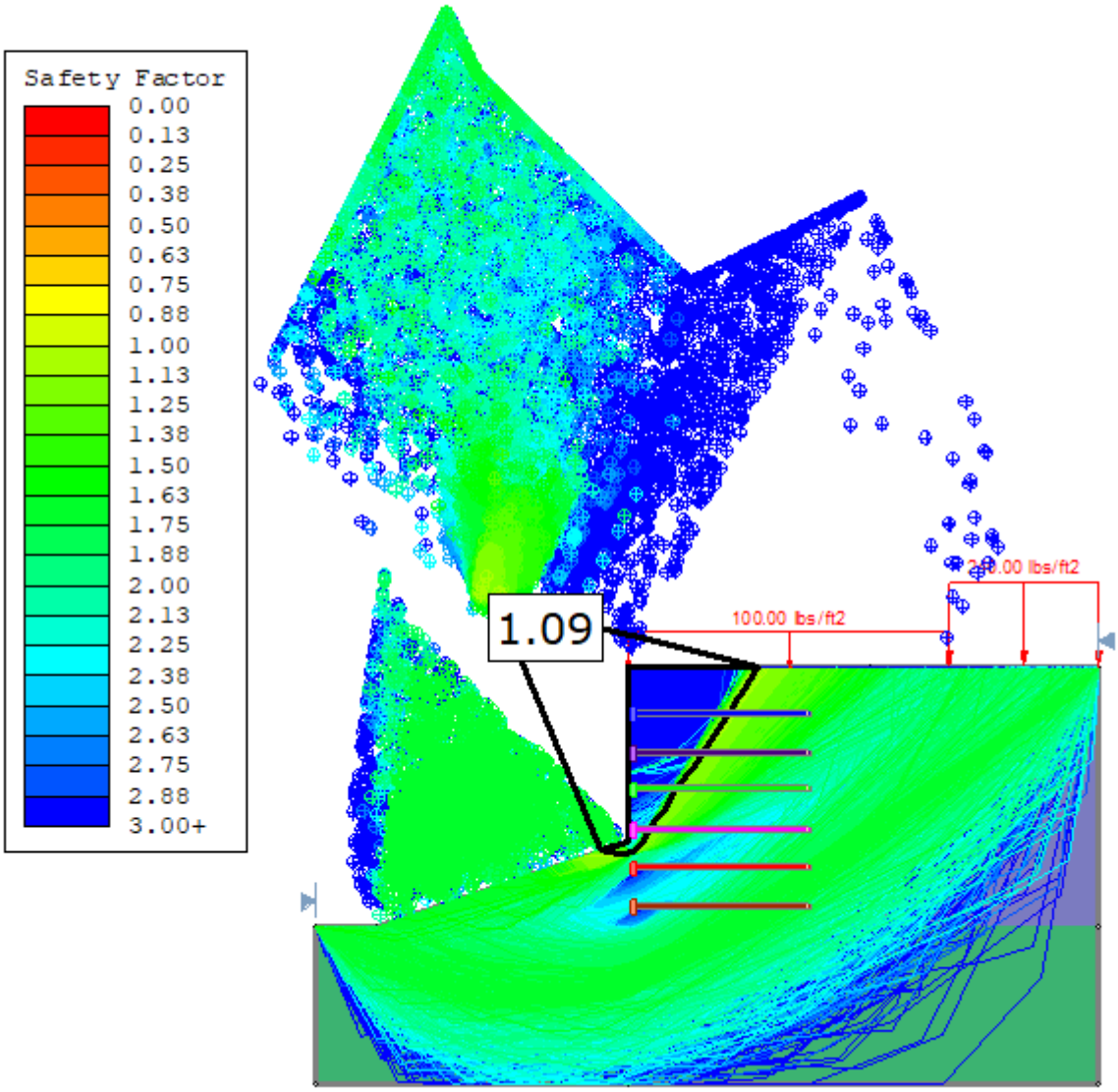

Figure 46. Critical slip surface after 42 years considering non-uniform corrosion loss.

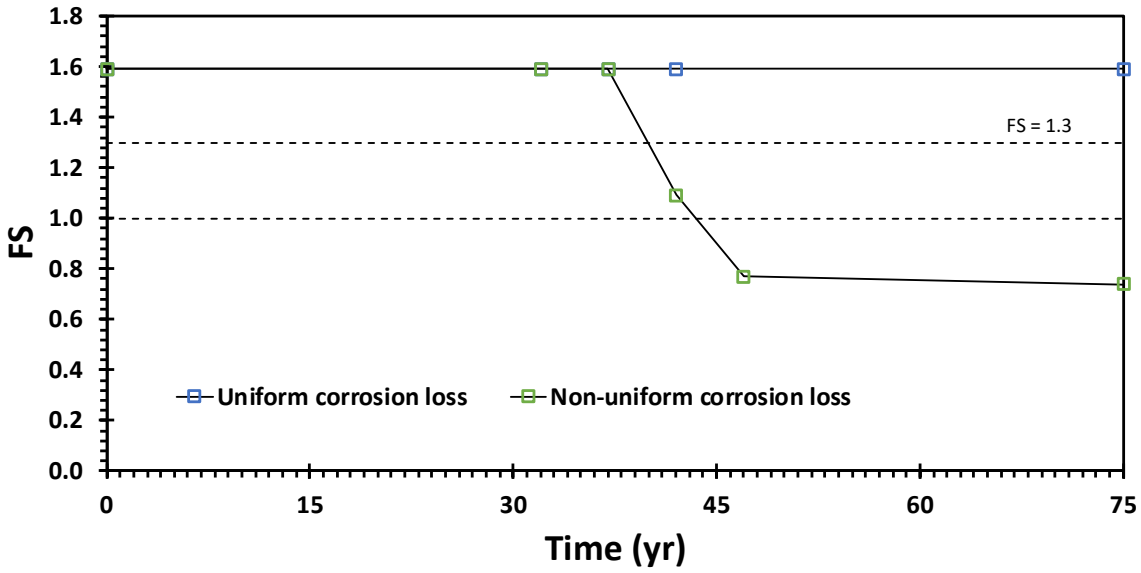

Figure 47. Global factor of safety (FS) reduction over time beginning at the construction of the MSE wall due to non-uniform corrosion loss.

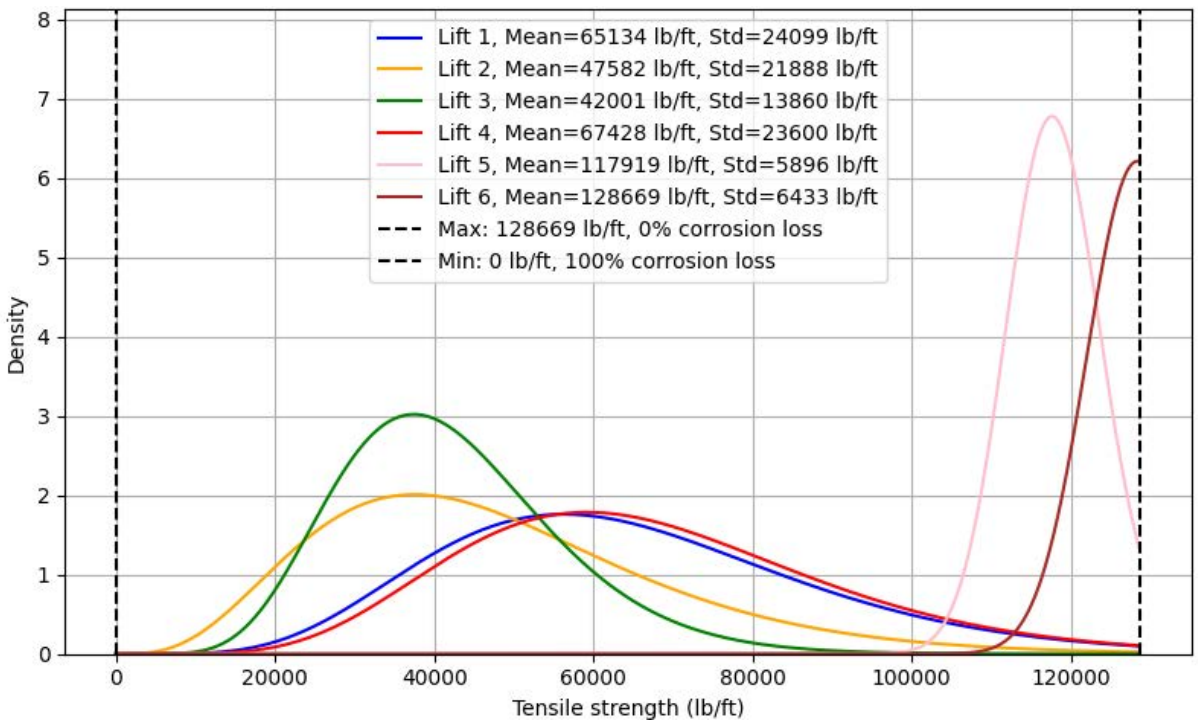

Figure 48. Probability distribution of tensile strength after 32 years for each lift.

APPENDIX B: TABLES

Table 1. Corrosion rates of galvanized steel buried in backfill soils meeting the electrochemical properties requirements provided by AASHTO and FHWA.

Material	**Corrosion Rate (mils/year) per side**	**Corrosion Rate (µm/year) per side**
Zinc in first 2 years	0.58	15
Zinc to depletion	0.16	4
Carbon Steel	0.47	12

Table 2. Electrochemical limits for select backfills based on FHWA guidelines.

Property	**Criteria**				**Test method**		
	1986	**1990**	**2000**	**2009**	**1990**	**2000**	**2009**
Minimum Resistivity (ohm/cm)	>3,000	>5,000	>3,000	>3,000	ASTM G-57-78	AASHTO T-288	AASHTO T-288
pH	5 to 10	4.5 to 9.5	5 to 10	5 to 10	Soil survey 8Cla	AASHTO T-289	AASHTO T-289
Chloride content (PPM)	<200	<100[5]	<100	<100	ASTM D512 ASTM D-4327	AASHTO T-291	ASTM D-4327
Sulfate content (PPM)	<1000	<200	<200	<200	ASTM D-516(B) ASTM D-4327	AASHTO T-291	ASTM D-4327
Organic content	-	0.01%	1% max	1% max	AASHTO T-267-86	AASHTO T-267	AASHTO T-267

[5] Elias (1990) states that soils with resistivities of less than 5,000 ohm/cm but greater than 2,000 ohm/cm may be accepted if they meet the requirements for chloride and sulfate.

Table 3. Design life of soil reinforced structures by Elias (1990).

Structure Classification	Design Life (yrs.)
Permanent Structure	75
Abutments	100
Rail Supporting Structures	100
Marine Structures	75

Table 4. Electrochemical limits for select backfills per AASHTO specifications and WisDOT Bridge Manuals.

Property	Criteria				Test Method
	AASHTO 1992	AASHTO 1996-2020	WisDOT 1996	WisDOT 2025	AASHTO 2002-2020
Minimum Resistivity (ohm/cm)	>3,000	>3,000	>3,000	>3,000	AASHTO T 289
pH	5 to 10	5 to 10	4.5 to 10	5 to 10	AASHTO T 288
Chloride content (PPM)	<50	<100[6]	<100	<100	AASHTO T 291
Sulfate content (PPM)	<500	<200	<200	<200	AASHTO T 290
Organic content	1% max	1% max	Free of organics	1% max	AASHTO T 267

[6] AASHTO (2002-2020) indicates that for soils with resistivities greater than 5000 ohm/cm, the chlorides and sulfates requirements may be waved.

Table 5. Recommended Sampling Protocol for Electrochemical Testing of MSE wall (Elias, et al., 2009).

Range of ρ_{min} (Ω-cm)	**General Description**	**Preconstruction**		**During Construction**	**Comments**
		No. Sample	**σ resistivity**	**Sample Interval (yd^3)**	
>10,000	Crushed rock and Gravel, <10% passing No. 10 sieve	1/3[1]	NA	NA	1. pH outside the specified limits is not allowed for any sample. 2. Backfill sources shall be rejected if ρ_{min} measured for any sample is less than 700 Ω-cm, CL >500 ppm or SO_4>1,000 ppm. 3. For materials with ρ_{min} < 5,000 Ω-cm, σ shall be less than 100 ppm and 200 ppm, respectively.
5,000 to 10,000	Sandy Gravel and Sands	3/6[1]	<2,000	4,000/2,000[1]	
< 5,000	Silty sands and Clayey sand, screenings	5/10[1]	<1,000	200/1,000[1]	
[1]# resistivity tests/ # tests for pH, CL, and SO_4					

Table 6. Key observations made by Geocomp during its initial site visit from the accessible area on top of the MSE wall.

Approximate station (feet)	Observations	Representative photo
0+00	The concrete barrier on top of the MSE wall facing was ¾ inches lower than the concrete barrier on top of the bridge abutment.	20231113_IMG_2132
0+00 to 0+20	Multiple joints in concrete approach slab on both the shoulder and the traffic lanes. A relatively large area of repaired pavement and a transverse crack on the concrete approach slab.	Figure 13.
0+23	Considerable depression was observed around a manhole.	20231113_IMG_2133
0+26 to 2+90	Almost continuous longitudinal (south to north) cracks extending from approximate station 0+26 to station 3+07 feet were observed. The crack was approximately 2.5 to 3 feet from the western edge of the coping concrete and had variable openings of less than ¼ inches to ½ inches.	20231113_IMG_2134 20231113_IMG_2137
1+51; 1+78; 1+90; 2+02; 2+20; 2+82; 3+53; 3+81; 4+56; 4+83; 5+00	Multiple transverse cracks (west to east) were observed at different locations. The crack openings were variable from less than ¼ inches to 1 inch. The cracks extended from the longitudinal crack up to the concrete barrier.	20231113_IMG_2149 20231113_IMG_2153 20231113_IMG_2155
Multiple locations	Pavement surface at the shoulder was between ½ inches to 2 inches lower than the design from approximately station 0+50 and station 3+00.	20231113_IMG_2163
1+51; 5+02	Surface storm sewer inlets were partially covered with dirt. Transverse and/or longitudinal cracks were observed around the drains.	20231113_IMG_2148 20231113_IMG_2193
2+90 to 4+30	Isolated longitudinal (south to north) cracks 2.5 to 3 feet from the western edge of the concrete coping.	Multiple photos

Table 7. Key observations made by Geocomp during its initial site visit from the MSE wall facing.

Approximate station (foot)	Observations	Representative photo
0+00	MSE wall facing panels and concrete coping moved outward (i.e., toward east) up to approximately 4 inches relative to the bridge abutment wing. Bulging was obvious between the concrete coping and the top panel. The top panel was rotated approximately 2 degrees.	20231113_IMG_2199 20231113_IMG_2200
0+00	Approximately ¾ inches opening observed between the MSE wall concrete facing panels and the bridge abutment wing.	20231113_IMG_2204
0+00 to 1+00	Approximately 2 to 3 degrees of rotation was measured for the top panels. The bottom panels had a measured rotation of approximately 0 to 1 degree.	20231113_IMG_2209
1+00 to 2+00	Approximately 1 to 2 degrees of rotation was measured for the top panels. The bottom panels had a measured rotation of approximately 0 to 1 degree.	20231113_IMG_2213
2+00 to 3+00	Approximately 0 to 1 degrees of rotation was measured for the top panels. The bottom panels had a measured rotation of approximately 0 to 1 degree.	
3+00 to 3+50	Approximately 0 to 2 degrees of rotation was measured for the top panels. The bottom panels had a measured rotation of approximately 0 to 1 degree.	
3+50 to 4+10	Approximately 1 to 2 degrees of rotation was measured for the panels.	
Multiple locations	Relative displacement of panels toward east was observed in multiple locations. The displacement ranged from 3/8 to ½ inches.	20231113_IMG_2215
Multiple locations	Signs of water seepage through the concrete copings and panels.	20231113_IMG_2210 20231113_IMG_2216 20231113_IMG_2222

Table 8. Geocomp's select excavation sections.

Section	Approximate STA (feet)	Approximate top of MSE wall pavement Elev (feet)	Design and visually observed features	Relative conditions
1	I43 Sta. 175+34.09 Wall Sta. 0+00	667.4	• Concrete slab joints on top of the MSE wall, and pavement distress (see Figure 13). • Bulging and approximately 4-inch outward movement of the MSE wall facing panel (see Figure 14)	Poor
5	I43 Sta. 176+02.70 Wall Sta. 0+68.61	666.8	• Longitudinal crack on top of the MSE wall pavement with up to ½ inches opening. • Up to 10% cross slope at the shoulder.	Poor
2	I43 Sta. 176+36.70 Wall Sta. 1+02.61	666.1	• Continuous longitudinal crack on top of the MSE wall asphalt concrete pavement with up to ½ inches opening. • Up to 10% cross slope at the shoulder.	Poor
3	I43 Sta. 177+49.70 Wall Sta. 2+15.61	664.0	• Discontinuous longitudinal and transverse cracks on top of the MSE wall asphalt concrete pavement with up to ½ inches opening. • Up to 10% cross slope at the shoulder.	Poor
4	I43 Sta. 178+53.48 Wall Sta. 3+19.39	660.7	• Minimal to no cracks on the asphalt concrete on top of the MSE wall.	Good

Table 9. Schedule of field testing and sampling.

Field test/measurement	Number of tests/samples
Moisture content	57
Density	60
Resistivity	38
Bulk soil samples	38
Metal straps	34

Table 10. Average dry and moist density and moisture content at the tested sections.

Section	Lift	Average Moist Density (pcf)	Average Dry Density (pcf)	Average Moisture Content (%)	Average degree of saturation (S_r)
1	1	139.2	131.8	5.6	54
1	2	135.8	129.0	5.2	46
1	3	134.9	127.3	6.0	50
1	4	136.7	129.1	5.9	53
1	5	134.9	127.8	5.6	48
2	1	129.2	122.1	5.8	41
2	2	131.9	125.3	5.2	42
2	3	135.7	129.7	4.6	43
2	4	135.8	128.6	5.6	50
3	1	131.9	126.3	4.4	36
3	2	134.3	128.9	4.2	38
3	4	135.7	130.3	4.2	38
3	5	137.7	130.1	5.9	54
4	2	134.4	129.5	3.8	35
4	4	145.4	133.5	9.0	92
5	1	132.9	124.7	6.7	52
5	2	132.3	123.5	7.1	53
Mean	-	135.2	128.2	5.5	48
STD	-	5.9	5.7	1.3	13
Mean+STD[7]	-	141.1	133.9	6.8	61
Mean-STD	-	129.4	122.4	4.3	36

[7] Mean+STD indicates average plus one standard deviation.

Table 11. Summary of maximum, minimum, and average measured field soil resistivity at sections 1 through 5.

Sample location	Field resistivity (ohm-cm)		
	Minimum	Maximum	Average
Section 1	1,532	22,981	5,589
Section 2	3,256	25,280	11,258
Section 3	2,451	30,642	14,055
Section 4	3,102	38,973	13,524
Section 5	2,834	32,557	16,125

Table 12. Summary of Gradation tests.

Section	Lift	Corner	Elevation (feet)	Gravel	Sand	Fines	Soil
2	1	SE	664	53.5	42.3	4.2	GW
1	3	NE	659.6	55	40.7	4.3	GP
3	2	SW	658.8	44.1	50.5	5.4	SP-SM
3	5	NW	651.5	49.4	47.3	3.3	GP
1	6	SE	652	51	45.1	3.9	GP
Retained soil				33.9	33.2	32.9	GC

Table 13. Summary of maximum, minimum, and average measured moisture content for the tested sections.

Sample location	Moisture content (%)		
	Minimum	Maximum	Average
Section 1	4	5.5	5.1
Section 2	3.7	5.8	4.6
Section 3	2.8	4.6	3.7
Section 4	3.3	3.3	3.3
Section 5	6		
Retained soil	17		

Table 14. Summary of Proctor tests.

Sample	Soil Type	In Place Dry Density (pcf)	Maximum Dry Density (pcf)	In Place Relative Density (%)	Optimum Moisture Content (%)
S3L2SW	SP-SM	136	139.2	97.7	10.2
S2L1SE	GW	122	137.9	88.5	8.4

Table 15. Summary of direct shear tests.

Sample	Soil Type	Initial Test Dry Density (pcf)	Peak friction angle (degree)	Peak cohesion (psf)
S3L2SW	SP-SM	136	48	217
S2L1SE	GW	122	38	166

Table 16. Summary of maximum, minimum, and average measured fill electrical resistivity at the tested sections compared to the WisDOT specified limit.

Sample location	ρ_{min} (ohm-cm)				
	Test results				WisDOT 2025 Bridge Manual limit
	Minimum	Maximum	Average	STD	
Section 1	895	4,774	2,354	1450	>3,000
Section 2	637	4,722	1,516	1444	
Section 3	1,260	5,090	3,183	1370	
Section 4	1,591	6,962	4,175	2338	
Section 5	2,345	2,345	2,345	-	
Retained soil	1,293			-	-

The values in red indicate results that are outside the WisDOT specified limits.

Table 17. Summary of maximum, minimum, and average chlorides of the samples from tested sections compared to the WisDOT specified limit.

Sample location	Chlorides (ppm)				
	Test results				WisDOT 2025 Bridge Manual limit
	Minimum	Maximum	Average	STD	
Section 1	35	512	177	156	< 100
Section 2	28	697	257	201	
Section 3	38	352	104	107	
Section 4	26	223	113	71	
Section 5	108		108	-	
Retained soil	131		-		-

The values in red indicate results that are outside the WisDOT specified limits.

Table 18. Summary of maximum, minimum, and average measured sulfates at different locations compared to the WisDOT specified limit.

Sample location	Sulfates (ppm)				
	Test results				WisDOT 2025 Bridge Manual limit
	Minimum	Maximum	Average	STD	
Section 1	<1	70	16	23	< 200
Section 2	<1	20	9	6	
Section 3	<1	20	6	7	
Section 4	<1	10	5	5	
Section 5	30			-	
Retained soil	10			-	-

Table 19. Summary of Coating and Steel thickness measurement.

Sample	Average coating thickness* (μm)	STD* (μm)	Average coating thickness** (μm)	Average steel thickness* (mm)	STD (mm)	Average total thickness (μm)
S1L5	94	34	110	4.23	0.11	4.45
S2L3	133	38	210	4.28	0.16	4.70
S3L5	107	13	120	4.11	0.06	4.35
S4L2	109	7	210	4.15	0.11	4.57

*measured according to ASTM B487
**measured according to ASTM A90

Table 20. Summary of Statistical Analysis Results for Two-Variable Correlations with Corrosion Loss.

Variable 1	p-value	Variable 2	p-value	R^2
Depth	0.004	Station	0.0006	0.72
Depth	0.023	Moisture content	0.004	0.68
Wall station	0.003	Dry density	0.003	0.59

Table 21. PCI index and depth to excessive corrosion loss.

Excavation Section	Representative PCI	Depth of excessive corrosion loss (feet)
1	67	12.8
2	72	7
3	71	5.2
4	78	2.9

Table 22. Parameters used to calculate crack infiltration rate in sections 1 through 4.

Parameters/results	Section 1	Section 2	Section 3	Section 4
N_c	2	1	0.6	0
W_c	20	5	3	0
W	20	20	20	20
C_s	10	12	20	-
q_i	0.48	0.17	0.09	0

Table 23. Summary of calculated *K* constant in Equation 1 for both uniform and non-uniform corrosion losses and reinforcing strips in each lift of excavation.

Lift	***K***	
	Uniform corrosion loss	**Non-uniform corrosion loss**
1	88	162
2	92	220
3	96	204
4	59	201
5	18	24

Table 24. Soil properties considered for stability analysis of the MSE wall at excavation Section 1.

Material Name	Color	Unit Weight (lb/ft^3)	Strength Type	Cohesion (psf)	Phi (deg)
Backfill		125	Mohr-Coulomb	0	38
Foundation		120	Mohr-Coulomb	0	30
Face		153	Mohr-Coulomb	10000	38
Retained		120	Mohr-Coulomb	0	30

Table 25. Calculated F* and strip coverage area for each row of reinforcing strips within excavation Section 1.

Lift number	F*	Coverage area (%)
1	1.8	6.6
2	1.7	8.2
3	1.5	8.2
4	1.4	9.8
5	1.2	8.2
6	1.1	8.2

Table 26. Load resistance factors for service and strength limit states AASHTO (2020).

Load/resistance	Service Limit State	Strength Limit State
	Load factors	
Live load surcharges	1	1.75
Earth load surcharges	1	1.5
Dead loads, maximum case	1	1.25
Dead loads, minimum case	1	0.9
Horizontal earth pressure	1	1.5
Vertical earth pressure, max	1	1.35
Vertical earth pressure, min	1	1
	Resistance Factors	
Passive resistance	1	0.5
Bearing resistance	1	0.65
Tensile resistance of reinforcement	1	0.75
Pullout resistance of reinforcement	1	0.9
Sliding resistance	1	1

Table 27. Unfactored tensile strength of reinforcing strips due to uniform corrosion loss during different times.

Lift	Tensile strength (lbs/ft)				
	Uncorroded	After 32 yrs	After 37 yrs	After 42 yrs	After 75 yrs
1	128,669	85,732	81,316	77,250	53,713
2	128,669	83,584	79,164	74,912	50,306
3	128,669	81,735	77,011	72,575	46,899
4	128,669	99,539	96,921	94,195	78,415
5	128,669	119,675	118,984	118,152	113,337
6	128,669	128,669	128,669	128,669	128,669

Table 28. CDR for bearing capacity, sliding, and overturning.

Failure mode	CDR – Service Limit State	CDR – Strength Limit State
Bearing	3.86	1.65
Sliding	1.62	1.04
Overturning	3.28	2.09

Table 29. CDR for pullout, service and strength limit states.

Lift	CDR, Service Limit State	CDR, Strength Limit State
1	0.69	0.46
2	1.61	1.07
3	1.56	1.04
4	1.90	1.41
5	1.93	1.36
6	2.13	1.42

The values in red indicate that the tensile capacity is less than the demand.

Table 30. Tensile strength CDR for initial construction and after 75 years, service and strength limit states.

Lift	CDR			
	Service limit state, initial construction	**Service limit state, after 75 yrs**	**Strength limit state, initial construction**	**Strength limit state, after 75 yrs**
1	10.88	4.54	6.05	2.52
2	15.02	5.87	8.34	3.26
3	11.19	4.08	6.22	2.27
4	10.52	6.41	5.84	3.56
5	7.72	6.80	4.29	3.78
6	6.56	6.56	3.64	3.64

Table 31. Unfactored tensile strength of reinforcing strips considering non-uniform corrosion loss at different times after the MSE wall construction.

Lift	Tensile strength (lbs/ft)					
	Uncorroded	**After 32 yrs**	**After 37 yrs**	**After 42 yrs**	**After 47 yrs**	**After 75 yrs**
1	128,669	49,036	41,497	34,010	26,830	0
2	128,669	20,772	10,286	120	0	0
3	128,669	29,019	18,896	9,469	428	0
4	128,669	30,019	20,510	11,222	2,314	0
5	128,669	117,128	115,755	114,646	113,582	108,227
6	128,669	128,669	128,669	128,669	128,669	128,669

Table 32. Summary of the factors of safety (FS) calculated by Slide2 considering uniform and non-uniform corrosion loss.

Time (yrs)	Factor of Safety	
	Uniform corrosion loss	**Non-uniform corrosion loss**
0	1.59	1.59
32	1.59	1.59
37	1.59	1.59
42	1.59	1.09
47	1.59	0.74
75	1.59	0.74

The values in red indicate that the calculated Factor of Safety is below the minimum required by WisDOT.

Table 33. Tensile strength CDR for initial construction, after 32, 37, and 42 years for service limit state.

Lift	CDR			
	Service limit state, initial construction	**Service limit state, after 32 yrs**	**Service limit state, after 37 yrs**	**Service limit state, after 42 yrs**
1	10.88	4.15	3.51	2.88
2	15.02	2.42	1.20	0.01
3	11.19	2.52	1.64	0.82
4	10.52	2.45	1.68	0.92
5	7.72	7.02	6.94	6.88
6	6.56	6.56	6.56	6.56

The values in red indicate that the tensile capacity is less than the demand.

Table 34. Tensile strength CDR for initial construction, after 32, 37, and 42 years for strength limit state.

Lift	CDR			
	Strength limit state, initial construction	**Strength limit state, after 32 yrs**	**Strength limit state, after 37 yrs**	**Strength limit state, after 42 yrs**
1	6.05	2.30	1.95	1.60
2	8.34	1.35	0.67	0.01
3	6.22	1.40	0.91	0.46
4	5.84	1.36	0.93	0.51
5	4.29	3.90	3.86	3.82
6	3.64	3.64	3.64	3.64

The values in red indicate that the tensile capacity is less than the demand.

Table 35. Nonlinear calibrated model for tensile strength prediction based on average value of all nonuniform corrosion loss.

Lift	**n**	**K**	**T (lb/ft) 32 yrs**	**T (lb/ft) 37 yrs**	**T (lb/ft) 42 yrs**	**T (lb/ft) 55 yrs**	**T (lb/ft) 57 yrs**	**T (lb/ft) 75 yrs**
1	0.65	130	65,134	58,846	52,850	38,324	36,202	18,144
2	0.65	166	47,582	39,557	31,904	13,366	10,658	0
3	0.65	177	42,001	33,424	25,244	5,430	2,535	0
4	0.65	125	67,428	61,367	55,588	41,587	39,541	22,136
5	0.65	22	117,919	116,855	115,841	113,383	113,024	109,968

Table 36. Summary of probabilities of failure against overall slope stability using nonuniform corrosion loss.

Years after construction	Probability of Failure (%)
32	0.00
37	0.00
42	0.00
55	1.06
57	2.06
75	50.11